

NASA CR-72754

CdS SOLAR CELL DEVELOPMENT

FINAL REPORT

by

N. E. Nastelin, P. L. DiRenzo and A. L. Gombach

CLEVITE CORPORATION
A Subsidiary of Gould Inc.

PREPARED FOR

NATIONAL AERONAUTICS AND SPACE ADMINISTRATION

NASA Lewis Research Center

CONTRACT NAS3-11845

L. R. Scudder, Project Manager

NOTICE

This report was prepared as an account of Government-sponsored work. Neither the United States, nor the National Aeronautics and Space Administration (NASA), nor any person acting on behalf of NASA:

- A.) Makes any warranty or representation, expressed or implied, with respect to the accuracy, completeness, or usefulness of the information contained in this report, or that the use of any information, apparatus, method, or process disclosed in this report may not infringe privately-owned rights; or
- B.) Assumes any liabilities with respect to the use of, or for damages resulting from the use of, any information, apparatus, method or process disclosed in this report.

As used above, "person acting on behalf of NASA" includes any employee or contractor of NASA, or employee of such contractor, to the extent that such employee or contractor of NASA or employee of such contractor prepares, disseminates, or provides access to any information pursuant to his employment or contract with NASA, or his employment with such contractor.

Requests for copies of this report should be referred to:

National Aeronautics and Space Administration
Office of Scientific and Technical Information
P. O. Box 33
College Park, Maryland 20740

NASA CR-72754
Project No. 303420

FINAL REPORT

DEVELOPMENT OF IMPROVED CADMIUM SULFIDE SOLAR CELLS

by

H. E. Nastelin, P. L. DiRenzo and A. L. Gombach

CLEVITE CORPORATION
A Subsidiary of Gould Inc.
540 E. 105th Street
Cleveland, Ohio 44108

Prepared for

NATIONAL AERONAUTICS AND SPACE ADMINISTRATION

September 1970

CONTRACT NAS3-11845

NASA Lewis Research Center
Cleveland, Ohio
L. R. Scudder, Project Manager
Direct Energy Conversion Division

FOREWORD

The work summarized in this report was done at the Electronic Technology Division of Gould Laboratories, Cleveland, Ohio, formerly known as Electronic Research Division of the Clevite Corporation. The work was performed under contract NAS3-11845 for Lewis Research Center, NASA, under the management of Mr. Larry R. Scudder, NASA Project Manager. The contractual effort covered a period of time from February 18, 1969, to March 18, 1970.

H. E. Nastelin was principal investigator. F. A. Shirland initially was Project Director followed later by Dr. D. B. Parkinson. P. L. DiRenzo was in charge of cell manufacturing and A. L. Gombach directed the quality control program. The contribution of the following individuals is acknowledged: J. Beller, T. R. Deucher, R. F. Didero, W. F. Dunn, J. R. Greene, J. P. Haugh, R. J. Kinley, and J. M. Smith III. The many helpful suggestions of L. R. Shiozawa of the Semiconductor Section are also acknowledged.

TABLE OF CONTENTS

	Page
FOREWORD	iii
ABSTRACT	v
LIST OF ILLUSTRATIONS	vi
LIST OF TABLES	vii

<u>Title</u>	
SUMMARY	1
INTRODUCTION	2
CELL FABRICATION	2
Standard Cell Production	2
Yields	4
Quality Control	10
CELL STABILITY	10
Dry Shelf Storage	11
Moisture Storage	19
100° C Vacuum Storage	27
CELL IMPROVEMENT PROGRAM	34
Roll Coated Substrates	34
1:1 Ag-Pyre ML Sprayed Substrates	37
Machine Sprayed Substrates	38
Zn-Pyre ML Substrates	39
Evaporated Grids	39
Gold Epoxy Application by Silk Screening	48
Chromium Interlayers	48
FEP Teflon Cover Plastic	57
Characterization of CdS Evaporation Process	66
(1) Evaporation Rate Profile	66
(2) Substrate Temperature Uniformity	67

ABSTRACT

Normal pilot line fabrication of standard process cells was limited by a period of low production yields. Long term storage stability testing has been continued for almost 4 years on three different tests, dry shelf storage, moisture storage and 100°C-vacuum storage. Machine roll-coated Ag-Pyre ML substrates were substituted for the standard sprayed substrates and showed an improved production yield as well as an apparent improvement in performance. Evaporated and electroplated chromium were unsuccessfully substituted for electroplated zinc as the interlayer material. FEP Teflon as a cover plastic was successfully attached to gridded cells with adhesives and heat bonding. Its evaluation is continuing. Evaporated grids were successfully deposited but their resistance was much greater than that of the present grid and no practical method of reducing this resistance was found. The CdS evaporation process was investigated and significant temperature gradients were found to exist on the substrate during simulated evaporation cycles. Their cause was traced to aluminum evaporation masks mounted in front of the substrate. The evaporation rate profiles of two designs of evaporation sources was also studied.

LIST OF ILLUSTRATIONS

Figure		Page
1.	I-V Characteristic at 0.01 AMO-25°C, Good Low Light Level Performance.	5
2.	I-V Characteristic at 0.01 AMO-25°C, Poor Low Light Level Performance.	6
3.	I-V Characteristic at AMO-25°C.	7
4.	I-V Characteristic at AMO-25°C.	8
5.	Average Relative Efficiency on Dry Shelf Storage.	16
6.	Average Relative Efficiency on Moisture Storage.	24
7.	Average Relative Efficiency on 100°C Vacuum Storage	31
8.	Effect of 100°C Storage on Cell Performance.	33
9.	I-V Characteristic of Evaporated Grid Cell. Fluorocarbon Spray Evaporation Mask.	43
10.	I-V Characteristic of Evaporated Grid Cell. Ni Foil Evaporation Mask.	44
11.	I-V Characteristic of Evaporated Grid Cell. Evaporated Pattern Built up With Silver Epoxy.	46
12.	I-V Characteristic of Evaporated Grid Cell. Evaporated Pattern Built up With Gold Epoxy.	47
13.	I-V Characteristic of Electroplated Chromium Interlayer Cell.	50
14.	I-V Characteristics of Back Junction With Electroplated Chrome Interlayer.	51
15.	I-V Characteristic of Electroplated Chromium Interlayer Cell.	52
16.	I-V Characteristic of Unexposed Evaporated Chrome Interlayer Cell.	54
17.	I-V Characteristic of Air Exposed Evaporated Chrome Interlayer Cell.	55
18.	I-V Characteristic of Cell With No Interlayer.	56
19.	I-V Characteristic of FEP Covered Cell.	59
20.	I-V Characteristics of Heat Sealed FEP Cell.	62
21.	I-V Characteristics of Class I Cell Subjected to Same Heating Cycles Used to Laminate FEP.	63
22.	I-V Characteristics of Cell With No Cover Subjected to Same Heating Cycles Used to Laminate FEP.	64
23.	Typical Evaporation Rate Profile of CdS Evaporation Source.	67

LIST OF TABLES

Table	Page
I. Average AM0-25°C Performance of 534 Cells.	2
II. Average AM0-60°C Performance of 534 Cells.	3
III. Average Performance of 200 Cells at 0.1 AM0-25°C and 0.01 AM0-25°C.	4
IV. Actual and Relative Efficiencies of 1966 Cells on Dry Shelf Storage.	12
V. Actual and Relative Efficiencies of 1967 Cells on Dry Shelf Storage.	13
VI. Actual and Relative Efficiencies of 1968 Cells on Dry Shelf Storage.	14
VII. Actual and Relative Efficiencies of 1969 Cells on Dry Shelf Storage.	15
VIII. Comparison of Initial and 42 Month Performance of Representative 1966 Cells on Dry Shelf Storage.	18
IX. Comparison of Average Relative Efficiencies of Mylar and Kapton Covered 1967 Cells on Dry Shelf Storage.	18
X. Comparison of Initial and Final Performance of Representative 1967 cells on Dry Shelf Storage (28 to 34 Months).	18
XI. Actual and Relative Efficiencies of 1966 Cells on Moisture Storage.	20
XII. Actual and Relative Efficiencies of 1967 Cells on Moisture Storage.	21
XIII. Actual and Relative Efficiencies of 1968 Cells on Moisture Storage.	22
XIV. Actual and Relative Efficiencies of 1969 Cells on Moisture Storage.	23
XV. Comparison of Initial and 40 Month Performance of 1966 cells on Moisture Storage.	19
XVI. Effect of Laminating and 15 Hour 135°C Vacuum Bake on Moisture Degraded Cells.	25
XVII. Effect of 15 Hour 135°C Vacuum Bake on Moisture Degraded Cells.	26
XVIII. Actual and Relative Efficiencies of 1966 and 1967 Cells on 100°C Vacuum Storage.	28
XIX. Actual and Relative Efficiencies of 1968 Cells on 100°C Vacuum Storage.	29

<u>Table</u>	<u>Page</u>
XX. Actual and Relative Efficiencies of 1969 Cells on 100° C Vacuum Storage.	30
XXI. Capacitance Measurements of Heat Degraded and Undegraded Cells.	32
XXII. AM0-25° C Performance of Kapton Covered Roll-Coated Substrate Cells.	35
XXIII. AM0-25° C Performance of Standard Process and 1:1 Roll-Coated Substrate Cells.	36
XXIV. Performance Comparison of Roll-Coated Substrate Cells and Standard Process Cells.	36
XXV. AM0-25° C Performance of 68 1:1 Spray Coated Cells.	38
XXVI. AM0-25° C Performance of 29 Standard Process Control Cells.	38
XXVII. Comparison of Machine Sprayed and Hand Sprayed Substrate Cells, AM0-25° C.	39
XXVIII. AM0-25° C Performance of 33 FEP Covered Cells.	57
XXIX. AM0-25° C Performance of 26 FEP Covered Class I Roll-Coated Substrate Cells.	58
XXX. Adhesives Evaluated for Attaching Type C FEP Teflon to Gridded Cells.	60
XXXI. AM0-25° C Performance of Heat Sealed FEP Cells.	65

SUMMARY

The design of the standard process cell remained unchanged over the contract period. Initial production yields were quite low in the manufacture of standard process cells. This necessitated a redirection of effort which curtailed cell production after the seventh month. As a result normal cell production was confined to a period of only five months.

Long term stability testing has continued on three separate tests, dry shelf storage, moisture storage, and 100°C vacuum storage. The average performance of cells on dry shelf storage, fabricated in 1966 and 1967, has remained within 10% of their initial performance. The averages of 1968 and 1969 cells have remained within 5% of initial performance. The 1966 cells on moisture storage have decreased to an average of 77% of their initial performance, while the 1967 cells had decreased to 70%. 1968 and 1969 cells had decreased to an average of 81% and 94% respectively. Wide fluctuations were present in the 100°C-vacuum storage test but general trends were apparent. The average performance of 1966 and 1967 cells had fallen to 40% of their initial values. The 1968 cells were at 76% while the average of the 1969 cells remained above their initial values. The best individual cell performance showed only a 2% decrease after 2 years on 100°C vacuum test.

A development program intended to improve the uniformity, stability and performance of thin film cells was also carried out. The substitution of machine roll coated Ag-Pyre ML substrates for sprayed substrates showed promise in that the manufacturing yields and apparently, cell performance, were somewhat improved.

FEP Teflon has been successfully attached to gridded cells as a cover plastic by the use of adhesives and by heat bonding. Its acceptability as a cover plastic is still being evaluated.

Evaporated and electroplated chromium were substituted for electroplated zinc as the interlayer material at the back junction. Both resulted in cell performance that was below standard cell performance. In addition, the difference in electrical behavior between evaporated and plated chrome interlayers suggests that the properties of this back junction are structure sensitive.

Evaporated gold grids of the required resolution and uniformity were successfully deposited on the barrier layer of standard process cells. However, their resistance was much greater than could be tolerated, and no practical method of reducing this resistance was found.

The standard CdS evaporation process was studied with respect to reproducibility from one evaporation cycle to the next. The evaporation rate profiles of two designs of evaporation sources were studied. The stability and long life of the design presently used was shown to be superior to an older type previously used. Fairly large temperature gradients were found to exist on the substrate during simulated evaporation cycles. Their cause was traced to the aluminum evaporation mask mounted in front of the substrate.

INTRODUCTION

The scope of the effort reported here covers a number of areas which were all part of a program intended to improve the uniformity, stability and performance of the thin film CdS solar cell. Included were the operation of a laboratory pilot line whose purpose was to fabricate 100 cells each month, the incorporation and maintenance of a quality control program on the pilot line, continuation of long term storage stability testing and a development program which included the investigation of a number of the cell fabrication steps and the substitution of other materials and processes in the standard design cell.

The design of the standard process cell remained essentially constant over the contract period and will not be detailed here since it has been frequently covered elsewhere.⁽¹⁾ This is basically the same cell that had been evolved and put into pilot manufacture in 1966.

CELL FABRICATION

Standard Cell Production

During the early portion of the reporting period standard cell manufacture was stymied by a severe slump in production yields. So much effort was spent in solving this problem during the first three months that a later redirection of the contract effort was necessary. As a result, normal cell production was confined to a five month period beginning in May, and continuing until September when the 100 cell monthly requirement was dropped. The total acceptable cell production then consisted of the 500 cells fabricated during the 5 months of normal production and 34 cells from the slump period.

The average AMO-25°C performance of these 534 acceptable cells, as well as their maximum and minimum values, are shown in Table I. The requirements for acceptance have been defined as a minimum efficiency of 2.8% and a minimum fill of 68.5%.

Table I. Average AMO-25°C Performance of 534 Cells

	<u>Max.</u>	<u>Min.</u>	<u>Av.</u>
OCV	.490 V	.440 V	.469 V
SCC	.975 A	.630 A	.761 A
P _{max}	.315 W	.213 W	.250 W
Eff.	4.1 %	2.8 %	3.3 %
Fill	72.9 %	68.5 %	70.1 %

⁽¹⁾ NASA CR 72534, Final Report on Contract NAS 3-9434.

Cells were also tested at AM0-60° C to qualify for NASA acceptance, the criteria being that the SCC shall not decrease by more than 2% of its AM0-25° C value. The ranges and averages of the 534 cell AM0-60° C performance are listed in Table II.

Table II. Average AM0-60° C Performance of 534 Cells

	Max	Min	Av.
OCV	.439 V	.389 V	.417 V
SCC	.960 A	.620 A	.751 A
P _{max}	.263 W	.166 W	.207 W
Eff.	3.4 %	2.2 %	2.7 %
Fill	71.5 %	60.0 %	66.6 %

Comparison of the 534 cell average performance at the two temperatures shows that the OCV has a temperature coefficient of $-1.49 \text{ mV}/^\circ\text{C}$, which is somewhat lower than the normally quoted value of $-1.6 \text{ mV}/^\circ\text{C}$. The reason for this difference is not known. The SCC at 60° C is well within the required 2% of the 25° C SCC. The maximum power, based on these 534 cells, shows a temperature coefficient of $-1.14 \text{ mW}/^\circ\text{C}$. The fill factor shows an average temperature coefficient of $-0.14\%/^\circ\text{C}$.

As part of an effort to further characterize the performance of the thin film CdS cell testing at light levels of 1/10 and 1/100 AM0 was initiated on a routine basis. In addition to the AM0-25° C and AM0-60° C testing all Class I monthly production cells were also tested at 0.1 AM0-25° C and 0.01 AM0-25° C during the first few months of the contract. This was later reduced to testing only representative cells at 0.01 AM0-25° C when cell production returned to normal levels and when it became apparent that only limited information was being obtained from the 0.1 AM0-25° C test.

Low light level performance has previously been thought to give some indication of future cell performance and stability.⁽²⁾ It was shown that the shunt resistance increases as light intensity decreases until saturating at some limiting value of leakage resistance. The magnitude of this limiting shunt resistance was thought to help determine cell performance, the higher the value of this resistance the better cell performance and stability. Unfortunately, this resistance does not seem to be obtainable from AM0 or AM1 or even dark I-V curves. It was hoped that correlation of these low light level measurements with the various cell stability testing programs would result in better methods of predicting cell performance.

⁽²⁾ ARL 68-0217, Dec. 1968, A. F. Final Report, Contract No. F33615-68-C-1182, H. E. Nastelin.

Table III shows the average performance parameters of 200 cells at 0.1 and 0.01 AM0 and 25° C.

Table III. Average Performance of 200 Cells at 0.1 AM0-25° C and 0.01 AM0-25° C.

	0.1 AM0-25° C	0.01 AM0-25° C
OCV	.410 V	.349 V
SCC	77.4 mA	8.0 mA
P _{max}	23.1 mW	1.7 mW
Eff.	3.0 %	2.2 %
Fill	70.8 %	63.4 %

The SCC shows a linear dependence on light intensity; the 1/10 and 1/100 AM0 SCC's are about 10% and 1% of the 534 cell AM0 averages. The 1/10 AM0 maximum power is about 10% of the AM0 average power; however, the 1/100 AM0 maximum power is only 0.7% of the AM0 maximum power, which indicates obviously that the power is not linearly dependent on light level. The behavior of the fill is quite interesting in that it parallels the variations in maximum power and efficiency. The low light level I-V characteristics indicate that a poor shunt resistance appears responsible for the low fill, which is in line with the earlier observation that an increasing shunt resistance with decreasing light level is a necessary requisite for good low light level performance. Figure 1 shows the I-V characteristic of a cell that had relatively good low light level performance, while Fig. 2 shows a cell with a poor low light level performance. It is interesting that both cells had very similar AM0-25° C curves, Figs. 3 and 4. These figures show that the AM0-25° C performance of a cell does not indicate how it will perform at low light levels.

Yields

Production yields of standard process cells varied considerably during the contract year, not only from month to month but within any given month as well. Hence overall yield figures for the entire year are relatively meaningless. The monthly values varied from a minimum of 1.7% in March to a high of 40.6% in July; meaning, for example, that 40.6% of all evaporated films in July finished as Class I cells.

As indicated before the Pilot Line was in a severe slump during the first few months of the contract period. The cause of the slump was never fully understood, there were a number of factors that apparently contributed to it. In addition to something actually out of control on the Pilot Line, more stringent requirements were made on cell acceptance because cell testing was changed from AM1 to AM0, and as a result, the 68.5% fill factor requirement became more difficult to meet. Also, the new quality control program was incorporated into the fabrication process during the same time period with its resultant increase in rejection rates. Finally, personnel changes and realignment of responsibilities in the fabrication and inspection areas were also reflected in the abnormally high rejection rates at that period.

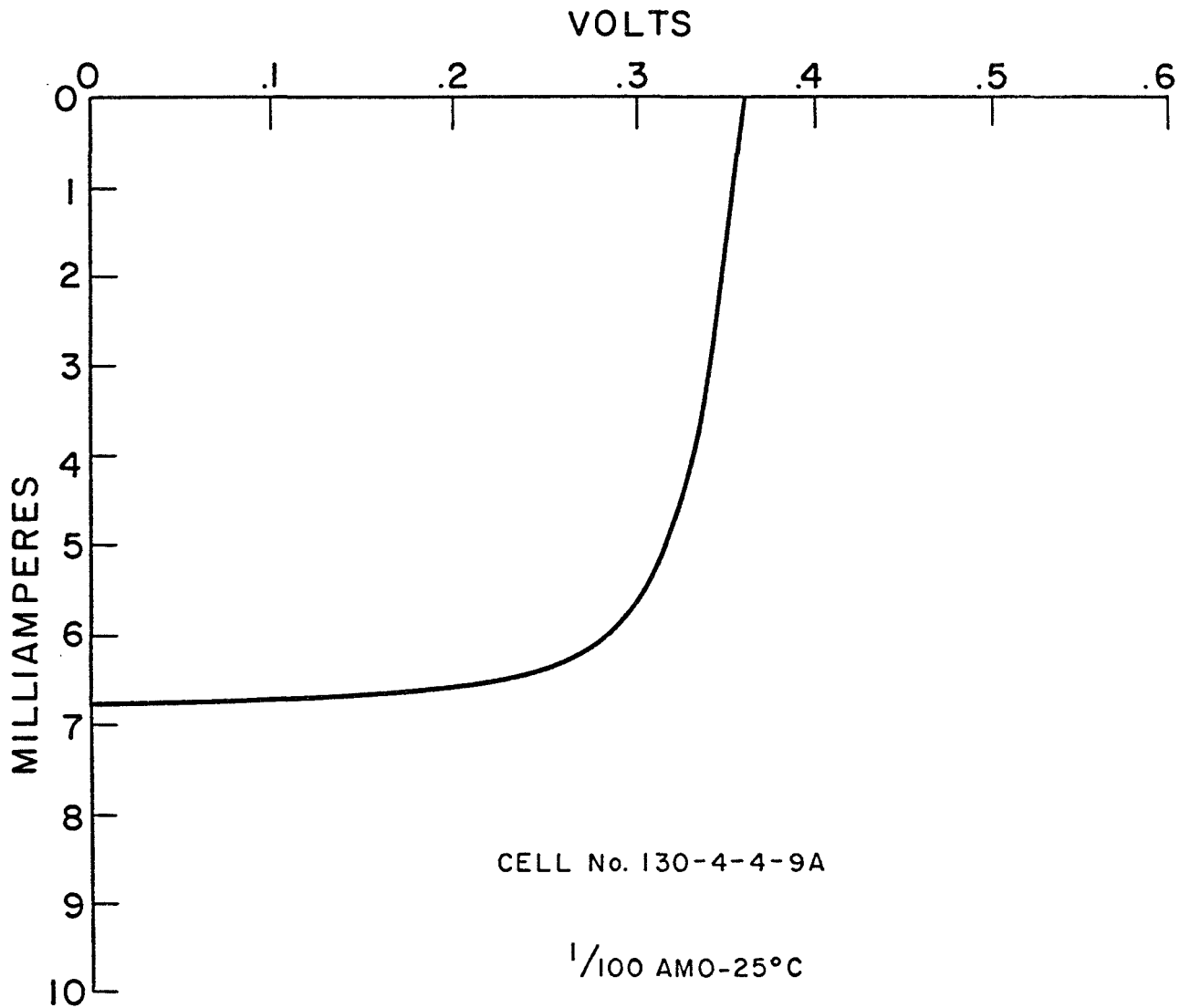


FIG. 1: I-V CHARACTERISTIC AT 0.01 AMO-25°C, GOOD LOW LIGHT LEVEL PERFORMANCE.

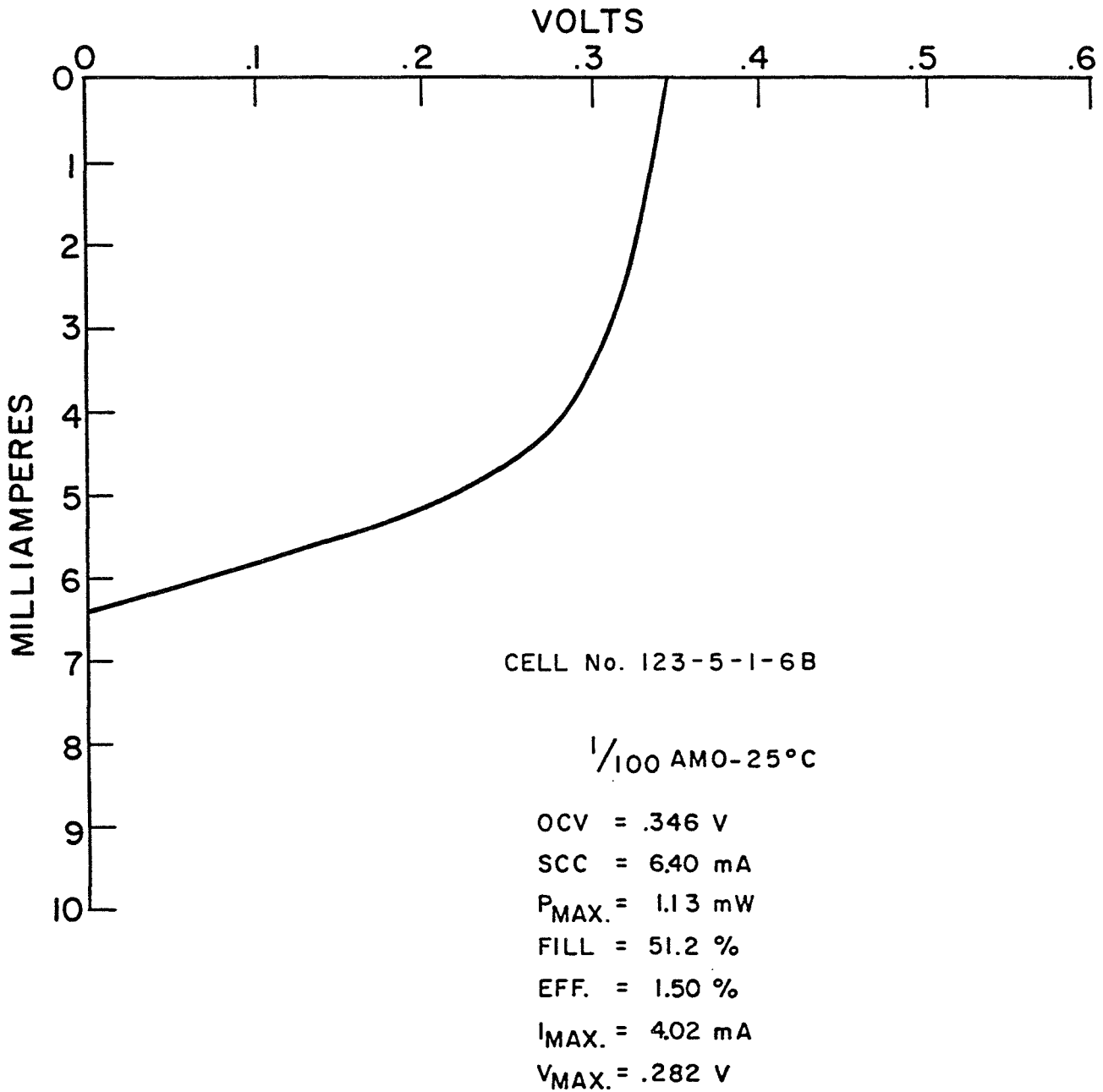


FIG. 2: I-V CHARACTERISTIC AT 0.01 AMO-25°C,
 POOR LOW LIGHT LEVEL PERFORMANCE.

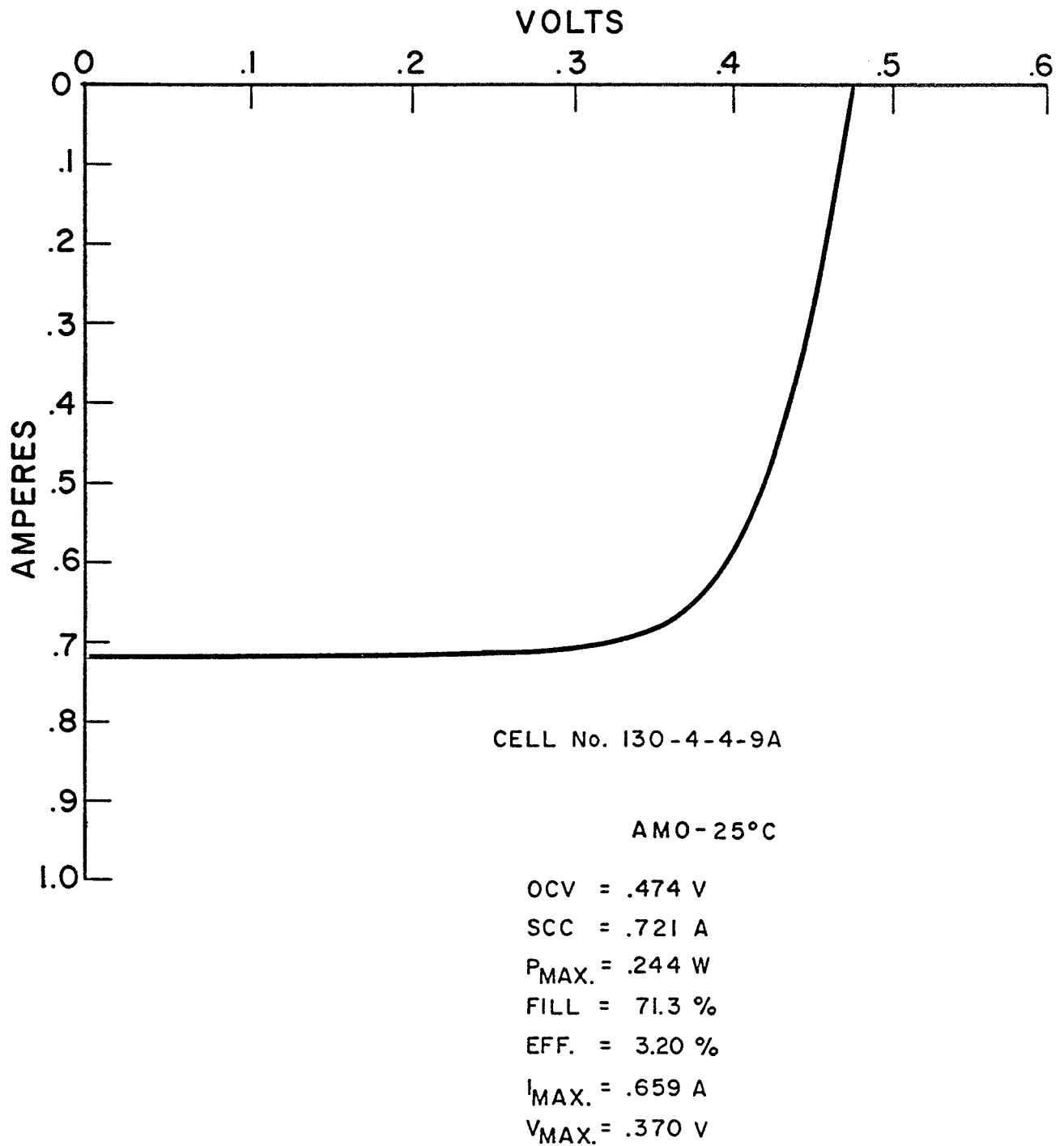


FIG. 3: I-V CHARACTERISTIC AT AMO -25°C .

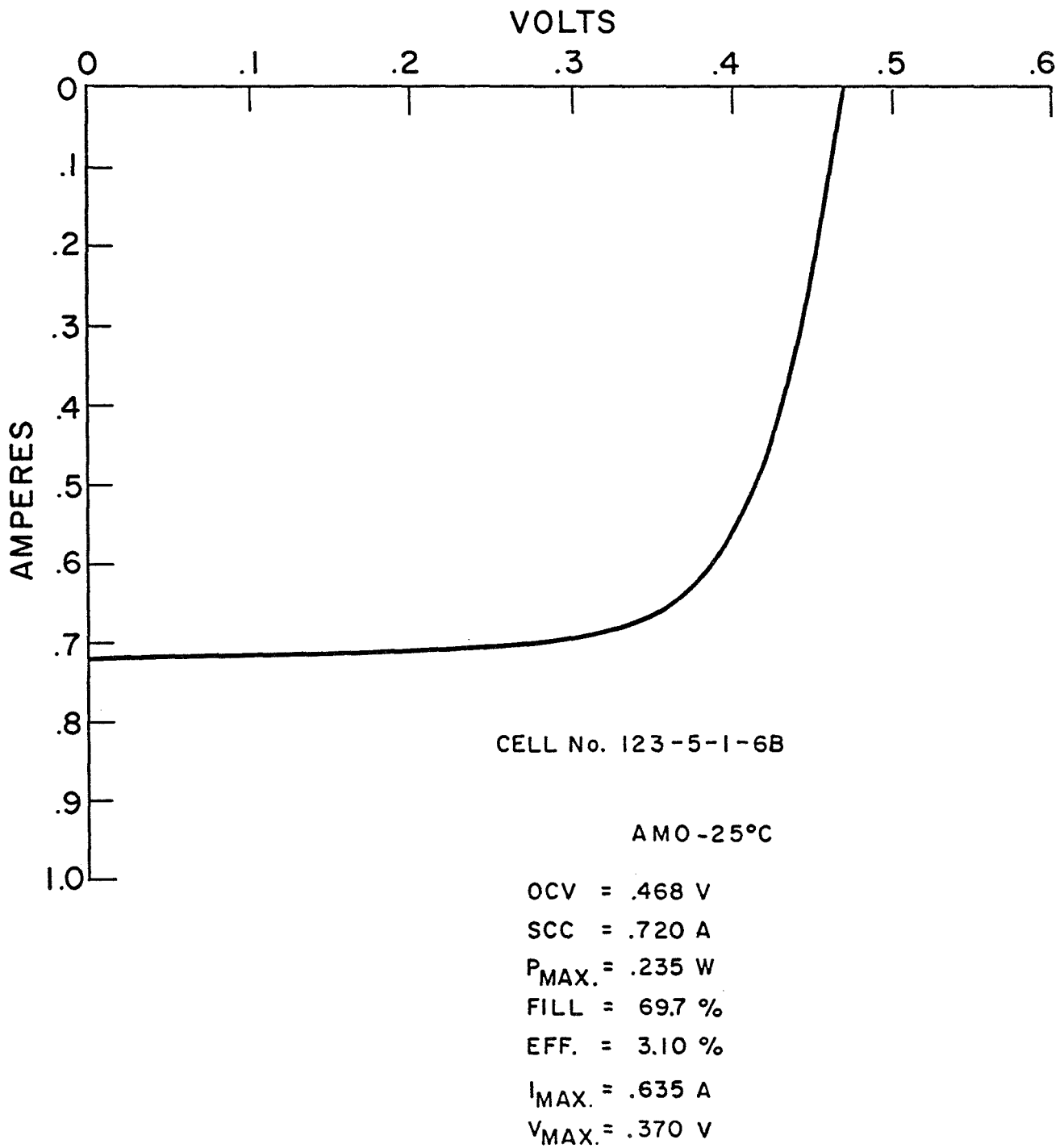


FIG. 4: I-V CHARACTERISTIC AT AMO-25°C.

There were two inspection stations that accounted for most of the high rejection rates, barrier inspection and final electrical testing. The main cause of rejections at the barrier inspection was the occurrence of copper precipitation on the barrier layer and the occurrence of pinholes in the barriered film. Both of these were suspected to be caused by faults in the substrate preparation area. At final testing the main cause of rejection was low fill factor and low output. It was first thought that there must have been a common cause for both of these rejections, but this was not fully established. The reason that a cell fill is just below 68.5% instead of being just above 68.5% is difficult, if not impossible, to identify. Only in the case of extremely poor fills is a definite cause assignable.

It wasn't until after a thorough and methodical examination of each step of the standard fabrication process was initiated that the slump started easing. By the time that the examination had proceeded through the barrier formation process yields had returned to acceptable levels. Surprisingly, the examination turned up no major faults in the process; only a number of minor deviations from the standard process that had apparently slowly crept in were found. Individually, none of the minor deviations could probably have accounted for the slump, but collectively they could, and probably did.

One of the additional benefits of the examination process was that a number of improvements were found that were incorporated into the design and construction of the new production facilities that the Pilot Line has recently been moved into. For example, the necessity of completely separating and isolating the substrate spraying and burnishing areas did not become apparent until the examination showed that dust and particle contamination in these steps was greater than had been assumed and only by completely isolating the two functions could an acceptable level of cleanliness be achieved.

The necessity of improving the method of mixing the Ag-Pyre ML mixture prior to substrate spraying was also stressed as a result of the examination. Previously, this mixture was hand mixed "as well as possible" and extremely varied results were usually obtained. One of the major faults was the occurrence of agglomerates of silver flake which usually resulted in pinholes during the burnish operation. Although a number of methods of mechanically stirring and mixing had been tried in the past with limited success the necessity of continuing the search was emphasized by the examination.

A Waring Blendor was used for the first time and extremely encouraging results were obtained. The occurrence of silver flake agglomerates was considerably reduced. The sheet resistance of the sprayed substrates was reduced to average values well below hand mixed values. The results from the Waring Blendor have been so encouraging that its use has been adopted as part of the standard process.

Quality Control

At the beginning of the contract period the existing quality control program was significantly expanded and upgraded. A new Q. C. program was essentially worked out, submitted to NASA-Lewis for approval and then incorporated into the standard process. The Q. C. Manual submitted to NASA early in the contract period, contains the details of the new Q. C. program.

The new Q. C. program was initiated at a time when, as mentioned before, the production yields were in a severe slump. Hence the effects of the new program were not immediately determinable. However, later on in the contract year when the Pilot Line had settled down to more normal operation, while still fluctuating considerably from month to month, the yields did occasionally reach higher levels than ever before.

A new cell numbering and card file system, which allows the easy traceability of all manufactured cells, was instituted early this contract year. The production record for each cell from the first step in its fabrication process, as well as inspection reports on all materials used in that cell, are readily available.

CELL STABILITY

One of the major tasks of this and the previous contracts has been the characterization of cell stability on long term shelf storage. Each month, beginning with Contract NAS3-8502 in 1966, cells have been selected from the current month's production and entered into three storage tests. The three tests are dry shelf storage, moisture storage and 100°C vacuum storage. All cells are removed from the test environment monthly for AMO-25°C testing for cells fabricated since 1969 and AM1-25°C testing for all cells fabricated prior to 1969. All of the cells on these tests are of the present standard construction; that is, sprayed Ag-Pyre ML substrates and gold plated copper grids held in place with conductive gold epoxy. The cover plastics are held in place with a transparent epoxy. The earlier cells are Mylar covered and those made since mid-1967, Kapton covered. Fluctuations in cell performance are obviously going to be present over such a long time period, approaching four years in the case of cells fabricated during 1966. Some of the fluctuations are due to actual instability or degradation in cell performance, however, much of it is due to variations in the test conditions. Attempting to maintain uniform test conditions over a period of several years is obviously difficult, and some changes are bound to occur. The tester has been modified considerably and completely replaced at least once since testing began. However, some general trends in cell performance are present and these will be reported.

In the tables that follow, the actual and relative efficiencies of each cell are reported. The relative efficiency is the percentage of pre-test efficiency; that is, $\frac{\text{present efficiency}}{\text{pre-test efficiency}} \times 100$. Some of the wide fluctuations in the data are due to using this pre-test performance as a basis of comparison because practically all cells seem to go through an adjustment period after fabrication. They then seem to settle down to a more constant performance afterwards. This is most apparent in the dry and moisture storage tests where the average performance seems to be marked by an initial more rapid degradation rate followed by a much slower rate.

Dry Shelf Storage

The dry shelf storage test consists of a standard laboratory type desiccator kept at room temperature and pressure. A chemical desiccant provides the dry atmosphere.

Tables IV through VII show the actual and relative efficiencies of cells while Fig. 5 shows plots of the average relative efficiency according to year of manufacture. As expected, no serious degradation problems appear to be present as indicated by the fact that after 42 months the average efficiency is still within 94% of the initial value. It is difficult to extract an average degradation value from such widely varying data. Probably of most significance is the fact that there are several cells that exceed their initial performance even after almost four years of testing.

An analysis of the I-V characteristics of the 1966 cells shows that the decrease in efficiency in all cells was accompanied by a decrease in SCC. Rather remarkably, in no instance was there a significant decrease in fill or OCV. The fill either improved or remained constant. However, their initial fills were quite low to begin with since they were fabricated at a time when specifications on fill were either quite low or non-existent. In those cases where the fill remained constant the decrease in relative efficiency was almost numerically equal to the decrease in relative SCC. And in those cases where the fill increased the loss in relative efficiency was less than the loss in relative SCC. This behavior is shown in Table VIII.

Table IV Actual and Relative Efficiencies of 1966 Cells and Dry Shelf Storage

Cell No.	Months														
	0	3	6	9	12	15	18	21	24	27	30	33	36	39	42
D315A	5.6/100	5.1/91	5.2/93	5.1/91	5.0/89	5.2/93	4.9/87	4.7/84	4.8/86	--	5.0/89	5.0/89	5.2/93	4.8/86	5.0/89
D289D	5.4/100	4.8/89	4.8/89	4.8/89	4.8/89	4.9/91	4.7/87	4.6/85	4.6/85	--	4.5/83	4.7/87	4.8/89	4.5/83	4.7/87
D292D	5.3/100	4.8/90	4.9/93	4.8/90	4.7/89	5.0/94	4.7/89	4.5/85	4.6/87	--	4.6/87	4.6/87	4.8/90	4.6/87	4.7/89
D296B	4.9/100	4.4/90	4.4/90	4.3/88	4.3/88	4.5/92	4.2/86	4.1/84	4.2/86	--	4.1/84	4.1/84	4.3/88	4.1/84	4.1/84
D306D	5.5/100	4.9/89	5.1/93	4.9/89	4.8/87	5.0/91	4.7/86	4.8/87	4.8/87	--	4.6/84	4.7/86	5.0/91	4.6/84	4.7/86
D336D	4.6/100	4.0/87	4.1/89	4.2/91	4.1/89	4.4/96	4.1/89	4.3/94	4.1/89	--	3.8/83	4.0/87	4.3/94	4.0/87	4.2/91
D355C	5.1/100	5.5/108	5.5/108	5.3/104	5.2/102	5.4/106	5.0/98	5.0/98	5.0/98	--	4.8/94	5.0/98	5.1/100	4.9/96	5.0/98
D364F	4.0/100	4.1/103	4.2/105	4.3/108	4.2/105	4.5/112	4.1/102	4.0/100	4.2/105	--	4.1/102	4.1/102	4.3/108	4.1/102	4.5/112
D375C	4.5/100	4.2/93	4.4/98	4.4/98	4.3/96	--	4.0/89	4.0/89	4.1/91	4.0/89	--	4.1/91	4.2/93	4.0/89	4.1/91
D385B	5.0/100	5.1/102	5.1/102	5.1/102	4.9/98	4.8/96	4.8/96	--	4.8/96	4.7/94	4.8/96	--	4.9/98	4.7/94	4.8/96
D386E	5.0/100	5.2/104	5.2/104	5.2/104	5.1/102	5.0/100	5.0/100	4.8/96	4.9/98	4.9/98	--	4.9/98	5.1/102	4.9/98	4.9/98
D391B	4.5/100	5.0/111	5.0/111	5.0/111	4.9/109	4.8/107	4.8/107	--	4.6/102	4.6/102	4.7/104	--	4.9/109	--	4.8/107
D395C	4.2/100	4.2/100	4.2/100	4.2/100	4.2/100	4.0/95	--	4.0/95	4.0/95	4.0/95	4.0/95	--	4.2/100	--	4.1/98
D403B	4.6/100	4.8/104	4.7/102	4.6/100	4.6/100	4.4/96	--	4.3/94	4.4/96	4.3/94	--	--	4.5/98	4.4/96	
D410B	4.9/100	4.9/100	--	4.7/96	4.5/92	4.5/92	4.3/88	--	--	4.2/86	4.4/90	4.5/92	4.2/86	4.5/92	
Average Relative Efficiency		97	98	97	96	97	93	90	93	94	91	91	96	91	94

Table V. Actual and Relative Efficiencies of 1967 Cells on Dry Shelf Storage

Cell No.	Months																		
	0	2	4	6	8	10	12	14	16	18	20	22	24	26	28	30	32	34	36
D513E	5.1/100	5.1/100	4.8/94	4.8/94	--	4.7/92	--	4.5/88	--	4.6/90	--	4.5/88	--	4.6/90	--	4.7/92	4.5/88	4.8/96	4.6/90
D522E	4.7/100	4.8/102	4.5/96	4.5/96	4.7/100	4.5/96	--	4.4/93	--	4.4/93	--	4.3/91	--	4.4/93	4.6/98	4.6/98	4.4/93	4.7/100	4.4/93
D551E	5.0/100	4.7/94	4.7/94	4.8/96	4.5/90	--	4.5/90	--	4.5/90	--	4.4/88	--	4.6/92	4.8/96	4.7/94	4.4/88	4.7/94	4.5/90	
D521F	4.4/100	4.6/104	4.4/100	4.3/98	--	4.3/98	4.4/100	--	4.5/102	--	4.2/95	--	4.4/100	--	4.6/104	4.6/104	--	4.7/107	
D563A	4.8/100	4.6/96	4.6/92	--	4.5/94	--	4.4/92	--	4.4/92	--	4.2/88	--	4.4/92	4.6/96	--	4.3/90	4.6/96	--	
D579B	5.0/100	4.6/92	4.6/92	--	4.4/88	--	4.4/88	4.5/90	--	--	4.4/88	--	4.5/90	4.7/94	--	4.4/88	4.7/94	4.4/88	
D583C	5.0/100	4.7/94	4.6/92	--	4.4/88	--	4.5/90	--	4.5/90	--	4.6/97	--	4.6/97	4.8/96	--	4.5/90	4.9/98	4.6/92	
N14B2	5.1/100	4.8/94	4.7/92	--	4.6/90	--	4.5/88	--	4.6/90	--	4.6/90	--	4.6/90	4.8/96	--	4.4/86	4.9/96	4.6/96	
N20B1	5.1/100	4.8/94	4.7/92	5.1/100	4.6/90	--	4.6/90	--	4.6/90	4.6/90	--	--	4.6/90	4.8/94	--	4.5/88	4.9/96	4.6/90	
N3 BK4	4.2/100	4.1/98	4.0/95	4.2/100	3.8/91	--	3.8/91	--	3.7/88	--	3.6/86	--	--	3.8/93	3.8/91	4.0/95	3.9/93	3.8/91	
N35B3	5.0/100	5.0/100	4.9/98	4.5/90	4.5/90	4.5/90	--	4.9/98	--	4.7/94	--	4.8/96	--	5.1/102	4.7/93	5.0/100	4.8/96		
N44B3	4.8/100	4.4/92	4.2/87	3.8/79	3.8/79	4.1/85	--	4.0/83	--	3.9/81	--	3.6/75	--	3.8/79	3.8/79	3.9/81	3.9/81		
N64BK5	4.2/100	4.1/98	4.1/98	4.0/95	4.0/95	--	3.8/91	--	3.9/93	--	4.0/95	--	4.0/95	4.0/95	4.2/100	4.0/95	4.2/100	4.0/95	
N65BK5	4.2/100	4.2/100	4.0/95	4.1/98	4.1/98	--	3.9/93	--	3.9/93	--	--	4.2/100	4.1/98	4.2/100	4.3/102	4.0/95	4.3/102	4.0/95	
N85BK3	4.2/100	4.2/100	3.9/93	3.9/93	3.9/93	--	3.7/88	--	3.8/91	--	3.9/93	--	3.8/91	3.8/91	4.1/98	3.9/93	4.1/98	3.9/93	
N86C5	6.6/100	5.8/88	5.4/82	5.4/82	5.3/80	--	5.5/83	--	5.5/83	--	5.5/83	--	5.6/85	5.3/80	5.7/86	--	5.7/86	--	
N71AK2	4.1/100	4.0/98	3.9/95	3.9/95	3.9/95	--	3.7/90	--	3.7/90	--	3.9/90	--	--	3.7/90	4.0/98	3.8/93	3.7/90	4.0/98	3.8/93
N78AK5	5.0/100	4.5/90	4.3/86	4.3/86	4.1/82	--	4.0/80	--	4.0/80	--	4.2/84	--	4.2/84	4.2/84	4.4/88	4.3/86	4.2/84	4.4/88	4.3/86
N80AK6	4.3/100	4.0/93	3.9/91	3.8/88	3.9/91	--	3.6/84	--	3.6/84	--	--	3.8/88	3.7/86	3.7/86	--	3.9/91	3.8/88	3.7/86	3.7/86
N99AK5	4.8/100	4.6/96	4.5/93	4.3/90	--	4.3/90	--	4.4/92	--	4.5/93	--	4.4/92	4.4/92	4.7/98	4.4/92	4.4/92	4.4/92	4.4/92	
N99AK6	4.6/100	4.4/96	4.2/91	4.3/93	--	4.1/89	--	4.2/91	--	4.3/93	--	4.2/91	4.2/91	4.4/96	4.2/91	4.2/91	4.2/91	4.4/96	4.2/91
N99AK8	4.8/100	4.6/96	4.5/93	4.4/92	--	4.3/90	--	4.3/90	--	4.4/92	--	4.4/92	4.4/92	4.5/94	4.4/92	4.4/92	4.4/92	4.5/94	4.4/92
N99AK9	4.5/100	4.5/100	4.4/98	4.4/98	--	4.3/93	--	4.3/96	--	4.4/98	--	4.3/96	4.3/96	4.6/102	4.3/96				
Average Relative Efficiency		96	93	93	90	91	89	91	90	92	90	91	92	93	94	92	93	94	

Table VI. Actual and Relative Efficiencies of 1968 Cells on Dry Shelf Storage

Cell No.	Months												
	0	2	4	6	8	10	12	14	16	18	20	22	24
N127CK3	4. 1/100	4. 0/98	3. 9/95	3. 9/95	--	3. 8/93	3. 8/93	--	4. 1/100	4. 0/98	4. 0/98	4. 1/100	4. 1/100
N128AK1	4. 2/100	3. 9/93	3. 8/91	3. 8/91	--	3. 8/91	--	--	4. 0/95	3. 9/93	3. 8/91	4. 0/95	4. 0/95
N128AK4	4. 3/100	4. 1/95	4. 1/95	3. 9/91	--	--	--	--	4. 0/93	4. 0/93	4. 1/95	4. 2/98	4. 4/102
N163BK1	4. 0/100	4. 0/100	4. 0/100	3. 9/98	--	4. 0/100	--	4. 1/102	4. 1/102	4. 1/102	4. 0/100	4. 2/105	
N163BK5	4. 2/100	4. 0/95	4. 0/95	3. 9/93	--	4. 0/95	--	4. 2/100	4. 1/97	4. 1/97	4. 0/95	4. 3/102	
N163BK9	4. 0/100	3. 9/98	3. 9/98	3. 8/95	--	3. 9/98	--	4. 1/102	4. 0/100	3. 9/98	3. 8/95	4. 1/102	
N167CK2	4. 0/100	3. 9/98	3. 8/95	3. 7/93	--	3. 8/95	--	3. 9/98	3. 8/95	3. 8/95	3. 9/95	4. 0/100	
N185BK3	3. 8/100	3. 6/95	3. 5/92	--	3. 7/97	--	3. 8/100	--	3. 6/95	3. 7/97	3. 8/100	3. 7/97	
N186AK2	3. 8/100	3. 6/95	3. 5/92	3. 6/95	--	3. 7/97	3. 7/97	--	3. 8/100	3. 8/100	3. 9/102	3. 7/97	
N186BK4	3. 8/100	3. 6/95	3. 5/92	3. 6/95	--	3. 7/97	--	3. 8/100	3. 7/97	3. 8/100	3. 9/102	3. 7/97	
N186BK7	3. 9/100	3. 6/92	3. 6/92	3. 6/92	--	3. 7/95	--	3. 8/98	3. 8/98	3. 8/98	3. 9/100	3. 7/95	
N190BK4	4. 3/100	4. 2/98	4. 2/98	--	4. 2/98	--	4. 3/100	--	4. 3/100	4. 3/100	4. 4/102	4. 3/100	
N196CK4	4. 0/100	3. 7/92	3. 7/92	--	3. 7/92	--	3. 8/95	--	3. 8/95	--	3. 9/98	3. 8/95	
N197AK1	4. 0/100	3. 8/95	3. 7/92	--	3. 7/92	--	3. 8/95	--	3. 8/95	3. 7/92	3. 9/98	3. 8/95	
N202BK9	4. 1/100	4. 0/98	3. 9/95	--	3. 9/95	--	4. 1/100	--	4. 0/98	3. 9/95	4. 1/100	4. 0/98	
N263AK7	3. 8/100	3. 5/92	3. 5/92	--	--	3. 6/95	--	3. 5/92	--	3. 6/95	3. 5/92		
N263CK8	3. 8/100	3. 6/95	3. 6/95	--	--	3. 7/97	--	3. 7/97	--	3. 8/100	3. 7/97		
N264BK6	4. 0/100	3. 7/93	3. 6/90	--	--	3. 8/95	--	3. 7/93	--	3. 8/95	3. 7/93		
N266AK1	4. 0/100	3. 8/95	3. 7/93	--	--	4. 0/100	--	3. 9/98	3. 9/98	3. 9/98	3. 8/95		
N279BK4	3. 8/100	3. 8/100	3. 9/103	--	3. 7/97	--	3. 8/100	--	3. 8/100	3. 9/103	3. 9/103		
N280AK1	3. 7/100	3. 5/95	3. 8/103	--	3. 9/105	--	3. 8/103	--	3. 7/100	3. 8/103	3. 8/103		
N280AK8	3. 8/100	3. 8/100	3. 8/100	--	3. 9/103	--	3. 8/100	--	3. 8/100	3. 9/103	3. 9/103		
N280AK3	3. 7/100	3. 7/100	3. 8/103	--	3. 8/103	--	3. 7/100	--	3. 8/103	3. 8/103	3. 7/100		
N289CK6	4. 1/100	4. 0/98	4. 1/100	4. 1/100	--	4. 1/100	4. 1/100	4. 1/100	4. 2/102	4. 1/100			
N290AK3	4. 1/100	4. 0/98	4. 1/100	4. 1/100	--	4. 0/98	4. 1/100	4. 1/100	4. 2/102	4. 1/100			
N291BK1	4. 1/100	4. 0/98	4. 1/100	4. 1/100	--	4. 0/98	4. 1/100	4. 1/100	--	4. 1/100			
N292AK2	4. 1/100	3. 9/95	4. 0/98	4. 0/98	--	3. 9/95	4. 0/98	4. 0/98	--	4. 1/100			
N300CK6	3. 9/100	3. 8/98	3. 9/100	--	3. 9/100	--	3. 9/100	4. 2/108	4. 1/105	3. 9/100			
N300CK9	3. 9/100	3. 8/98	3. 9/100	--	3. 8/98	--	3. 8/98	4. 0/103	4. 0/103	3. 9/100			
N301AK3	3. 9/100	4. 0/103	4. 0/103	--	3. 9/100	--	3. 9/100	4. 0/103	4. 0/103	4. 0/103			
N301BK5	3. 9/100	3. 8/98	3. 8/98	--	3. 8/98	--	3. 8/98	3. 9/100	4. 0/103	3. 8/98			
N308CK9	3. 9/100	3. 8/98	3. 8/98	4. 0/103	--	3. 9/100	3. 9/100	4. 0/103	3. 9/100				
N309AK1	3. 8/100	3. 8/100	3. 7/97	3. 8/100	--	3. 8/100	3. 8/100	--	3. 8/100				
N313AK4	4. 0/100	3. 8/95	3. 8/95	3. 9/98	--	3. 8/95	3. 9/98	--	3. 8/95				
N314CK8	4. 0/100	3. 9/98	3. 9/98	3. 8/95	--	4. 0/100	3. 9/98	--	3. 9/98				
N326BK8	4. 2/100	4. 2/100	4. 3/102	4. 3/102	4. 3/102	4. 2/100	4. 2/100	4. 4/105	4. 2/100				
N326CK5	4. 2/100	4. 3/102	4. 4/105	4. 4/105	--	4. 3/102	4. 3/102	4. 5/107	4. 4/105				
N327BK7	4. 1/100	4. 1/100	4. 1/100	4. 1/100	--	4. 1/100	4. 1/100	4. 3/105	4. 1/100				
N327CK3	4. 2/100	4. 2/100	4. 3/102	4. 2/100	--	4. 2/100	4. 2/100	4. 4/105	4. 3/102				
N348AK6	4. 0/100	3. 9/98	4. 0/100	--	3. 9/98	--	4. 1/102	4. 1/102	3. 9/98				
N348CK1	4. 1/100	4. 1/100	4. 2/102	--	4. 2/102	4. 1/100	4. 3/105	4. 3/105	4. 2/102				
N349CK2	4. 0/100	4. 0/100	4. 0/100	--	4. 0/100	4. 0/100	4. 2/105	4. 1/102	3. 9/98				
N350BK4	4. 1/100	4. 0/98	4. 1/100	--	3. 4/83	3. 4/83	3. 5/86	4. 1/100	4. 0/98				
Average Relative Efficiency			97	97	98	97	99	101	99	99	98	99	99

Table VII. Actual and Relative Efficiencies of 1969 Cells on Dry Shelf Storage Months

Cell No.	0	1	2	3	4	5	6	7
7264	3.2/100	3.3/103	3.2/100	3.2/100	3.2/100	3.2/100	3.3/103	3.3/103
7265	3.2/100	3.2/100	3.2/100	3.2/100	3.2/100	3.1/97	3.1/97	3.2/100
30546	3.5/100	3.5/100	3.5/100	3.6/103	3.6/103			
30862	3.7/100	3.7/100	3.6/97	3.7/100	3.7/100	3.7/100	3.8/103	
51542	3.5/100	3.5/100	3.5/100	3.6/103				
51545	3.6/100	3.6/100	3.6/100	3.7/103				
76868	3.4/100	3.3/97	3.4/100	3.5/103				
86764	3.5/100	3.4/97	3.4/97	3.6/103				
98654	3.0/100	3.2/107	3.2/107					
98652	3.2/100	3.2/100	3.2/100					
98566	3.0/100	3.0/100	3.1/103					
105651	3.1/100	3.1/100	3.2/103					
132262E	2.8/100	3.0/107						
135256F	3.0/100	3.1/103						
Average Relative Efficiency		101	101	102	101			

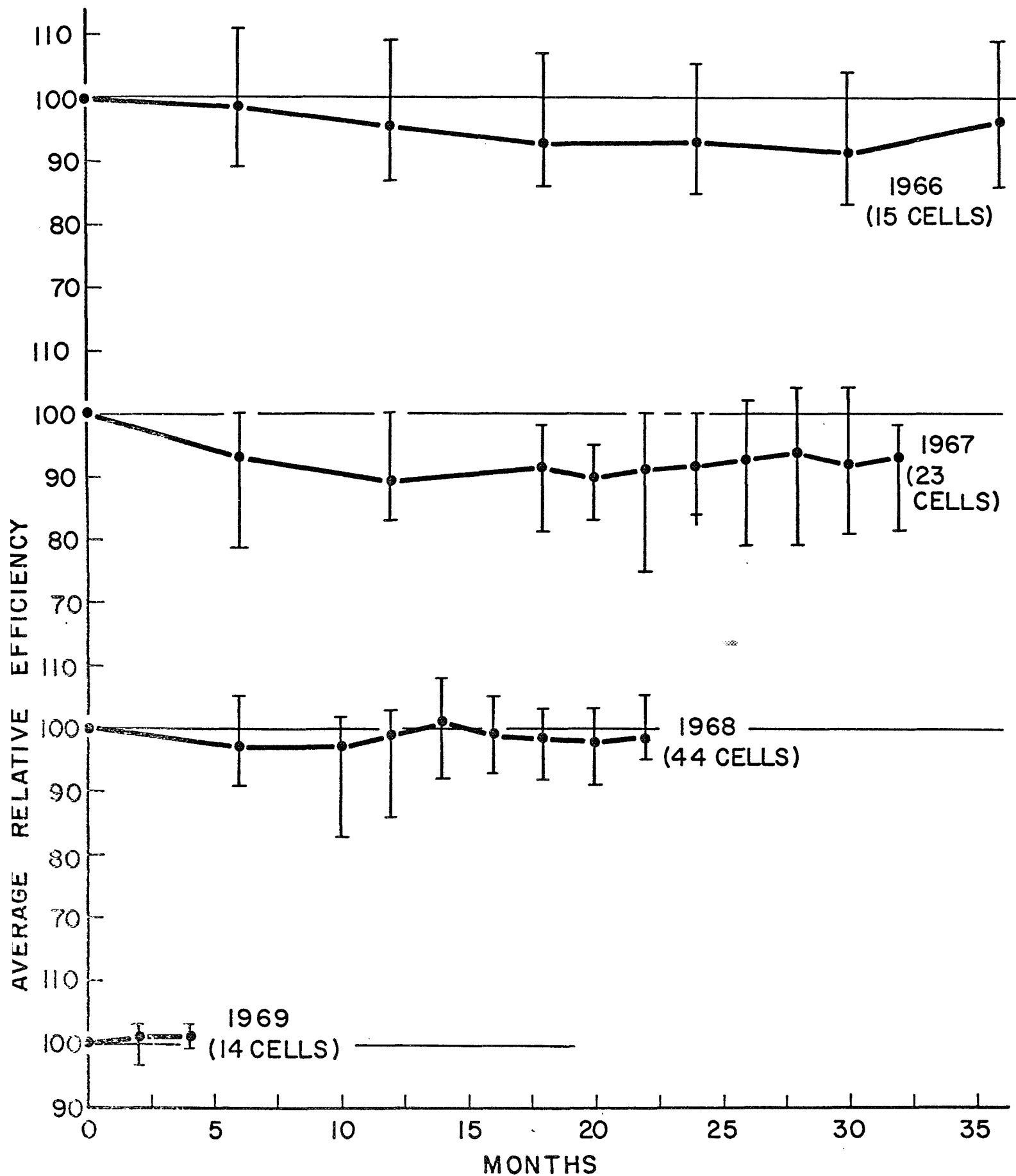


FIG. 5: AVERAGE RELATIVE EFFICIENCY ON DRY SHELF STORAGE.

Cells D385B and D410B show that the decrease in relative efficiency is almost numerically equal to the decrease in relative SCC for the case where the fill remained relatively constant. Cells D296B and D391B show both mechanisms in effect, a loss of SCC and an increase in fill, but the loss in efficiency is less than the loss in SCC.

Loss of SCC with no corresponding loss in fill can be caused by a decrease in area or a decrease in light transmission. Since these early cells were all covered with Mylar it is tempting to conclude that the loss of SCC was due primarily by a loss of transmission in the Mylar, which is known to be somewhat susceptible to aging. However, the cells fabricated in 1967, Table V, half of which were Mylar and half Kapton covered, showed no essential improvement in degradation rate. In fact a comparison of efficiencies between Mylar and Kapton covered cells fabricated during 1967, Table IX, shows no significant difference. Numbers in parenthesis indicate the number of cells in the averages. Hence if the loss of SCC is actually caused by a loss in transmission in the cover plastic then these data indicate that Kapton and Mylar lose their transmission at almost equal rates. Or, another, as yet unknown, mechanism may be responsible for this decrease in SCC. Loss of area is difficult to reconcile with the observed data.

Table V and Fig. 5 shows that cells fabricated during 1967 did not perform as well as did the 1966 cells. This was probably caused by the fact that during early 1967 the transition to 100 cells per day pilot line production was started. Although none of the fabrication steps was changed in concept, they were changed to handle larger numbers of cells. Such changes in fabrication steps have always been followed by periods of readjustment during which cell performance was usually quite poor before returning to previous levels.

The 1967 cells showed much the same patterns that the 1966 cells did with the exception that a decreasing fill was now present. Increasing fills as well as constant fills were also present. This is shown in Table X.

Again, if the fill remained constant the loss in relative efficiency was numerically equal to the loss in relative SCC. This is shown by cells N78AK5 and N14B2. Cells N44B3 and N31BK4 show that if the fill decreases the loss in relative efficiency is greater than the loss in relative SCC. Cells N35B3 and N86C5 show that if the fill increases the loss in relative efficiency is not as great as the loss in relative SCC.

Table VI shows the actual and relative efficiencies of the 1968 cells. It appears that there is no serious degradation problem with these cells on dry shelf storage.

Table VII shows the results of the cells fabricated during 1969. Obviously it is too soon to remark on their stability, but the short term data indicate no problems as yet.

Table VIII. Comparison of Initial and 42-Month Performance of Representative Cells From 1966 on Dry Shelf Storage.

Cell No.	Initial Eff. %	Final Eff. %	$\frac{\text{Eff}_F}{\text{Eff}_I} \times 100$	Initial SCC mA	Final SCC mA	$\frac{\text{SCC}_F}{\text{SCC}_I} \times 100$	Initial Fill %	Final Fill %	$\frac{\text{Fill}_F}{\text{Fill}_I} \times 100$
D385B	5.0	4.8	96%	965	921	96%	60.0	61	102%
D410B	4.9	4.3	88	845	754	89	67.3	67	100
D296B	4.9	4.1	84	921	745	81	62.4	66	106
D391B	4.5	4.8	107	880	840	95	62.0	66	107

Table IX. Comparison of Average Relative Efficiencies of Mylar and Kapton Covered Cells from 1967 Dry Shelf Storage Test.

	6 Mo.	12 Mo.	20 Mo.	26 Mo.
Mylar	91.9% (8)	90.1 (8)	89.9 (7)	92.4 (11)
Kapton	93.4 (11)	88.1 (7)	89.6 (7)	93.5 (11)

Table X. Comparison of Initial and Final Performance of Representative 1967 Cells on Dry Shelf Storage (28 to 34 Months)

	Eff. Initial	Eff. Final	Relative Eff.	SCC Initial	SCC Final	Relative SCC	Fill Initial	Fill Final	Relative Fill
N35B3	5.0	4.8	96%	840	786	94%	68.2	69.9	102%
N86C5	6.6	5.4	84	1100	908	83	67.5	69.8	103
N78AK5	5.0	4.3	86	857	740	86	65.2	65.5	100
N14B2	5.1	4.6	90	886	799	90	66.6	66.1	100
N44B3	4.8	3.9	81	892	824	92	61.3	56.4	92
N31BK4	4.2	3.8	91	700	660	94	69.4	67.6	98

Moisture Storage

Cells on the moisture storage test are kept at room temperature and pressure and at a relative humidity of 80%. Tables XI through XIV show the actual and relative efficiencies of cells according to year of manufacture. Figure 6 shows plots of average relative efficiencies, also according to year of manufacture.

The type of degradation seen on the moisture test, strangely enough, is quite similar to that seen on the dry shelf storage, except that the rates are greater. All of the moisture degradation is accompanied by a corresponding loss in SCC in those cases where the fill remained constant. The largest decreases were registered by those cells whose fills also decreased. There was also some loss in OCV in some of the cells but it could not be correlated with the variation in fill. Table XV again shows how the variation in relative efficiency can be numerically equal to the variation in relative SCC when the fill remains fairly constant.

Table XV. Comparison of Initial and 40 Month Performance of 1966 Cells on Moisture Storage

Cell No.	Eff. Initial	Eff. Final	Eff. Relative	SCC Initial	SCC Final	SCC Relative	Fill Initial	Fill Final	Fill Relative
D350F	4.7	4.0	85 %	988	718	73%	55.0	63.7	115%
D357E	5.2	3.9	75	860	642	75	67.0	67.9	101
D401B	5.0	3.6	69	885	715	81	69.1	59.4	86

Cell D357E which had practically no change in fill shows a decrease in efficiency that is numerically equal to the decrease in SCC. Cell D350F, whose fill increased, showed a decrease in efficiency that was much less than its decrease in SCC; while Cell D401B, whose fill decreased, showed an efficiency decrease that was greater than its loss in relative SCC.

The 1966 cells and most of the 1967 cells are Mylar covered, but again it appears that there is little difference attributable to the type of cover plastic. Hence, it appears that there are two separate mechanisms affecting both dry and moisture storage degradation. The one mechanism, loss in SCC, appears to be present in all cells, while the second one, which affects the fill, is more difficult to characterize because its effects are variable. The first one has been associated with a loss of area or loss of transmission, but thus far has eluded a more precise definition. There are a number of reasons that could cause the observed variation in fill, but they all concern themselves with effects on either the series or shunt resistance. Unfortunately, the observed variations in fill do not neatly fall into one or the other category, so a more precise definition of this failure mechanism isn't possible at this time.

Table XI. 66 Cells on Long Term Moisture Testing -- All are Mylar Covered -- AM1 Efficiencies

	0	4	8	12	16	20	24	28	32	36	40	44
D187B*	6.2/100	6.1/99	5.3/86	5.3/86	5.2/83	5.1/82	5.0/81	4.8/78	5.0/81	4.9/79	4.9/79	4.7/76
D297C	5.1/100	4.2/82	4.4/86	4.3/84	4.3/84	4.0/78	4.0/78	3.8/75	3.8/75	3.8/75	3.8/75	3.8/75
D348C	5.4/100	4.4/82	4.2/82	4.4/82	4.6/85	4.1/76	4.0/74	4.0/74	4.0/74	4.0/74	4.0/74	4.0/74
D350C	4.3/100	4.4/102	4.4/102	4.1/95	3.7/86	3.7/86	3.7/86	3.6/84	3.3/77	3.5/81	3.3/77	
D350F	4.7/100	3.9/83	3.7/79	4.2/89	4.3/92	3.8/81	3.7/79	3.7/79	3.8/81	3.8/81	4.0/85	4.3/92
D357E	5.2/100	4.3/83	4.3/83	4.3/83	4.0/77	3.9/75	3.8/73	3.8/73	3.8/73	3.7/71	3/5/67	3.7/71
D372A	4.5/100	4.3/96	4.0/89	4.0/89	3.8/85	3.6/80	3.7/82	3.7/82	3.7/82	3.7/82	3.5/78	
D401B	5.2/100	5.0/96	4.7/90	4.8/92	4.2/81	4.0/77	3.8/73	3.8/73	3.6/69	3.5/67	3.6/70	
D405A	4.8/100	4.5/93	4.3/90	4.4/92	4.1/85	--	3.9/81	3.9/81	3.9/81	3.7/77	3.8/79	
D411F	4.6/100	4.3/94	4.2/91	4.3/94	4.0/87	3.9/85	3.8/83	3.7/81	3.7/81	3.2/70	3.8/83	
D424E	5.6/100	5.3/95	5.3/95	5.1/91	4.7/84	--	4.4/79	--	4.5/80	4.2/75	4.4/79	
Average Relative Efficiency		91	89	89	85	80	79	78	78	76	77	77

* Cu Foil Substrate.

Table XII. 67 Cells on Long Term Moisture Testing

	0	2	4	6	8	10	12	14	16	18	20	22	24	26	28	30	32	34	36
D436E	5.0/100	4.6/92	4.5/90	4.3/86	4.2/84	--	4.0/80	4.0/80	--	--	3.7/74	--	3.5/70	3.7/74	--	3.7/74	3.5/70	--	3.7/74
D454A	4.9/100	4.4/90	4.2/86	--	3.9/80	--	3.5/71	--	3.4/69	3.4/69	--	--	3.4/69	--	3.5/71	3.5/71	3.2/65	3.3/67	3.2/65
D376A	4.9/100	4.7/96	4.6/94	4.5/92	4.1/84	--	4.3/88	4.2/86	4.2/86	4.1/84	--	4.0/82	--	--	4.1/84	4.2/86	3.9/80	4.1/84	4.1/84
D480B	4.8/100	4.5/94	4.4/92	4.3/90	4.1/86	--	4.0/82	--	--	3.7/77	--	--	3.6/75	3.5/75	--	3.6/75	3.3/69	3.5/73	3.4/71
D485A	5.0/100	4.7/94	4.5/90	4.5/90	4.5/90	--	4.2/83	4.1/82	4.1/82	--	4.0/80	--	4.0/80	--	4.0/80	4.0/80	3.7/74	3.9/78	3.9/78
D487C	5.2/100	5.0/96	4.9/94	4.8/92	4.9/94	--	4.5/87	--	4.5/87	--	4.5/87	--	4.4/85	--	4.4/85	4.4/85	4.1/79	--	4.5/87
D506B	5.4/100	5.3/98	4.9/91	4.7/87	4.9/91	4.5/83	4.4/82	4.4/82	--	4.4/82	--	4.4/82	--	4.4/82	--	4.3/80	4.1/76	4.3/80	
D509E	5.1/100	4.8/94	4.4/86	4.3/84	4.4/86	4.0/79	3.8/75	3.7/73	--	3.7/73	--	3.7/73	3.6/71	--	3.2/63	3.2/63	3.1/61	3.1/61	
D516D	5. /100	4.9/98	4.4/88	4.3/86	4.5/90	4.1/82	4.0/80	4.0/80	--	3.8/76	--	3.8/76	--	3.8/76	--	3.7/74	3.5/70	3.5/70	
D526C	4.3/100	4.3/100	3.8/88	3.8/88	4.0/93	3.7/86	3.6/84	3.6/84	--	3.4/79	--	3.3/77	--	--	--	3.3/77	3.1/72	3.2/74	
D554A	5.3/100	5.0/94	5.0/94	--	4.5/85	4.5/85	4.3/81	--	4.3/81	4.3/81	--	4.2/79	--	4.2/79	4.0/76	--	4.0/76		
D580E	4.7/100	4.0/85	3.9/83	4.1/87	3.7/79	3.6/77	3.6/77	--	3.6/77	--	3.6/77	--	3.6/77	--	3.5/75	3.5/75	3.5/75		
D585C	5.3/100	4.7/89	4.5/85	4.7/88	4.2/79	4.0/76	3.9/74	--	3.6/68	--	3.3/62	--	2.8/53	--	2.5/47	2.3/43	2.2/42		
N14B8	4.9/100	4.7/96	4.7/96	5.0/102	4.5/92	4.5/92	4.4/90	--	4.4/90	--	4.4/90	--	4.3/88	--	4.3/88	4.3/88	4.3/88		
N17B3	4.9/100	4.2/86	4.1/84	4.1/84	3.6/74	3.5/72	3.2/65	--	3.1/63	--	2.8/57	--	2.7/55	--	2.6/53	2.5/51	2.5/21		
D615C	5.3/100	4.8/91	4.8/91	--	4.4/83	4.2/79	3.8/72	--	4.1/77	--	4.1/77	--	3.9/74	3.9/74	3.8/72	--	3.7/70		
N38B7	4.4/100	4.1/93	3.9/89	--	3.6/82	3.6/82	3.2/73	--	3.1/73	--	3.0/68	--	3.0/68	--	2.6/59	--	2.6/59		
N51B8	5.3/100	4.9/93	4.8/91	--	4.2/79	4.0/76	3.7/70	--	3.9/74	--	3.7/70	--	3.4/64	--	3.3/62	--	3.3/62		
N52B4	4.9/100	4.8/98	4.6/94	--	3.7/76	3.5/72	3.3/67	3.5/72	--	--	3.5/72	--	3.3/67	3.4/69	3.1/63	--	3.2/65		
D639CK	4.6/100	--	--	3.8/83	3.7/81	3.6/78	3.4/74	--	3.4/74	--	3.3/72	--	3.3/72	3.3/72	3.3/72	3.0/65			
N72B5	5.4/100	5.8/107	5.3/98	5.0/93	--	5.3/98	--	--	4.7/87	--	4.7/87	--	4.7/87	4.5/83	4.7/87	--			
NH194CK9	3.9/100	3.5/90	3.4/87	3.2/82	3.1/80	3.0/77	3.2/82	--	--	3.1/80	--	3.2/82	3.1/80	3.1/80					
N97BK2	4.7/100	4.1/87	4.5/96	3.9/83	3.8/83	3.6/77	3.7/79	--	3.7/79	--	3.7/79	3.5/75	--	3.5/75					
N99BK3	4.7/100	4.5/96	4.2/89	4.0/85	3.9/83	3.8/81	3.8/81	--	3.9/83	3.8/81	--	3.8/81	3.7/79	3.8/81					
N99BK5	4.9/100	4.7/96	4.3/88	4.0/82	3.9/80	3.9/80	4.0/82	--	--	4.0/82	4.0/82	3.9/80	--	3.8/78					
Average Relative Efficiency				88			79		78		76		73		71				

Table XIV. Actual and Relative Efficiencies of 1969 Cells on Moisture Storage
Months

Cell No.	0	1	2	3	4	5	6	7	8	9	10
N400AK3	3.6/100	3.6/100	3.5/ 97	3.5/ 97	--	--	3.4/95	3.4/95	--	3.3/92	3.2/89
20362	3.3/100	3.2/ 97	3.2/ 97	3.2/ 97	--	--	3.1/ 93	3.1/93	--	3.0/91	3.0/91
30542	3.6/100	3.4/ 94	3.4/ 94	--	--	3.2/89	3.3/92	--	3.2/89	3.1/86	--
32851	3.2/100	3.2/100	3.2/100	--	--	3.1/97	3.1/97	--	3.1/97	3.1/97	--
40665	3.6/100	3.5/ 97	3.5/ 97	3.6/100	--	3.5/97	3.5/97	--	--	--	--
44346	3.7/100	3.6/ 97	3.6/ 97	3.7/100	--	3.6/97	3.5/95	--	--	--	--
76861	3.5/100	3.4/ 97	3.3/ 94	3.4/ 97	--	3.5/97	3.3/94	--	--	--	--
98658	3.3/100	3.4/103	3.4/103	--	3.0/91	3.0/91	--	--	--	--	--
98659	3.3/100	3.1/ 94	3.2/ 97	--	3.2/97	3.1/94	--	--	--	--	--
105652	3.2/100	3.1/ 97	3.1/ 99	--	3.0/94	2.9/91	--	--	--	--	--
105654	3.2/100	2.9/ 91	2.9/ 91	--	2.8/88	2.7/85	--	--	--	--	--
134762E	2.9/100	2.9/100	--	2.9/100	2.8/ 97	--	--	--	--	--	--
134765E	2.9/100	2.9/100	--	2.8/ 97	2.8/97	--	--	--	--	--	--
Average Relative Efficiency			97	98	94	94	95				

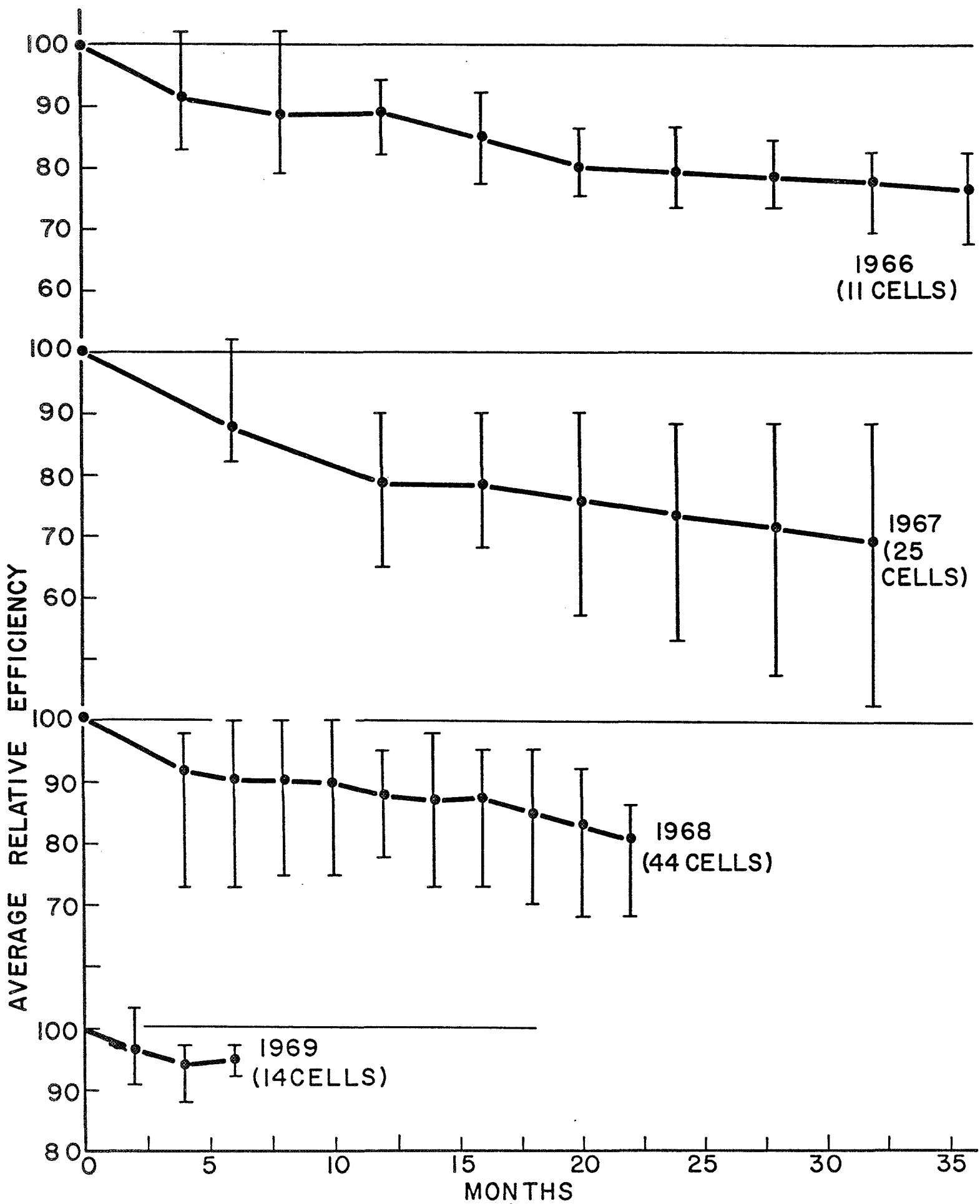


FIG. 6: AVERAGE RELATIVE EFFICIENCY ON MOISTURE STORAGE.

The simple fact that exposure to water vapor resulted in a greater degree of degradation than exposure to the desiccated atmosphere suggests that water vapor by itself can cause degradation. In a previous cell design, in which the grid was kept in pressure contact with the barrier layer simply by the cover plastic-barrier layer bond, degradation by exposure to high humidity conditions was a common failure mechanism. It was shown later that the cover plastic bond was moisture sensitive and exposure to water vapor resulted in a weakening of the bond which loosened the grid contact and raised the series resistance. Ordinarily, subjecting the cell to the same laminating conditions that were used initially to attach the cover plastic was sufficient to restore the bond and cell performance to their initial states.

A number of cells on moisture test which had degraded to below 75% of their initial efficiencies were removed from the test to determine if any similar recovery tendencies were present. Four of the cells were put through a 180°C lamination cycle for 10 minutes at 100 psi which was initially used to bond the cover plastic epoxy to the barrier during cell fabrication. The cells were also given a 15 hour vacuum bake at 135°C after laminating, a step also used during cell fabrication. Table XVI shows the results.

Table XVI. Effect of Laminating and 15 Hour 135° C Vacuum Bake on Moisture Degraded Cells

Cell No.	OCV mV	SCC mA	MP mW	Fill %	Eff. %	
D385C	400	498	112	56.5	2.05 (A)	Initial Perf.
	420	665	153	54.9	2.80 (B)	After Lamination
	382	610	82	35.0	1.49 (C)	After Vacuum Bake
N38B-7	450	600	146	54.1	2.66 (A)	
	455	690	180	57.4	3.29 (B)	
	425	630	99	36.8	1.80 (C)	
D454A	435	620	176	65.2	3.20 (A)	
	430	748	211	65.6	3.85 (B)	
	440	690	197	64.9	3.60 (C)	
D357E	478	646	205	66.5	3.74 (A)	
	465	610	191	67.5	3.49 (B)	
	470	600	187	66.3	3.41 (C)	

There was a noticeable improvement in 3 of the 4 cells as a result of the lamination but a decrease in the fourth cell. Of the cells that improved the major change was an increase in SCC, but significantly, there was no major change in fill. If the main effect of the lamination was to improve the gold epoxy bond it wasn't apparent from these data. The fact that all cells decreased in performance after the vacuum bake was another indication that the effect of the laminating cycle was not permanent but only temporary.

Another group of four cells that had degraded on moisture testing was put directly into the vacuum bake. The purpose was to determine if the 15 hour vacuum heat treatment without the lamination cycle would improve the cells. Table XVII shows the results.

Table XVII. Effect of 15 Hour 135° C Vacuum Bake on Moisture Degraded Cells

Cell No.	OCV mV	SCC mA	MP mW	Fill %	Eff. %		
N17B3	426	525	130	58.2	2.40	(A)	After removal from test. After bake.
	425	495	112	53.2	2.04	(B)	
	414	495	93	45	1.7	(C)	Taken in immediate succession
	352	490	44	25	0.8	(D)	
D509E	465	598	177	63.6	3.2	(A)	
	450	570	145	56.5	2.7	(B)	
	430	570	105	43.0	1.9	(C)	
N52B4	455	628	169	59.3	3.1	(A)	
	385	600	66	28	1.2	(B)	
	360	600	58	27	1.1	(C)	
D480B	480	605	191	65.9	3.5	(A)	
	475	640	196	64.6	3.6	(B)	

Again in 3 of the 4 cells the effect of the vacuum bake was a large decrease in cell performance, which again, is probably an indication of the unstable nature of moisture degraded cells. In fact, successive curves taken after the bake show an even more rapid deterioration of cell performance than before baking.

Why should the vacuum bake add to the woes of these already badly deteriorated cells? Two such bakes are part of the standard process that is used in the manufacture of the cells initially, so they should be able to withstand this treatment easily. Also, this bake is usually quite effective in restoring cell performance lost as a result of degradation. The data show no specific pattern other than a general deterioration of practically all cell parameters. Hence, it appears that after moisture degradation these cells are beyond recovery but the actual degradation mechanism escapes identification.

Figure 6 shows that the average performance of the 1967 cells is somewhat worse than the 1966 cells, probably for the reasons listed before. The 1968 cells show an improvement over both previous years' cells, probably because most of the earlier difficulties were gradually being eliminated. Again, the 1969 cells have not been on test long enough to conclude anything about their performance.

100° C Vacuum Storage

Cells on the 100° C vacuum storage test are kept in a heated vacuum system maintained at a pressure of 10^{-5} Torr by an oil diffusion pump and a liquid nitrogen trap. Each month the system is cooled down and opened up to allow the cells to be tested and to enter new cells on test. There is no in situ testing.

Tables XVIII through XX show the actual and relative efficiencies of cells manufactured by year from 1966 to 1969. Figure 7 shows the plots of the average relative efficiencies also by year. 1966 and 1967 cells are averaged together since there were only 5 of the 1966 cells that survived this long.

This test is the most severe of the three tests and as a result cell response shows the greatest variation. This is shown in Fig. 7 by the extreme width of the error bars, which indicates that cell performance ranged between almost complete failure to only a slight degradation. However, the important conclusion here is that the best performance observed, even if it occurs only in a single cell, represents the limit of any intrinsic degradation that may be present in the thin film solar cell. Hence, in Fig. 7, the upper limit of the error bars is of as much significance as are the averaged data points themselves. For example, we can see that after 24 months in 100° C vacuum storage the average cell performance is at 60.8% of its initial value, while the best performance, registered by Cell D586B, is at 98% of its initial performance.

An indication of the mechanism responsible for heat degradation has been given by Shiozawa.⁽³⁾ During barrier layer formation copper from the newly formed Cu_2S layer is assumed to diffuse into the CdS layer, resulting in a very thin copper-compensated photoconductive insulating layer. The presence of this layer appears necessary for efficient operation of the cell. The most efficient cell operation calls for an optimum thickness of this insulating layer and the proposed mechanism of high temperature degradation is a thickening of this layer caused by the continued diffusion of copper. An increased thickness of this insulating layer should appear as an increased series resistance of the cell, and indeed, this is actually what is observed during the various stages of high temperature degradation. Similar performance has been observed by the deliberate introduction of external resistance in series with the cell.

The first indications of high temperature degradation are a decreased fill and efficiency as a result of the series resistance increase. As the I-V curve continues to flatten out a point is reached where the SCC begins

⁽³⁾ARL 69-0155, Final Report on Contract AF33(615)-5224 (Oct. 1969).

Table XVIII. Relative and Actual Efficiencies of 1966 and 1967 Cells on 100°C Vacuum Storage

Cell No.	Months												
	0	3	6	9	12	15	18	21	24	27	30	33	36
D379E	5. 1/100	5. 0/98	4. 9/96	4. 5/88	4. 0/78	3. 4/67	--	2. 6/51	--	--	1. 5/30		
D388F	4. 8/100	4. 9/102	4. 5/94	4. 2/88	3. 9/81	3. 6/75	--	3. 3/69	--	2. 8/58	--	2. 6/54	2. 4/50
D392A	5. 1/100	5. 1/100	4. 7/92	4. 4/86	4. 1/80	3. 6/71	--	3. 4/67	--	2. 7/53	--	0. 8/15	
D401F	4. 5/100	4. 7/104	4. 5/100	4. 0/89	4. 0/89	3. 6/80	--	3. 6/80	--	2. 3/51	--	0. 7/15	
D407D	4. 9/100	2. 5/51	4. 0/82	4. 0/82	3. 3/67	3. 2/65	2. 8/57	--	--	2. 5/51	2. 2/45	2. 3/47	
D412F	4. 1/100	4. 4/107	4. 4/107	3. 9/95	3. 9/95	3. 8/93	--	--	3. 6/88	3. 3/81	3. 1/76	2. 4/59	2. 5/61
D438D	5. 6/100	5. 6/100	4. 8/86	4. 6/82	4. 3/77	3. 9/70	3. 3/59	--	2. 2/39	1. 5/27	--	1. 0/18	
D462E	6. 1/100	5. 7/94	5. 3/87	5. 2/85	5. 1/84	5. 2/85	4. 8/79	--	4. 7/77	4. 5/74	4. 6/75	4. 2/69	4. 5/74
D504E	5. 5/100	5. 5/100	4. 8/87	4. 6/84	4. 0/73	3. 9/71	--	2. 5/46	--	1. 4/25	1. 4/25	1. 0/18	
D514E	4. 9/100	4. 6/94	4. 0/82	3. 9/80	3. 4/70	3. 4/70	--	1. 5/31	--	0. 6/12	1. 5/31		
D554E	5. 2/100	4. 9/94	4. 9/94	4. 6/89	4. 1/79	3. 5/67	--	2. 7/52	2. 4/46	2. 0/38			
D579E	4. 6/100	4. 5/98	4. 3/94	4. 2/91	3. 1/89	4. 0/87	--	1. 7/37	1. 9/41	1. 0/22			
D586B	5. 0/100	4. 9/98	4. 8/96	4. 5/90	4. 6/92	4. 5/90	--	4. 9/98	4. 9/98	4. 3/84	4. 1/82		
H107B8	5. 0/100	5. 2/104	5. 1/102	5. 0/100	4. 5/90	--	5. 0/100	4. 8/96	4. 7/94	4. 6/92			
H108A4	5. 0/100	5. 3/106	4. 7/94	5. 0/100	4. 4/88	--	4. 6/92	4. 4/88	4. 1/82	4. 2/84			
H108B5	5. 1/100	5. 0/98	5. 0/98	5. 0/98	4. 7/92	--	4. 7/92	4. 7/92	4. 3/84	4. 3/84			
N74B8	5. 1/100	4. 6/90	4. 5/88	3. 5/69	--	3. 3/65	3. 1/61	2. 6/51	2. 7/53				
N85BK7	4. 5/100	4. 5/100	4. 0/89	4. 0/89	3. 4/76	--	3. 2/71	2. 8/62	3. 0/67	2. 9/65			
N98BK4	4. 9/100	4. 8/98	4. 3/88	3. 4/70	--	2. 5/51	1. 5/31	1. 7/35	1. 5/31				
N98BK5	5. 0/100	4. 6/93	4. 5/90	3. 7/74	--	2. 6/52	1. 8/36	--	1. 5/30				
N99BK4	4. 7/100	4. 5/96	4. 3/92	3. 2/68	--	2. 0/43	1. 5/32	--	1. 0/21				
Average Relative Efficiency		96	92	86	82	71	65	64	61	56	52		

Table XIX. Actual and Relative Efficiencies of 1968 Cells on 100°C Vacuum Storage

Cell No.	Months											
	0	2	4	6	8	10	12	14	16	18	20	22
D111AK2	4.0/100	3.7/91	3.3/81	2.3/56	2.5/61	2.5/61	2.2/54	--	2.4/59	2.4/59	2.7/66	2.1/52
D112AK5	4.2/100	4.3/102	4.2/100	4.0/95	4.0/95	4.0/95	4.1/98	--	3.9/93	4.1/98	4.0/95	3.9/93
D113CK8	4.2/100	4.2/100	4.1/98	3.7/88	3.7/88	3.8/91	3.8/91	--	3.5/83	3.6/86	3.7/88	3.4/81
N116AK8	4.5/100	4.6/101	4.5/100	4.3/96	4.4/98	4.5/100	4.4/98	--	4.2/93	4.4/98	4.3/96	4.3/96
N127BK2	4.4/100	4.5/101	4.4/100	4.0/91	4.0/91	4.0/91	4.0/91	3.3/75	3.3/75	3.4/77	3.3/75	3.3/75
N128BK5	4.8/100	4.6/96	4.5/94	4.5/94	3.8/79	3.8/79	3.5/73	2.9/60	2.9/60	2.8/58	2.7/56	2.6/54
N128BK6	4.4/100	4.2/96	4.1/93	3.8/86	3.8/86	3.8/86	3.9/89	3.6/82	3.5/80	3.6/82	3.7/84	3.5/80
N163BK3	4.0/100	3.8/95	3.4/85	3.4/85	3.3/83	3.2/80	--	2.8/70	2.5/62	2.7/67	2.5/62	
N163BK8	4.1/100	4.0/98	3.9/95	3.9/95	3.9/95	3.95/95	--	3.5/85	3.2/78	3.4/83	3.2/78	
N164AK2	4.2/100	4.0/95	4.0/95	4.0/95	4.1/98	4.2/100	--	4.0/95	4.0/95	--	3.9/93	
N165BK9	4.2/100	4.0/95	4.0/95	4.1/98	4.1/98	4.1/98	--	--	4.2/100	4.3/102	4.0/95	
N171BK4	4.0/100	3.8/95	3.6/90	3.5/88	3.4/85	3.3/83	--	2.8/70	2.8/70	3.0/75	2.8/70	
N185BK4	4.0/100	4.0/100	3.6/90	3.4/85	3.4/83	3.1/78	--	2.4/60	2.6/65	2.8/70	2.5/63	
N186CK5	3.9/100	4.0/103	3.7/95	3.7/95	3.7/95	--	3.4/87	3.2/82	3.0/77	3.3/85	3.1/80	
N187AK5	4.2/100	4.0/95	4.0/95	3.9/93	3.9/93	3.5/83	--	3.1/74	3.1/74	3.0/72	2.8/67	
N199BK5	4.4/100	4.3/98	4.3/98	4.3/98	4.3/98	--	3.9/89	3.8/86	3.9/89	3.8/86		
N200CK9	3.7/100	3.5/95	3.5/95	3.5/95	3.5/95	--	3.6/97	3.4/92	3.5/95	3.3/89		
N199AK4	4.1/100	4.0/98	4.0/98	3.9/95	4.0/98	--	3.9/95	3.8/93	4.0/98	3.8/93		
N202BK6	4.1/100	4.0/98	4.0/98	4.0/98	4.0/98	--	3.9/95	3.9/95	--	3.8/93		
N262BK5	4.0/100	4.0/100	3.9/98	3.9/98	3.8/95	--	3.4/85	3.4/85	3.4/85	3.2/80		
N262BK7	4.0/100	4.0/100	4.0/100	4.0/100	4.0/100	--	3.6/90	3.7/93	3.7/93	3.5/88		
N264BK7	3.9/100	3.9/100	3.8/98	3.8/98	3.7/95	--	3.4/87	3.5/90	3.4/87	3.3/85		
N265BK1	4.0/100	4.1/103	4.0/100	4.0/100	4.1/103	3.9/98	3.8/95	4.0/100	3.9/98	3.7/93		
N278AK1	3.9/100	3.8/98	3.8/98	3.8/98	3.8/98	3.9/100	3.7/95	3.9/100	3.9/100	3.8/98		
N278AK5	3.8/100	3.8/100	3.8/100	3.8/100	3.8/100	3.7/97	3.6/95	3.7/97	3.7/97	3.5/92		
N278AK7	3.8/100	3.8/100	3.7/97	3.7/97	3.8/100	3.9/103	3.7/97	4.0/105	3.8/100	3.7/97		
N279BK5	3.8/100	3.8/100	3.3/87	2.9/76	2.6/68	1.6/42	1.5/39					
N290AK5	4.5/100	4.5/100	4.3/96	4.4/98	4.4/98	--	4.1/91	4.2/93	4.3/96			
N290BK1	4.2/100	4.3/102	4.1/98	4.1/98	4.1/98	--	3.8/90	3.9/93	3.8/90			
N290BK4	4.5/100	4.5/100	4.4/98	4.4/98	--	4.0/89	3.9/87	3.9/87	3.9/87			
N290BK7	4.3/100	4.4/102	4.3/100	4.3/100	4.4/102	--	4.0/93	4.0/93	4.0/93			
N300CK2	4.0/100	3.9/98	3.9/98	3.9/98	--	3.6/90	3.4/85	3.5/88	3.3/83			
N301AK8	4.0/100	3.9/98	3.9/98	3.9/98	--	3.7/73	3.7/93	3.8/95	3.5/88			
N301CK2	4.1/100	4.2/103	4.2/103	4.1/100	--	4.0/98	4.1/100	--	3.9/95			
N301CK7	4.0/100	4.0/100	4.0/100	4.0/100	--	3.8/95	3.8/95	4.0/100	3.7/93			
N309BK5	4.1/100	4.1/100	4.1/100	--	--	3.8/93	3.7/90	3.8/93	3.6/88			
N313BK7	4.1/100	4.2/102	4.2/102	4.2/102	--	4.0/98	4.0/98	--	3.9/95			
N314CK5	4.0/100	4.1/102	4.1/102	4.1/102	--	3.9/97	4.0/100	4.0/100	3.8/95			
N314CK6	4.1/100	4.1/100	4.1/100	4.1/100	--	4.0/98	4.0/98	--	3.9/95			
N324BK5	4.3/100	4.4/102	4.5/105	--	3.9/91	3.8/88	4.0/93	3.7/86				
N324CK4	4.3/100	4.5/105	4.4/102	--	4.2/98	4.1/95	4.2/98	4.3/100				
N329BK4	4.4/100	4.4/100	4.4/100	--	4.1/93	3.9/89	4.1/93					
N330BK7	4.5/100	4.5/100	4.6/102	--	4.2/93	4.0/89	4.2/93	4.2/93				
N353AK5	4.4/100	4.5/102	4.4/100	--	--	3.6/82	--	3.6/82				
N350AK2	4.1/100	4.2/102	3.9/95	--	--	3.7/90	--	3.6/88				
N348BK5	4.1/100	4.3/105	4.2/102	--	3.8/93	3.9/95	--	3.8/93				
N348CK4	4.2/100	4.3/102	4.3/102	--	--	4.3/102	4.1/98	3.9/93				
Average Relative Efficiency			97	94	93	90	90	88	88	84	78	76

Table XX. Actual and Relative Efficiencies of 1969 Cells on 100°C Vacuum Storage

Cell No.	Months										
	0	1	2	3	4	5	6	7	8	9	10
5268	3.2/100	3.2/100	--	--	3.4/106	3.2/100	3.2/100	3.3/103	--	3.3/103	3.1/97
19861	3.7/100	3.9/105	--	--	3.8/103	3.8/103	3.8/103	4.0/108	--	3.9/105	3.7/100
N388C5	3.5/100	--	--	3.5/100	3.5/100	3.5/100	3.6/103	--	3.6/103	3.3/94	
28655	3.9/100	3.9/100	3.7/95	4.0/103	--	3.9/100	3.6/92				
39762	3.9/100	3.9/100	3.9/100	4.0/103	--	4.0/103	--	3.7/95			
40664	3.6/100	3.7/103	3.6/100	3.8/105	--	3.8/105	--	3.6/100			
27548	3.3/100	3.4/103	3.4/103	3.5/106	--	3.5/106	--	3.2/97			
39764	3.6/100	3.8/105	3.8/105	3.9/108	--	3.9/108	--	3.6/100			
98656	3.3/100	3.5/106	3.7/112	--	3.6/109	--	3.4/103				
98655	3.1/100	3.4/110	3.5/115	--	3.5/113	--	3.4/110				
105655	2.9/100	3.2/110	3.3/114	--	3.4/117	3.1/107					
107261	2.9/100	3.0/103	3.2/110	--	3.2/110	3.0/103					
132144C	2.9/100	3.2/110	--	3.1/107	3.0/103						
132145C	2.8/100	3.1/111	--	3.2/114	3.0/107						
Average Relative Efficiency		105	106	106	108	104	102	101			

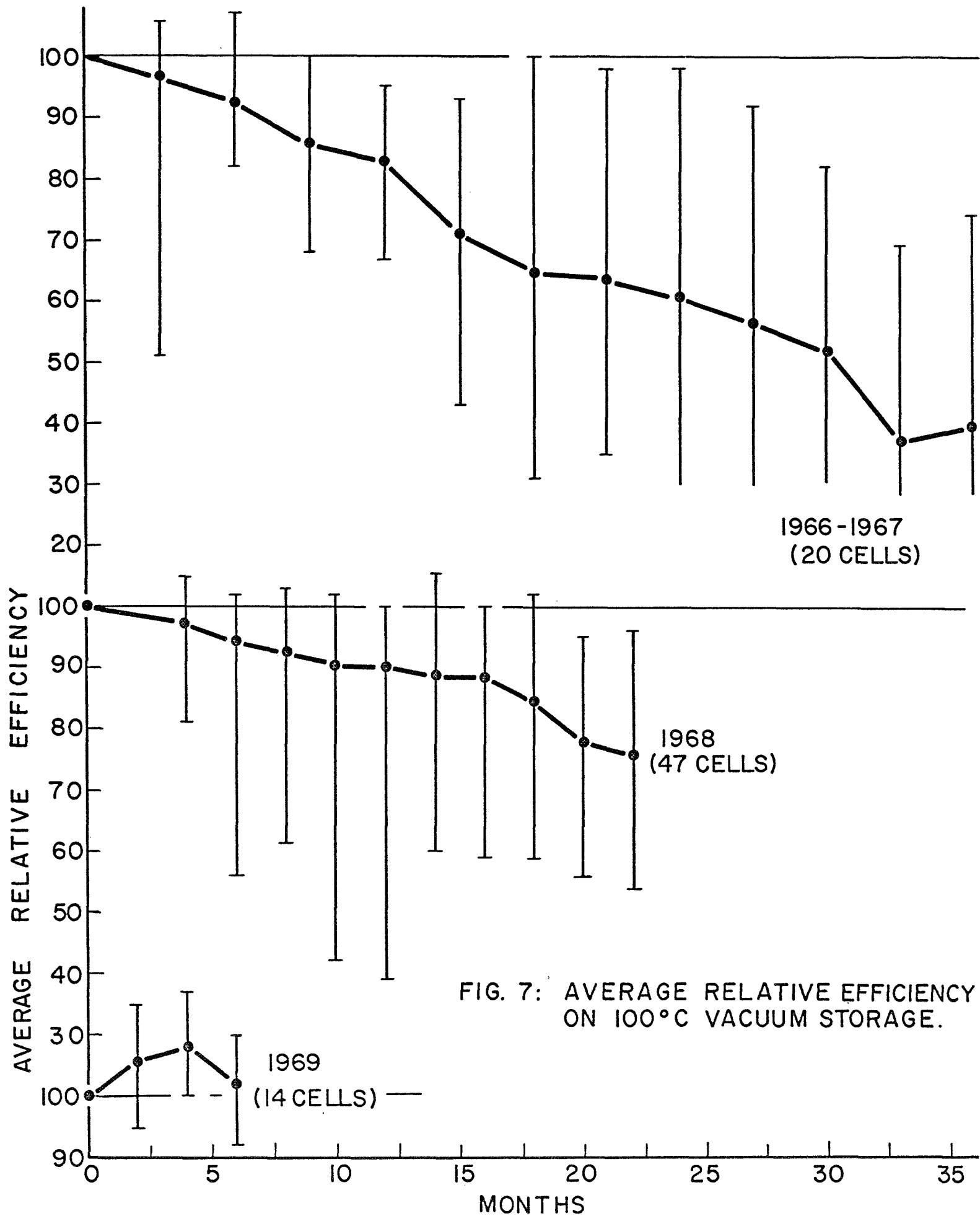


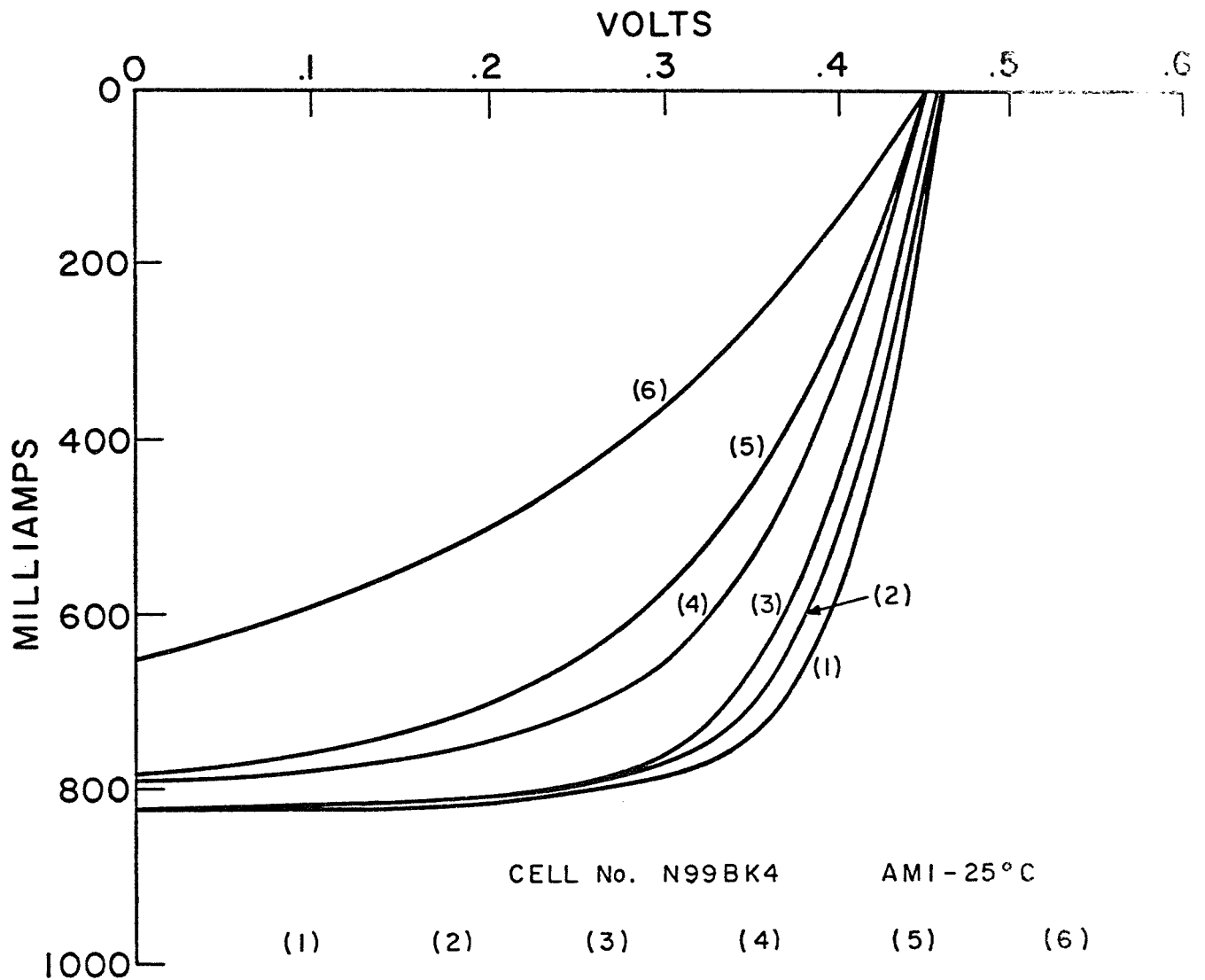
FIG. 7: AVERAGE RELATIVE EFFICIENCY ON 100°C VACUUM STORAGE.

to decrease. As a rule the OCV is seldom affected by an increasing series resistance until an extreme is reached. Figure 8, which was prepared by superimposing I-V curves from a cell that degraded on the 100°-vacuum test, shows this effect. The great amount of scatter in the data however is difficult to reconcile with a common degradation mechanism. It may be that the variation of some, as yet unknown, cell property from cell to cell may determine the degradation rate more than the intrinsic mechanism, the intrinsic mechanism merely representing the best that can be achieved.

Capacitance measurements of heat degraded cells would be expected to show smaller values of capacitance than undegraded cells. This is because if the insulating layer is assumed to be the dielectric separating the plates of the parallel plate capacitor formed by the grid and the substrate, then the thickness of this layer should be inversely proportional to the capacitance. Actual measurements show this. Cells D407D and D392A were tested on an HP Model 4800 Vector Impedance Meter and were compared with cells that were very recently fabricated, i. e., no heat degradation, 255321D and 255218C. Table XXI shows the results of this measurement. The heat degraded cells, by virtue of the increasing capacitance with decreasing frequency, are obviously extremely non-uniform and result in a dispersion type behavior. The undegraded cells show much more stable behavior over the same frequency range, their capacitance remaining fairly constant.

Table XXI. Capacitance Measurements of Heat Degraded and Undegraded Cells.

Frequency Hz	Capacitance, Microfarads			
	D407D	D392A	255321	255218
100 k	.0238	.0231	--	--
10 k	.049	.030	.318	.244
1 k	.405	.171	.331	.270
100	4.0	1.62	.356	.500
10	40	16	--	--



	CELL No. N99BK4				AMI - 25 °C	
	(1)	(2)	(3)	(4)	(5)	(6)
OCV . =	.460	.460	.458	.450	.450	.450 V
SCC =	.822	.820	.820	.790	.785	.650 A
V_{mp} =	.359	.340	.330	.310	.293	.250 V
I_{mp} =	.720	.720	.710	.632	.580	.440 A
MAX. PWR. =	.258	.245	.236	.196	.170	.110 W
FILL =	68.4	65.0	62.4	55.0	48.1	37.6 %
EFF. =	4.72	4.48	4.28	3.58	3.10	2.01 %
DATE =	11/67	1/68	6/68	10/68	12/68	5/69

FIG. 8: EFFECT OF 100°C VACUUM STORAGE ON CELL PERFORMANCE.

CELL IMPROVEMENT PROGRAM

Roll Coated Substrates

The preparation of Ag-Pyre ML substrates by machine roll-coating was studied as a possible substitute for the standard process sprayed substrate. During standard process substrate preparation a mixture of two parts Pyre-ML varnish to one part Ag flake, by weight, is sprayed onto Kapton film. The viscosity is adjusted to a sprayable mixture by the addition of a one to one mixture of dimethyl formamide and toluene. After spraying the substrate is given two heat treatments; the first, at low temperatures, drives off the solvents, while the second, at much higher temperatures, actually cures the Pyre ML varnish. Since each substrate is prepared individually its cost is high and the probability of obtaining uniformity from one substrate to the next is not very high. It was felt that if the Kapton could be coated by a roller machine process, such as is presently used* to coat the cover plastic with epoxy, both greater uniformity and a reduced cost could be achieved. The same vendor that supplies the epoxy coated cover plastics was also asked to prepare the roll coated Ag substrates. Three ratios of varnish to silver were studied, one to one, one and a half to one and two to one, all by weight. A nominal thickness of 0.3 mil was specified.

Inspection after receiving indicated that the thickness, light transmission, and resistance of the roll coated substrates were very non-uniform, and if the same inspection standards that are used in evaluating sprayed substrates had been applied to these roll coated substrates, they would have been rejected. The variations were rather erratic and occurred randomly throughout a roll, rather than as a gradual variation from one end to the other. The thickness was found to vary between 0.1 and 0.35 mils. As expected, the resistance varied with varnish to silver ratio. The 1:1 material ranged between 0.012 and 0.030 ohms/square; the 1-1/2:1 ranged from 0.025 to 0.056, while the 2:1 material consistently was greater than 0.06 ohms/square. An upper limit of 0.030 ohms/square is presently the upper inspection limit tolerated for sprayed substrates.

During the roll coating process the material apparently was heated enough to remove the solvents. For evaluating purposes the material received the same cure cycle as did the standard process material. Also in the standard process substrates are given a light burnish prior to zinc plating. Since the effect of burnishing roll coated substrates was unknown, about half of the roll coated substrates were given the standard burnish treatment and the other half not. Comparison of finished cells later indicated that there was no significant difference between the burnished and nonburnished substrates.

Of the three weight ratios the 1:1 material resulted in cells with the best performance. The 1-1/2:1 material was next best and the 2:1 was worst. Table XXII shows these results by comparing the performance of cells fabricated from the three different materials. The substrates were

all cured in the same way. All of the cells that were completed are included in the data; however, a number of cells were rejected at various stages of fabrication.

Table XXII. AM0-25°C Performance of Kapton Covered Roll-Coated Substrate Cells

	Min	Max	Av.
58 1:1 Roll Coated			
OCV	.449 V	.482 V	.469 V
SCC	.717 A	.975 A	.867 A
P _{max}	.240 W	.313 W	.281 W
Eff.	3.2 %	4.1 %	3.7 %
Fill	65.0 %	71.4 %	69.2 %
18 1-1/2:1 Roll Coated Cells			
OCV	.460 V	.491 V	.476 V
SCC	.750 A	.900 A	.826 A
P _{max}	.253 W	.291 W	.268 W
Eff.	2.9 %	3.6 %	3.4 %
Fill	59.4 %	69.1 %	67.0 %
12 2:1 Roll Coated Cells			
OCV	.461 V	.478 V	.470 V
SCC	.700 A	.959 A	.839 A
P _{max}	.217 W	.287 W	.258 W
Eff.	2.8 %	3.7 %	3.3 %
Fill	57.8 %	68.9 %	65.6 %

A comparison of the performance of roll-coated substrate cells with standard process cells was made several times. Table XXIII shows the performance of 1:1 roll coated and standard process cells fabricated together, beginning with zinc plating and CdS evaporation.

Table XXIII. AM0-25°C Performance of Standard Process and 1:1 Roll Coated Substrate Cells

	Max.	Min.	Av.
43 Roll Coated Cells			
OCV	. 470 V	. 445 V	. 463 V
SCC	. 920 A	. 700 A	. 796 A
P _{max}	. 292 W	. 222 W	. 258 W
Eff.	3. 80 %	2. 90 %	3. 36 %
Fill	73. 0 %	66. 5 %	70. 3 %
27 Standard Process Cells			
OCV	. 480 V	. 450 V	. 467 V
SCC	. 890 A	. 668 A	. 781 A
P _{max}	. 281 W	. 229 W	. 255 W
Eff.	3. 67 %	2. 98 %	3. 33 %
Fill	73. 0 %	65. 4 %	70. 2 %

These data indicate that there is little difference between the performances of these two types of cells.

A further evaluation of 1:1 roll coated substrate cells was made by comparing their performance with standard cell performance at AM0-60°C and at 1/10 and 1/100 AM0-25°C. These roll coated cells were the 48 best of the 58 cells reported on previously while the standard cells were the 100 Class I cells fabricated during the month of May. Table XXIV shows the averages of the important performance parameters from the two groups of cells, as well as their relative averages.

Table XXIV. Performance Comparison of Roll Coated Substrate Cells and Standard Process Cells

	AM0-25°C	AM0-60°C	0. 1 AM0-25°C	0. 01 AM0-25°C
48 Roll Coated Cells				
OCV	. 469 V	. 415 V/88. 5	. 415 V/88. 5	. 354 V/75. 5
SCC	. 812 A	. 791 A/97. 4	. 080 A/9. 85 ^h	. 0078 A/. 96
P _{max}	. 265 W	. 216 W/81. 5	. 024 W/9. 1	. 0018 W/. 68
Eff.	3. 4%	2. 8%/82	3. 1%/91	2. 4%/70. 6
Fill	69. 6%	66. 0%/94. 8	70. 9%/102	66. 4%/95. 4
100 Standard Process Cells				
OCV	. 465 V	. 409 V/87. 6	. 410 V/88. 2	. 347/74. 6
SCC	. 754 A	. 751 A/99. 6	. 076 A/10. 1	. 0077/1. 02
P _{max}	. 242 W	. 203 W/83. 9	. 022/9. 1	. 0018/0. 74
Eff.	3. 2%	2. 6%/81. 3	2. 8/87. 5	2. 2%/68. 8
Fill	69. 4%	66. 4%/95. 7	71. 1/102	63. 9%/92. 1

All of the previous data appear to indicate that the substitution of roll coated substrates for standard sprayed substrates had no significant effect on cell performance. However, as indicated before, the Pilot Line was just coming out of a severe yield slump and this may have masked any minor effects that the roll coated substrates caused. More recent commercial production from the Pilot Line, in which the number of cells involved is much greater than during the initial evaluation, shows that roll coated substrate cells perform at a somewhat higher level than sprayed substrate cells. The average output power from roll coated cells is about 10% greater than sprayed substrate cells. Also, the yields from roll coated substrates were significantly higher during the initial evaluation than were the yields from sprayed substrates. The yields from roll coated substrates presently are even greater than before, which is another indication of the preference of the roll coated substrates over the sprayed ones.

However, all of these data were collected from cells prepared from a single roll of roll coated silver Pyre ML on Kapton, and the possibility exists that the manufacture of identical rolls cannot be duplicated. The fortuitous occurrence of a number of optimized parameters may have been responsible for the observed higher yields and performance but it may be that their occurrence was a random event which has little possibility of reoccurring.

The reason that roll coated substrates result in better performance is, of course, unknown but must be related to the manner in which the zinc plate deposits on its surface, which in turn determines the manner in which the CdS layer is grown. As is mentioned in the section covering the chromium interlayer work, the purpose of the zinc interlayer appears to be more than merely providing an ohmic contact between the CdS film and the Ag-Pyre ML substrate, because an ohmic contact was demonstrated to occur without the presence of the zinc.

1:1 Ag-Pyre ML Sprayed Substrates

The better yields and performance obtained from the 1:1 roll coated substrates prompted another investigation of 1:1 spray coated substrates. The substitution of 1:1 spray coated substrates has been attempted in the past but with limited success only. Intuitively, one would expect better performance from cells fabricated with substrates of higher metallic content than from lower metallic content substrates.

The viscosity of the 1:1 experimental mixture was adjusted to the same viscosity as the standard process mixture. The resistances of the resulting substrates ranged between .004 and .010 ohm/square, which is considerably lower than the .030 ohms/square tolerated as the upper limit for standard process substrates. The adherence of the 1:1 sprayed substrates, as determined by the cellophane-tape pull test, was much poorer than the standard substrates, a fact previously observed in the earlier attempts at using 1:1 substrates.

Four CdS evaporation runs were involved, each consisting of two 1:1 substrates and one 1:2 substrate. All of the resulting films were processed normally. 68 of the 72 starting cells were processed into finished cells. Their AM0-25°C performance averages and ranges are shown in Table XXV.

Table XXV. AM0-25°C Performance of 68 1:1 Spray Coated Cells

	Max.	Min.	Av.
OCV	.478 V	.423 V	.454 V
SCC	.903 A	.400 A	.635 A
P _{max}	.296 W	.124 W	.205 W
Eff.	3.8 %	1.6 %	2.8 %
Fill	73.6 %	67.1 %	69.9 %

29 of the 32 standard process cells were finished into completed cells and Table XXVI shows their AM0-25°C performance averages and ranges.

Table XXVI. AM0-25°C Performance of 29 Standard Process Control Cells

	Max.	Min.	Av.
OCV	.481 V	.415 V	.466 V
SCC	.850 A	.620 A	.700 A
P _{max}	.276 W	.130 W	.232 W
Eff.	3.6 %	1.7 %	3.0 %
Fill	72.6 %	68.0 %	70.7 %

These data indicate that the use of 1:1 substrates doesn't result in any particular advantage over standard process substrates. In fact, all of the average parameters of the 1:1 substrate cells are somewhat lower than the corresponding parameters of the standard cells.

Machine Sprayed Substrates

It has long been recognized that dependence on operator skill at the various stations on the standard process fabrication line is one of the major deterrents to uniform and reproducible cell production. As part of a corporate sponsored effort to reduce that dependence a mechanized substrate sprayer was fabricated and permanently installed as part of the standard process line. Two separate motions were incorporated in the design of the unit; the spray gun moves horizontally while the substrate moves vertically stepwise. At the end of each traversal

of the spray gun a limit switch is actuated which turns off the spray and initiates a single step of the vertical drive. After the vertical drive has ended the spray starts again and the gun begins its return trip. The operator needs only to mount the substrate initially and rotate it after the unit has gone through a complete cycle. The unit was put on-line in mid-September and as part of an initial evaluation a number of cells fabricated with machine sprayed substrates were compared with hand sprayed substrate cells. No selection criteria were imposed on either group of cells other than the fact that they were sprayed and fabricated during the same time period.

The comparison of their AM0-25° C average parameters are shown in Table XXVII.

Table XXVII. Comparison of Machine Sprayed and Hand Sprayed Substrate Cells, AM0 - 25° C.

	65 Machine Sprayed Substrate Cells	75 Hand Sprayed Substrate Cells
Av. OCV	.467 V	.469 V
Av. SCC	.751 A	.731 A
Av. Fill	69.0 %	69.3 %
Av. Eff.	3.1 %	3.1 %

There appears to be no significant difference between the two groups of cells, so that the greatest benefit from the adoption of the machine sprayer lies in the ease and uniformity of fabrication from one substrate to another.

Zn-Pyre ML Substrates

The direct substitution of zinc flake for silver in the fabrication of a zinc-Pyre ML substrate was also attempted. Unfortunately, the zinc flake apparently acts as a catalyst for the polymerization of the Pyre ML varnish and within a few minutes after its addition a definite increase in the viscosity of the mixture was noted. After 30 minutes or so a molasses thick mixture resulted. No attempt was made to spray the material since it was obviously too thick. No further plans are being considered utilizing this approach.

Evaporated Grids

Of all the process steps in the fabrication of the thin film CdS solar cell the one step that appears to be most in need of further refinement is the application of the grid. An etched half mil thick copper mesh, plated with a gold flash, is attached to the cell surface with a gold filled conductive epoxy. The epoxy is cured in a two-step process; first, the cure is initiated in a lamination press at a temperature of 196° C for a period of 20 minutes under a pressure of 100 psi. The cure is then completed by a 15 hour vacuum bake at 135° C. The integrity of the grid contact is therefore dependent on the gold epoxy maintaining an intimate and reliable contact

between the grid and the cell surface. Unfortunately, the following process step, cover plastic application, requires an almost identical cure cycle to cure the transparent cover plastic epoxy. The effects of subjecting the already cured gold epoxy to this second cure cycle are unknown but have long been suspected of weakening its bond strength and causing other unknown effects.

The concept of an evaporated grid is obviously appealing since it eliminates most of the problems associated with the gold epoxy. The bond between an evaporated grid and the barrier layer ought to be quite stable and unaffected by the cover plastic lamination cycle. Also, a low resistance ohmic contact can be established uniformly over the entire cell area avoiding the bridges that the rather stiff and springy copper foil grid tends to form. A completely evaporated grid, however, didn't appear feasible because previous experience had shown that obtaining a uniform pattern over the entire cell area with the required resistance and light transmission was a difficult problem. It was decided to use a combination of two grids, an evaporated grid and a coarse overlay grid. The evaporated grid was intended to serve as the actual current collector while the overlay grid was to be a current carrier, merely providing a low resistance path between the evaporated grid and the positive tab. The overlay grid was to be attached with the same conductive gold epoxy as is presently used but its application would be much less critical since its purpose was to contact the evaporated lines and not the barrier layer.

Since the evaporated portion of the grid was to be the current collector it would have to have about the same geometry as the presently-used etched copper foil grid, which has a line density of 60 lpi in one direction and 10 lpi in the other. The line width in both directions is a nominal 2 mils. The calculated light transmission is 86.3% and in order to be competitive any possible substitute grid should have at least the same transmission. The evaporated pattern was thus selected to be 2 mil wide parallel lines spaced 60 lines to the inch. This pattern has a calculated light transmission of 88% and if an overlay grid density of 10 lpi in both directions is selected then the transmission of the combined grid calculates to 84.5%, which is less than the 86.3% of the copper foil grid. But merely decreasing the overlay grid line density to 5 lpi or less in both directions increases the overall transmission to above the required 86.3%.

Since the resistance of the evaporated lines determines the density, or spacing between adjacent lines, of the overlay grid, obtaining a low resistance evaporated pattern was recognized as a requisite for the successful development of a combined grid. Hence, much effort was expended during the contract period in devising methods of reducing this resistance.

Gold was selected as the evaporated grid material because it had been shown earlier to provide the lowest resistance ohmic contact to the Cu_2S barrier layer of a number of possible materials. (2) The evaporation parameters that resulted in the lowest resistance evaporated gold lines were initially determined and although a bulk value resistivity of 2.4×10^{-6} ohm-cm is often quoted values around 10^{-5} ohm-cm were most consistently obtained on the evaporated gold lines. Since the resistance of the evaporated pattern could also be reduced by increasing its thickness, the upper limit of evaporated pattern thickness was also established. Thicknesses up to a micron were usually obtained with no difficulty but above that adherence became a problem. Lines thicker than a micron peeled and spalled readily so only line thicknesses less than a micron could be used.

Several methods of masking during gold evaporation were used. First, a spray fluorocarbon mold-release was used because it had been used in the past with some success. These mold release masks were put down on the barrier layer through masks specially fabricated for this purpose or through the standard etched foil grids as positives. After gold deposition, acetone, or some other suitable solvent, was used to remove the mold-release mask leaving only the desired grid pattern on the barrier layer. Photoresists were also used but with limited success only. When it became apparent that extremely thick evaporated patterns were required both the mold release and photoresist masks suffered in that complete removal of the mask after deposition was not possible. Apparently, as the thickness of the evaporated deposit increased it prevented the solvent from completely removing the mask and resulted in very non-uniform evaporated patterns.

In addition, the resolution of the mold release mask was limited by the particle size in the spray mixture. Microscopic examination revealed that the edges of the evaporated 2 mil lines were very coarse and rough, and in extreme cases, discontinuities in the lines were also present. A large number of commercially available mold releases, both silicone and fluorocarbon, dry lubricants, and other possible candidates, were evaluated for this application, which obviously was not their intended purpose. The best results were obtained with Miller-Stephenson spray mold releases, MS-122 and MS-136.

The photoresist masks generally resulted in evaporated patterns that had much better line definition than patterns from masks of mold-release, but they were confined to impractically thin layers of evaporated gold. Microscopic examination usually showed many discontinuities in these lines which contributed to the series resistance so characteristic of these cells.

Figure 9 is a typical I-V characteristic obtained from a cell whose evaporated grid was deposited through a mold-release mask. The high series resistance, which apparently causes the low SCC, fill and efficiency, was common to all of these cells, photoresist as well as mold-release prepared. And the high series resistance is presumed caused by the thin and discontinuous evaporated grid lines. The thickness of the lines on this particular cell was estimated to be in the 0.3 to 0.5 micron range.

The possibility that the fluorocarbon and photoresist masks were contaminating the barrier layer was never completely eliminated. Several attempts were made to determine if there were any effects and although no immediate and obvious effects were detected the possibility that subtle and more gradual effects were occurring was not ruled out.

The best results in evaporating heavy deposits of gold were obtained with metal foil masks which had no mask removal problems. The first attempts with metal foil masks were with magnetic foil and were held in place during gold evaporation with a magnet. Unfortunately, the vendor was not able to fabricate a mask with the required resolution uniformity over the entire 3" x 3" area by electro-etching. The resulting evaporated patterns also suffered from a lack of uniformity in resolution. It was necessary to resort to an electroformed mask which meant that the foil material was confined to Ni, Au, Cu or Ag. Ni was selected since it had some magnetic properties. The vendor was successful in electroforming a mask with the required resolution over the entire area. However, because of the buckling and flexible nature of the cell at this stage of fabrication temporary attachment of the mask during gold evaporation became a greater problem. A spray-on adhesive that was soluble in acetone was resorted to and was fairly successful in producing grid patterns of acceptable quality. After gold evaporation the masked cell was immersed in acetone and the mask usually parted from the cell with no difficulty. The particle size of the spray-on adhesive was quite large and resulted in frequent bridging over the 2 mil gaps in the mask and caused discontinuities in the evaporated lines if not removed. The bridges were removed with a fine camel hair brush soaked in acetone but unfortunately some of the adjacent adhesive was also weakened by the acetone and resulted in a number of areas where mask contact to the cell was poor. This in turn resulted in widened grid lines during gold evaporation.

Figure 10 shows the I-V trace of a typical cell with an evaporated gold grid that used the Ni foil as a mask. The thickness of the evaporated gold line is estimated between 0.1 and 1.0 μ . An overlay grid of 10 lpi in both directions was also used. A high series resistance is still quite

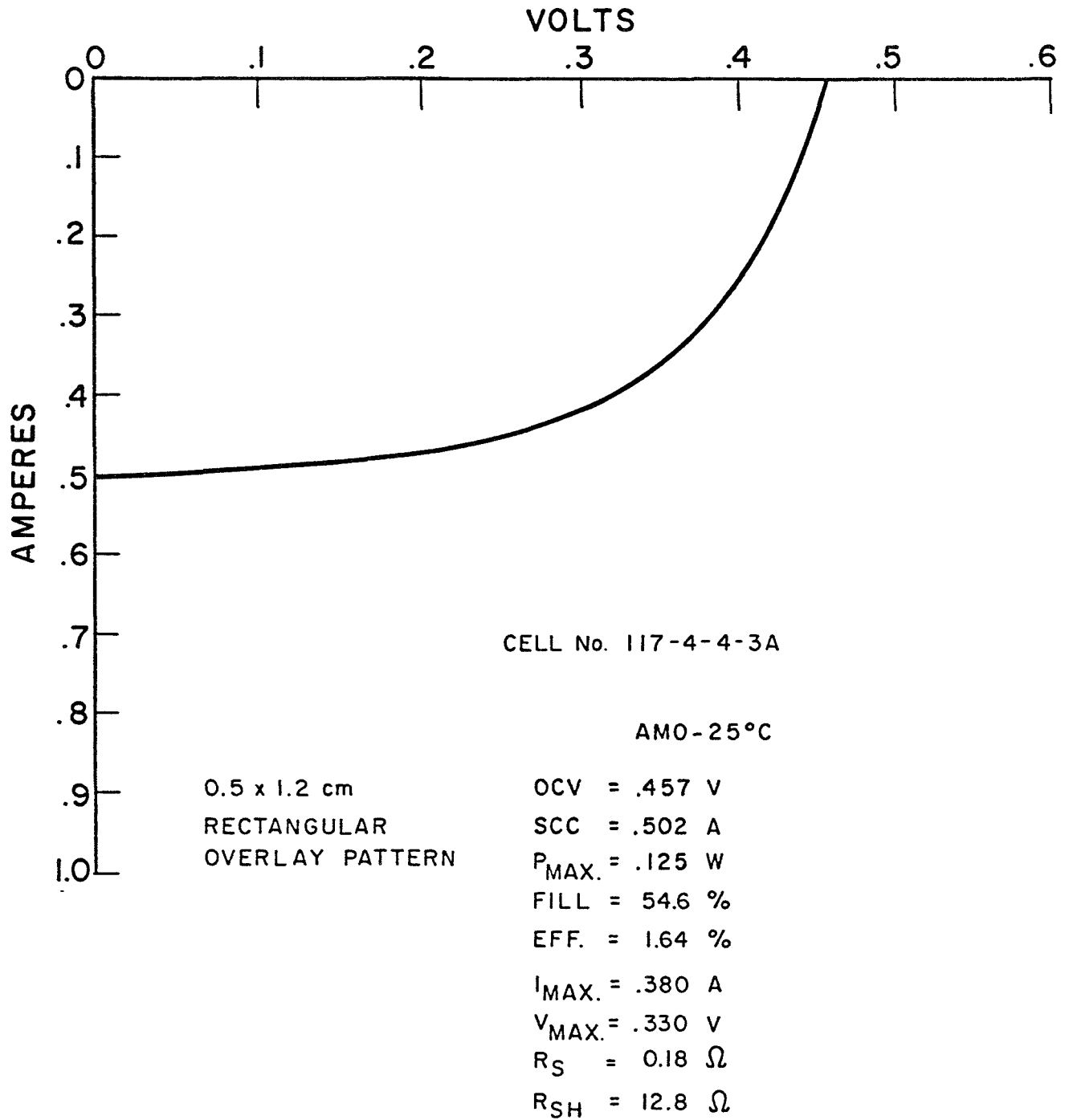


FIG. 9: I-V CHARACTERISTIC OF EVAPORATED GRID CELL. FLUOROCARBON SPRAY EVAPORATION MASK.

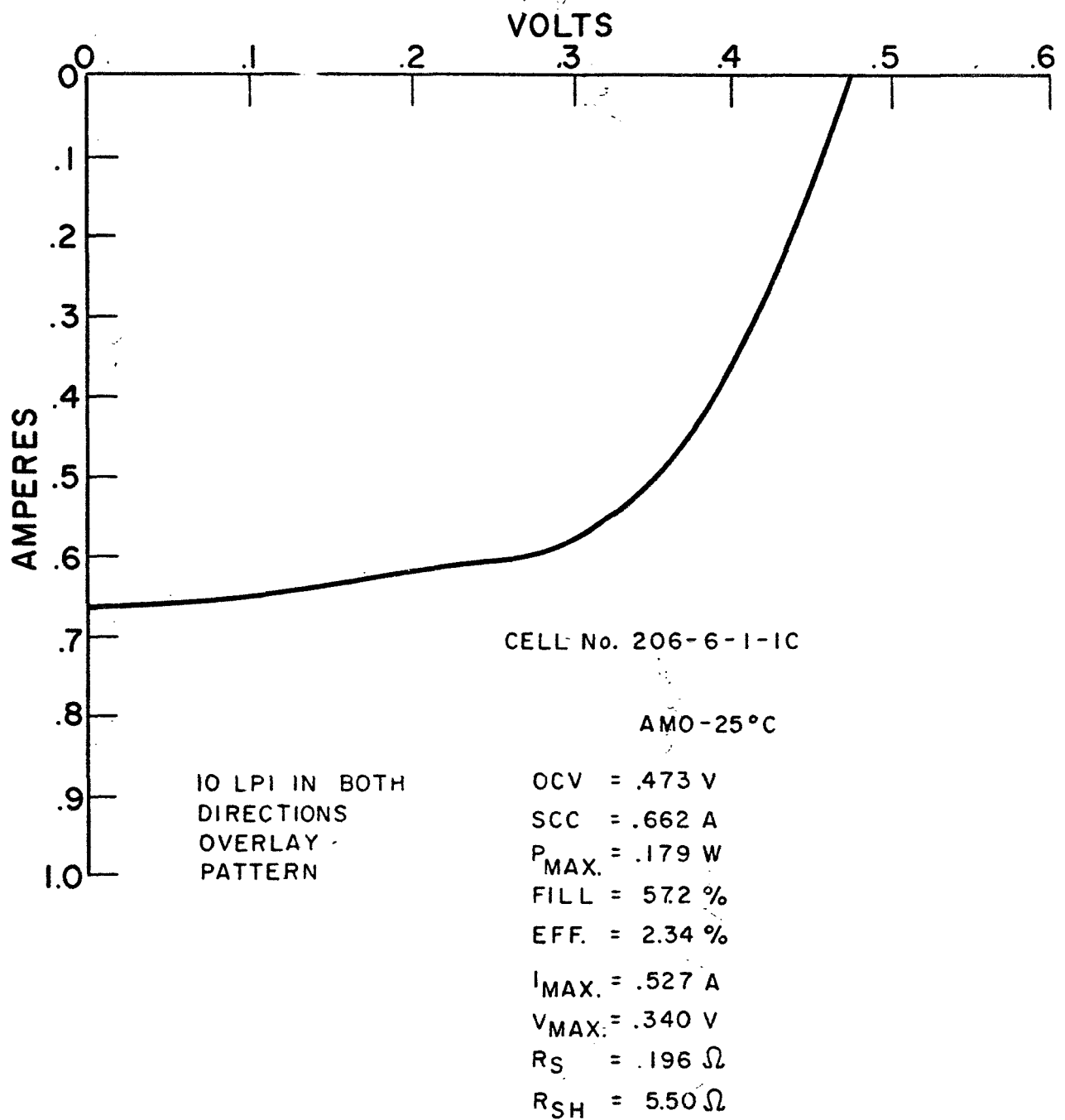


FIG. 10: I-V CHARACTERISTIC OF EVAPORATED GRID CELL. Ni FOIL EVAPORATION MASK.

prominent; however, an increased SCC seemed to result from these cells. A poor shunt also appears to contribute to the low fill. A poor shunt was quite common to all evaporated grid cells and can be considered as one of its drawbacks. It is assumed to be caused by pinholes or other imperfections in the CdS film which the evaporated gold can easily penetrate and, under the right circumstances, cause a low resistance path between the substrate and the barrier layer. The epoxied electro-etched grid tends to bridge these small imperfections in the film and thus avoids this disadvantage.

Since gold apparently could not be deposited in thicknesses much greater than about a micron, at least on the barrier layer of the CdS film, several alternative methods of increasing the thickness of the gold deposit were studied. Dipping in molten solder was attempted but the solder did not wet the gold lines uniformly and resulted in a very non-uniform pattern. Also, this high temperature treatment of the barrier cell usually reduced the OCV considerably. Dipping in several low melting temperature bismuth alloys was also attempted but with the same results.

A solder cream, originally intended for use in printed circuit applications, was also evaluated. It was applied to the grid pattern by squeegeeing through the evaporation mask and a silk screen mesh after gold evaporation. After a low temperature cure the mask was removed and the cell was then vacuum heated to above the liquidus temperature of the solder. The resulting pattern appeared uniform but microscopic examination revealed that the lines were not continuous. Apparently not enough of the solder cream could be applied so that continuous lines could be formed.

Conductive gold and silver epoxies were also used to build up the grid lines. The epoxy was squeegeed through the evaporation mask after gold evaporation. After removal of the mask the cell was given the required heat treatment to cure the epoxy. There was considerable spreading of the epoxy resulting in a non-uniform and somewhat messy appearing pattern. Figures 11 and 12 show the resulting I-V curves from these cells. The low fill appears to be dominated by both a low shunt and high series resistance so no apparent advantage was gained by this method of grid fabrication.

It was concluded that the performance of these evaporated grid cells was limited by their series resistance and was apparently caused by discontinuities and the thinness of the evaporated lines. None of the attempts at reducing the resistance of the as-evaporated pattern was successful and it was concluded that unless a more conductive evaporated pattern could be deposited the concept of the evaporated grid was limited.

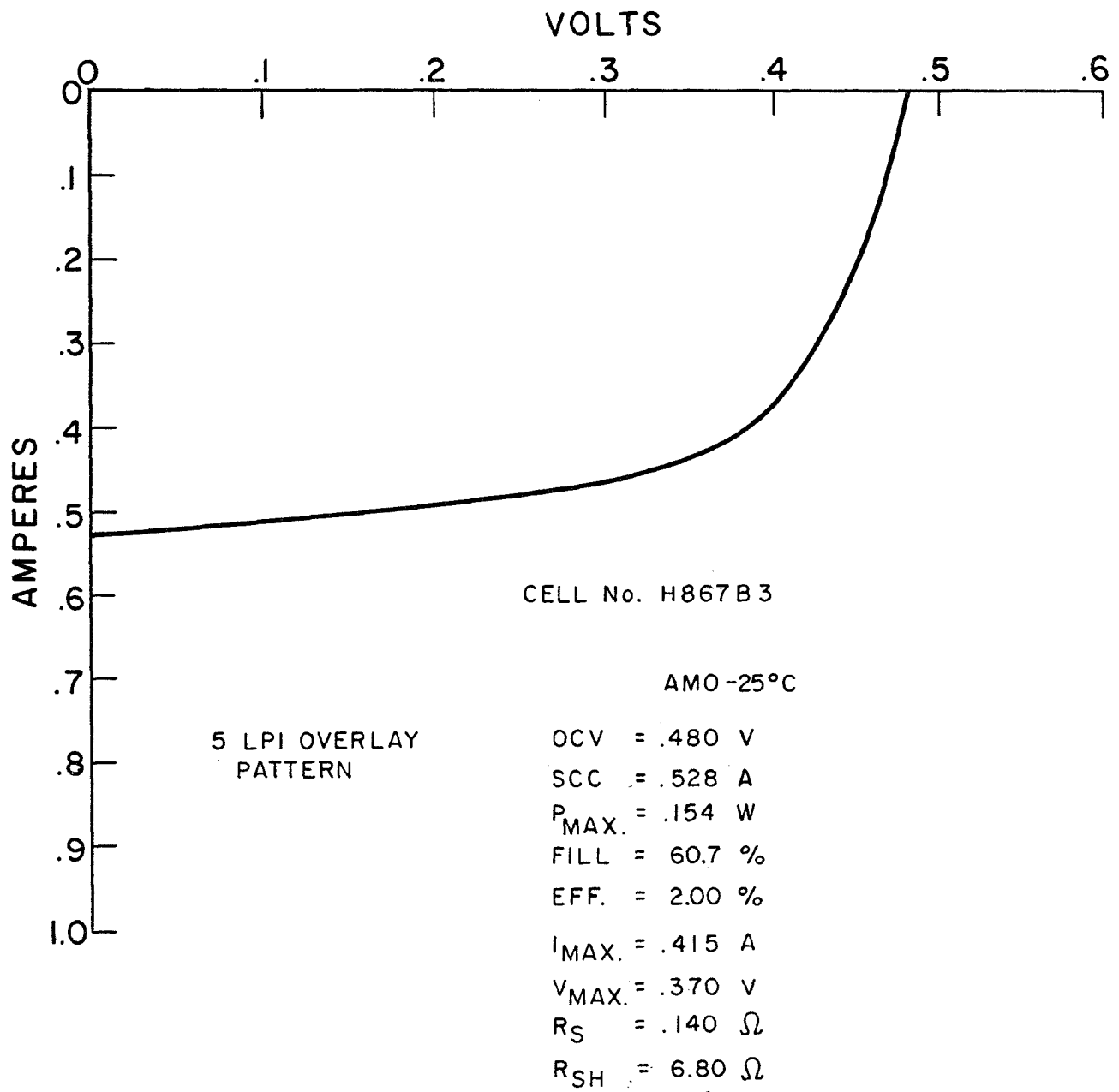


FIG. II: I-V CHARACTERISTIC OF EVAPORATED GRID CELL. EVAPORATED PATTERN BUILT UP WITH SILVER EPOXY.

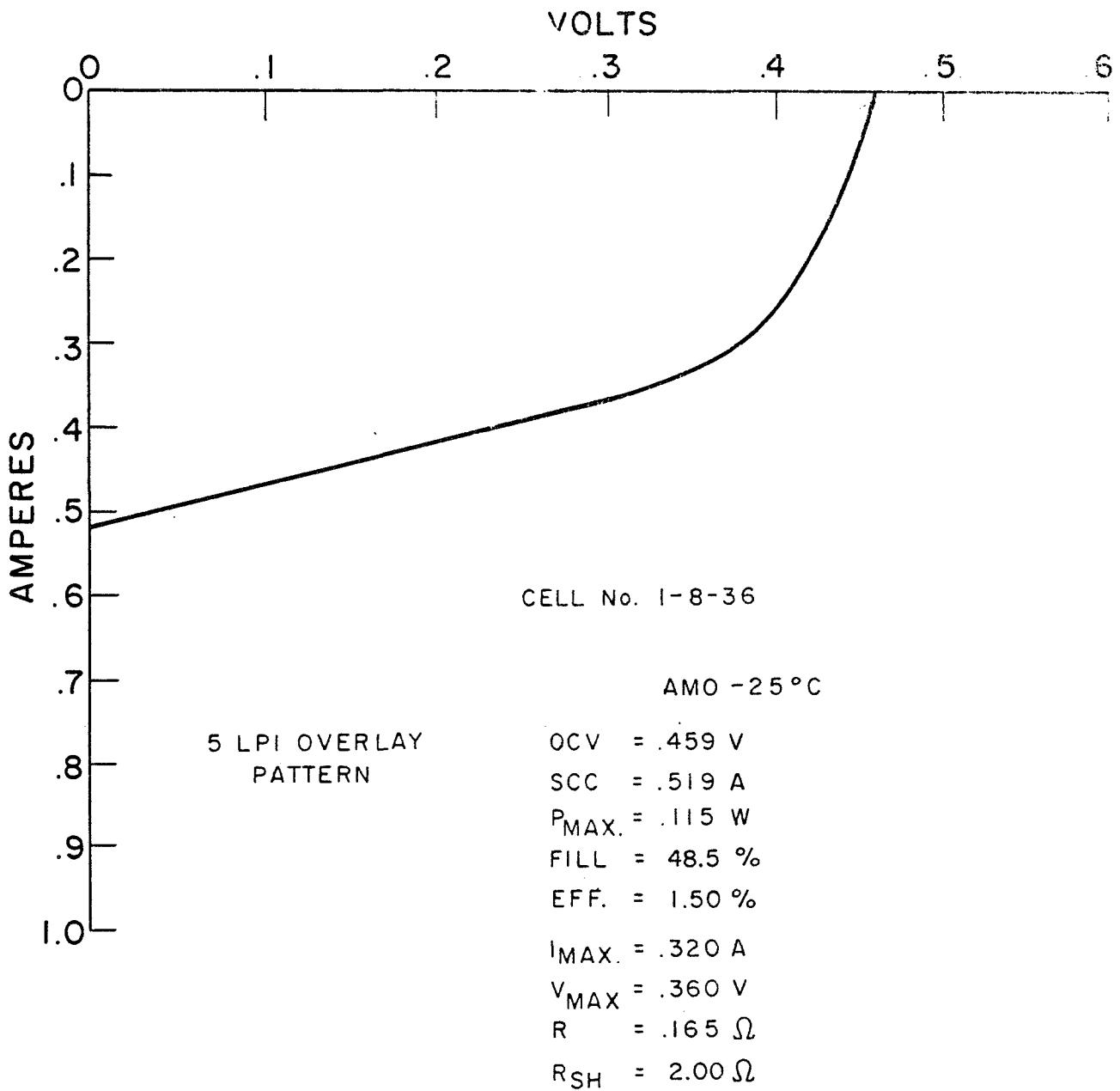


FIG. 12: I-V CHARACTERISTIC OF EVAPORATED GRID CELL. EVAPORATED PATTERN BUILT UP WITH GOLD EPOXY.

Gold Epoxy Application by Silk Screening

As an additional effort in reducing the dependence on operator skill a different method of applying the conductive gold epoxy to the grid was initiated. Previously, the epoxy was applied to the grid simply by squeegeeing the grid down into a film of the gold epoxy which had been spread over a sheet of Teflon. A uniform layer was quite difficult to obtain reproducibly and wasn't always confined to the intended side of the grid, some spreading usually occurred. Prior to positioning on the cell an attempt was made to smooth out the epoxy layer on the grid by means of a cotton swab, but usually at the expense of wrinkling the already fragile grid, or breaking some of its wires.

By silk screening the gold epoxy onto the grid a much more uniform coating is obtained. The silk screen, by acting as a metering device, assures that each grid receives the same amount of gold epoxy and that it is uniformly applied over its entire surface. Microscopic comparison of silk screen epoxied grids with hand epoxied grids indeed does show that silk screening is a much more uniform process.

The use of silk screen epoxied grids doesn't appear to result in any advantage in cell performance. However, the main advantage with the silk screen process lies in its ease of use and, as such, is much less dependent on operator skill. This method was incorporated into the standard process at the end of August.

Chromium Interlayers

In the present standard process of cell fabrication a very thin layer of zinc is electroplated onto the Ag-Pyre ML substrate just prior to CdS evaporation. The necessity of this zinc layer has been established empirically and has long been assumed to provide a low resistance ohmic contact at the CdS and the Ag-Pyre ML interface. The presence of this zinc layer, however, has many disadvantages, among them its high vapor pressure during the CdS evaporation cycle which has been thought to result in a Zn doped CdS film. Also any zinc that has not been covered by CdS during the evaporation process will result in the precipitation of metallic copper when dipped in the copper chloride solution during the barrier formation process. This copper usually results in badly shunted cells.

Substitutes for the zinc have long been sought and chromium has appeared to be one of the more promising candidate materials. Previous attempts at using chromium resulted in cell performance with normal OCV's and fills but low SCC's and efficiencies.⁽⁵⁾ These attempts were

⁽⁵⁾ Shirland, Hietanen, and Bower, NASA CR-72159, Final Report on Contract NAS 3-8502, dated December 30, 1966.

confined to evaporated chromium and it was logical to attempt substituting electroplated chromium since electroplated zinc has been shown previously to result in better cell performance than evaporated zinc.

Standard process Ag-Pyre ML substrates were electroplated with chromium layers about 1000 Å thick. These substrates were then processed into otherwise standard process cells. The I-V characteristics of these cells showed double inflection S-shaped curves. See Fig. 13. Such behavior is usually associated with back-to-back diodes, which in the case of the CdS cell means that an additional rectifying junction has appeared in the cell.

Suspecting that the chrome-CdS junction was rectifying, I-V curves were taken between the substrate and the base CdS film. In-Hg amalgam, which is known to make ohmic contact to CdS, was used to contact the CdS film. Figure 14 shows the curves obtained. Curve B was obtained between two In-Hg contacts on the CdS film to show that no rectification was present at the In-Hg-CdS contact. Curve A was obtained between the substrate and the In-Hg contacts and clearly shows a rectifying characteristic which could very well explain the abnormal I-V curves obtained from completed cells made from these substrates. The Inset in Fig. 14 shows the experimental arrangement used in obtaining these curves.

The previous attempts at chromium substitution for the interlayer material used evaporated chrome and showed no such behavior. It was assumed that the reason for the present behavior in the electroplated chrome substrates was the formation of chrome oxides due to the exposure of the plated chrome substrate to room atmosphere. The best results obtained in the earlier work from the evaporated chrome substrates were obtained when the CdS evaporation followed chrome evaporation without exposing the evaporated chrome to room air. Several attempts were then made to reduce the effects of chrome oxide formation prior to CdS evaporation. The time between chrome plating and mounting in the CdS evaporator was minimized, but some exposure to room air was unavoidable. In addition, the evaporator was back-filled with argon and the substrate given an extended ion bombardment in hopes of removing any chrome oxides that may have formed. However, these attempts were to no avail, the only improvement being the reduction of the second inflection in the curve, Fig. 15, but an extremely high series resistance still remained. I-V curves of the back junction still revealed a rectifying contact present.

It was then decided to repeat the evaporated chrome interlayer experiments to see if the earlier results could be duplicated. The earlier results showed that if the evaporated chrome interlayer was exposed to room air prior to CdS evaporation the same double inflection curves were obtained from cells processed from these substrates. However, cells processed from evaporated chrome interlayers not exposed to room air prior to CdS evaporation resulted in the more normal cells referred to earlier. These experiments were repeated, particularly to see if the

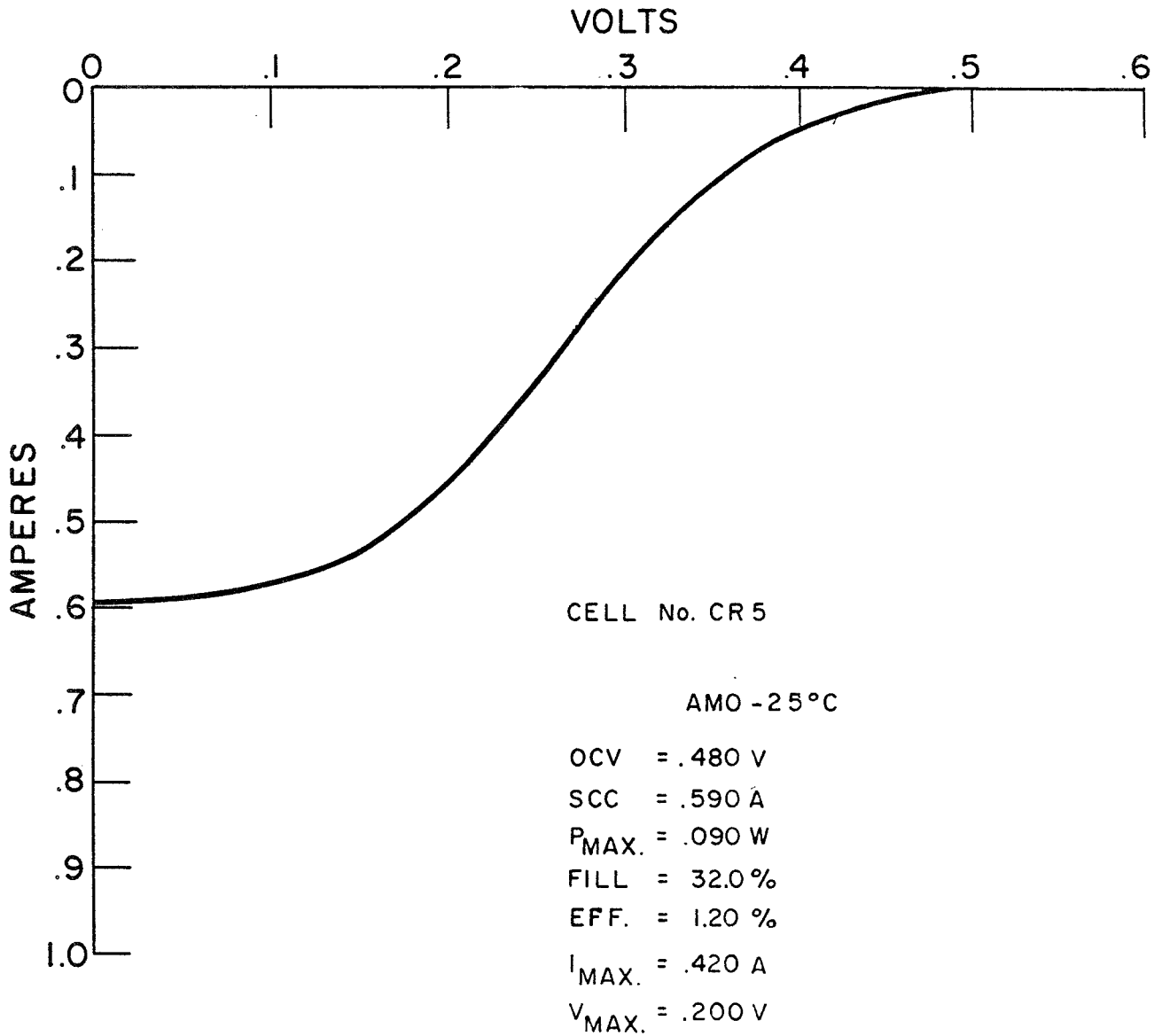


FIG. 13: I-V CHARACTERISTIC OF ELECTROPLATED CHROMIUM INTERLAYER CELL

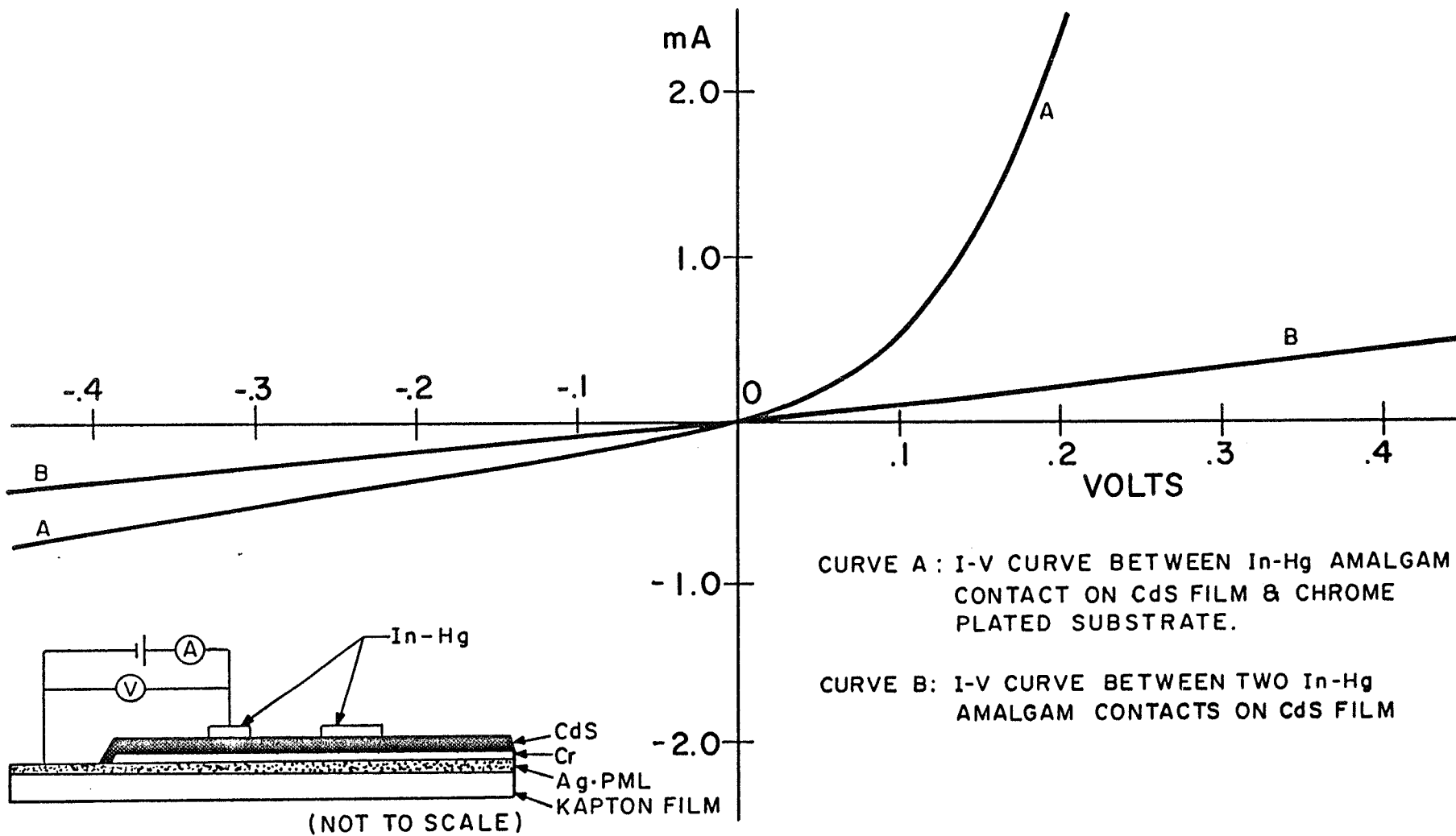


FIG. 14: I-V CHARACTERISTIC OF BACK JUNCTION WITH ELECTROPLATED CHROME INTERLAYER.

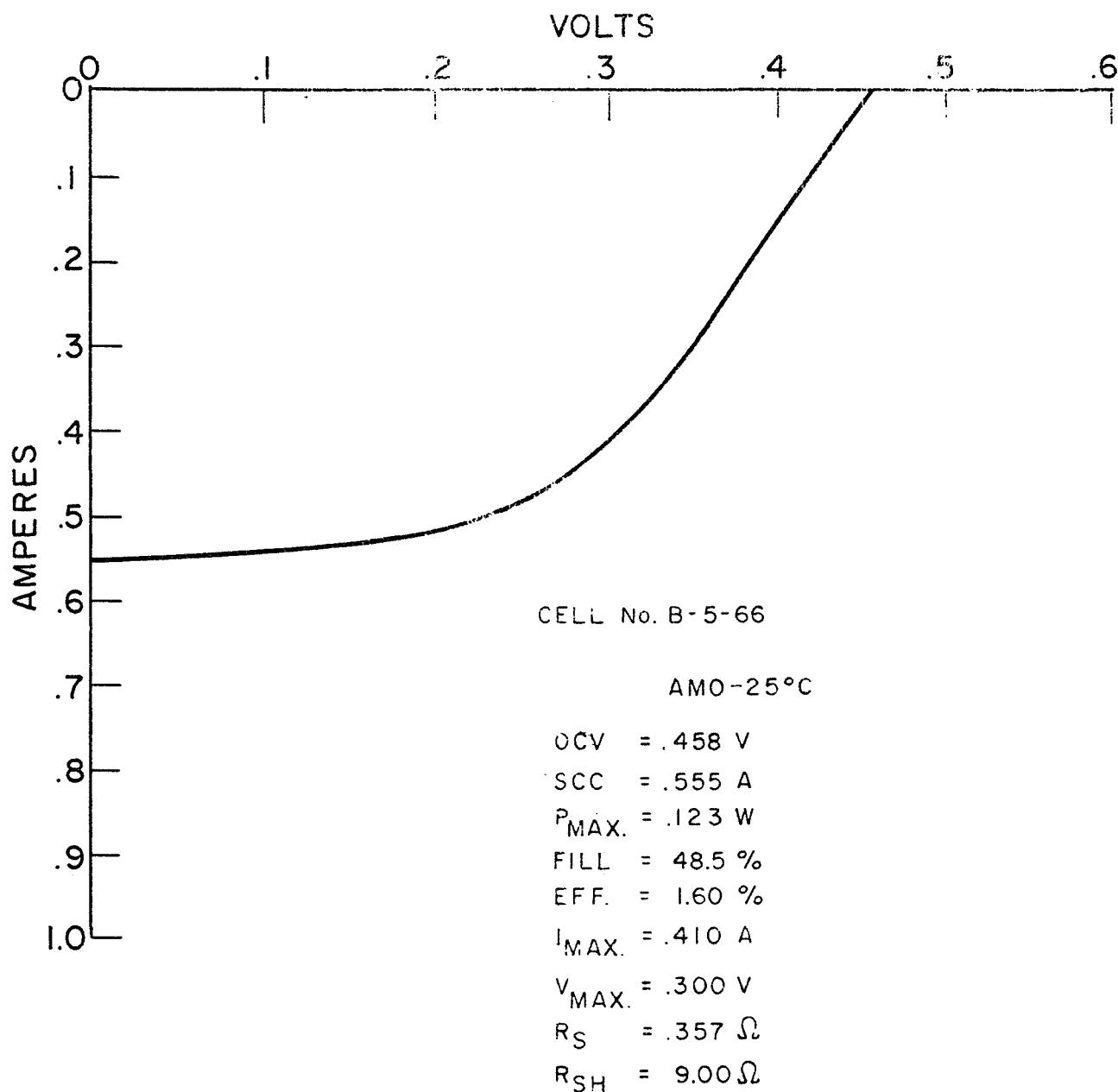


FIG. 15: I-V CHARACTERISTIC OF ELECTROPLATED CHROMIUM INTERLAYER CELL.

exposure to room air resulted in rectifying back junction, which would help explain the results obtained from the electroplated chrome cells.

Somewhat surprisingly, very little difference was observed between the exposed and unexposed chrome substrates, both on the back contact measurements as well as on the completed cells. Figures 16 and 17 show typical I-V curves from these cells. These curves are considerably different from those obtained from electroplated chrome substrate cells. The high series resistance and double inflection curve, characteristic of the plated samples, are not present, however, a low SCC is present. In addition a poor shunt condition is present which seems to be responsible for the low fill and low OCV. However, a poor shunt is difficult to explain in terms of the rectifying properties of the back junction. I-V curves of the back junction were linear, indicating that an ohmic contact had been established in both cases. Hence it appears that the back junction is more fabrication sensitive than it is materials sensitive.

These rather confusing results prompted an attempt to evaporate CdS directly onto an Ag-Pyre ML substrate, i. e., with no interlayer present. The main purpose was to determine if a non-ohmic contact would result at the CdS-Ag-Pyre ML interface. I-V curves of the CdS-Ag-Pyre ML junction surprisingly were linear, only at extremely high voltages and currents was there any indication of nonlinearity, but in the range of interest, within ± 100 mV, the curve was linear. Several of these substrates were processed into completed cells and Fig. 18 is typical of their resultant I-V curves. Obviously, this is a curve from a rather poor cell, but interestingly, the absence of the very high series resistance and double inflection curve affirm that an ohmic back junction is present. Again this curve seems somewhat dominated by a poor shunt resistance as evidenced by the very low OCV. However, the SCC is respectable, only slightly below average.

Hence, the conclusion to be drawn from these experiments is that chromium interlayers, either evaporated or electroplated, cannot be directly substituted for the electroplated zinc presently used. The immediate effect of these substitutions is somewhat confusing but does indicate that some other properties of the back contact, as yet unknown, may be of as much significance as its ohmic nature. The implication being that the manner of deposition seems to be as important as the material itself. This was also demonstrated earlier by the difference between evaporated and electroplated zinc.

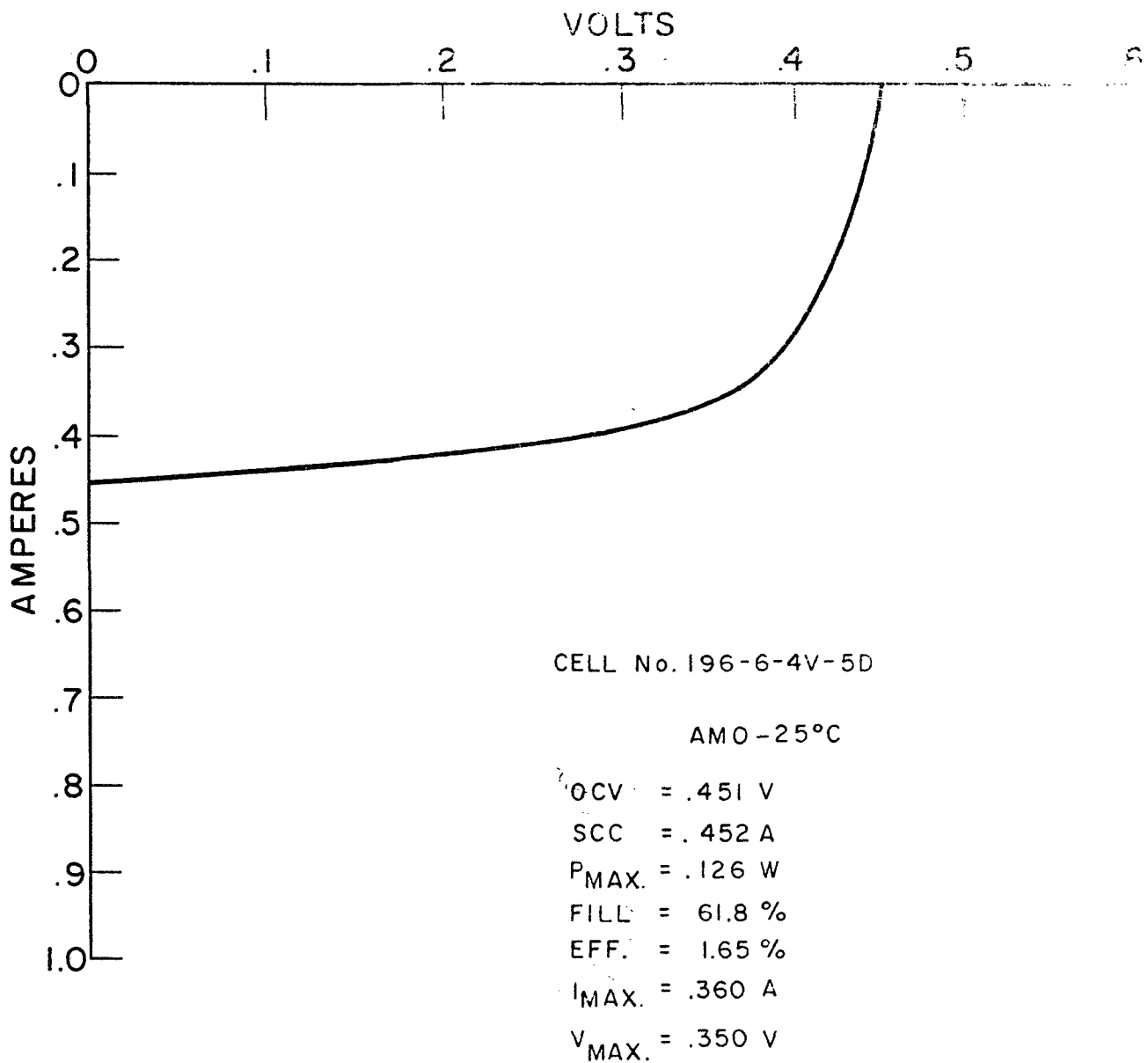


FIG. 16: I-V CHARACTERISTIC OF UNEXPOSED CHROME INTERLAYER CELL.

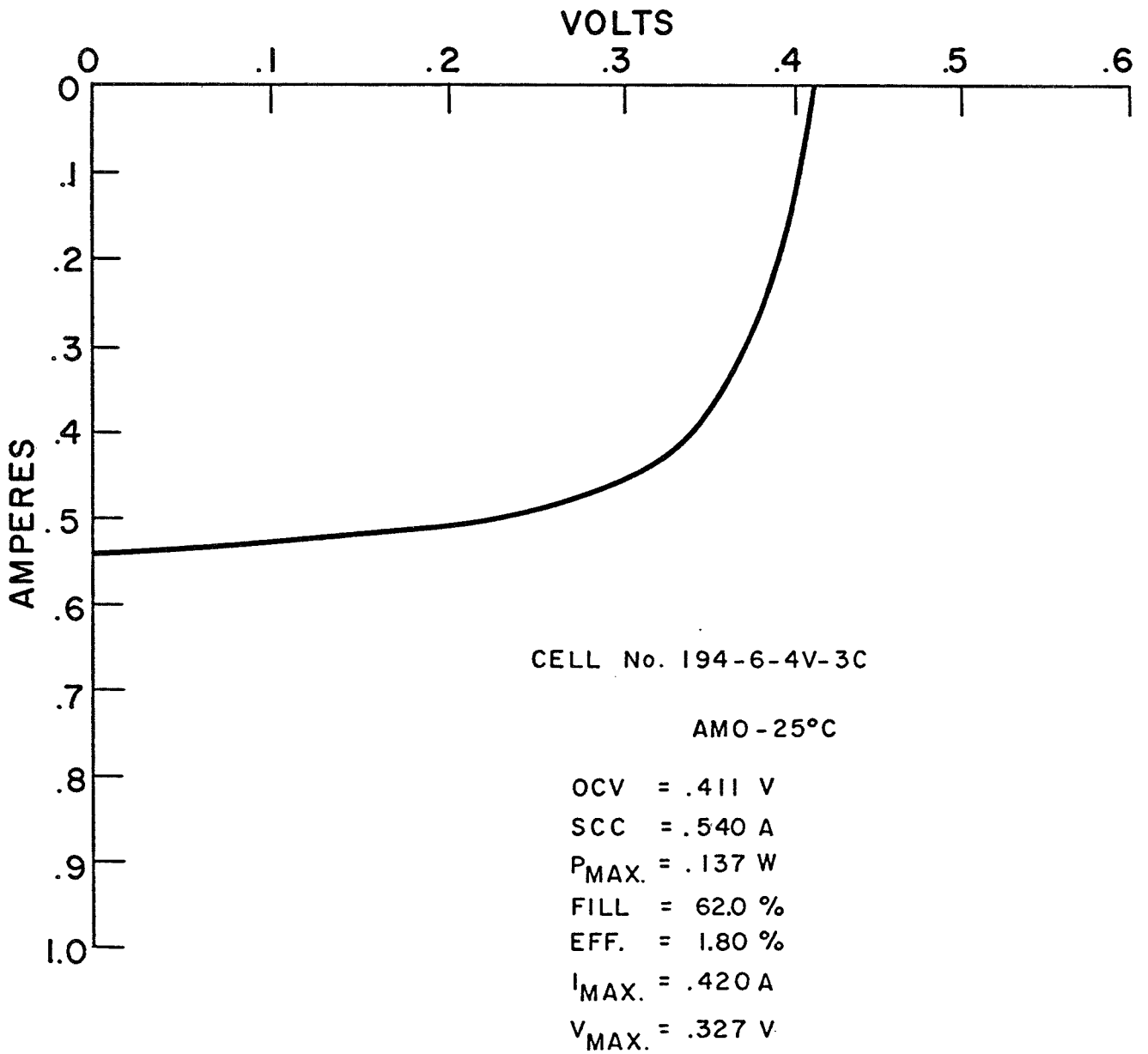


FIG. 17: I-V CHARACTERISTIC OF AIR EXPOSED CHROME INTERLAYER CELL.

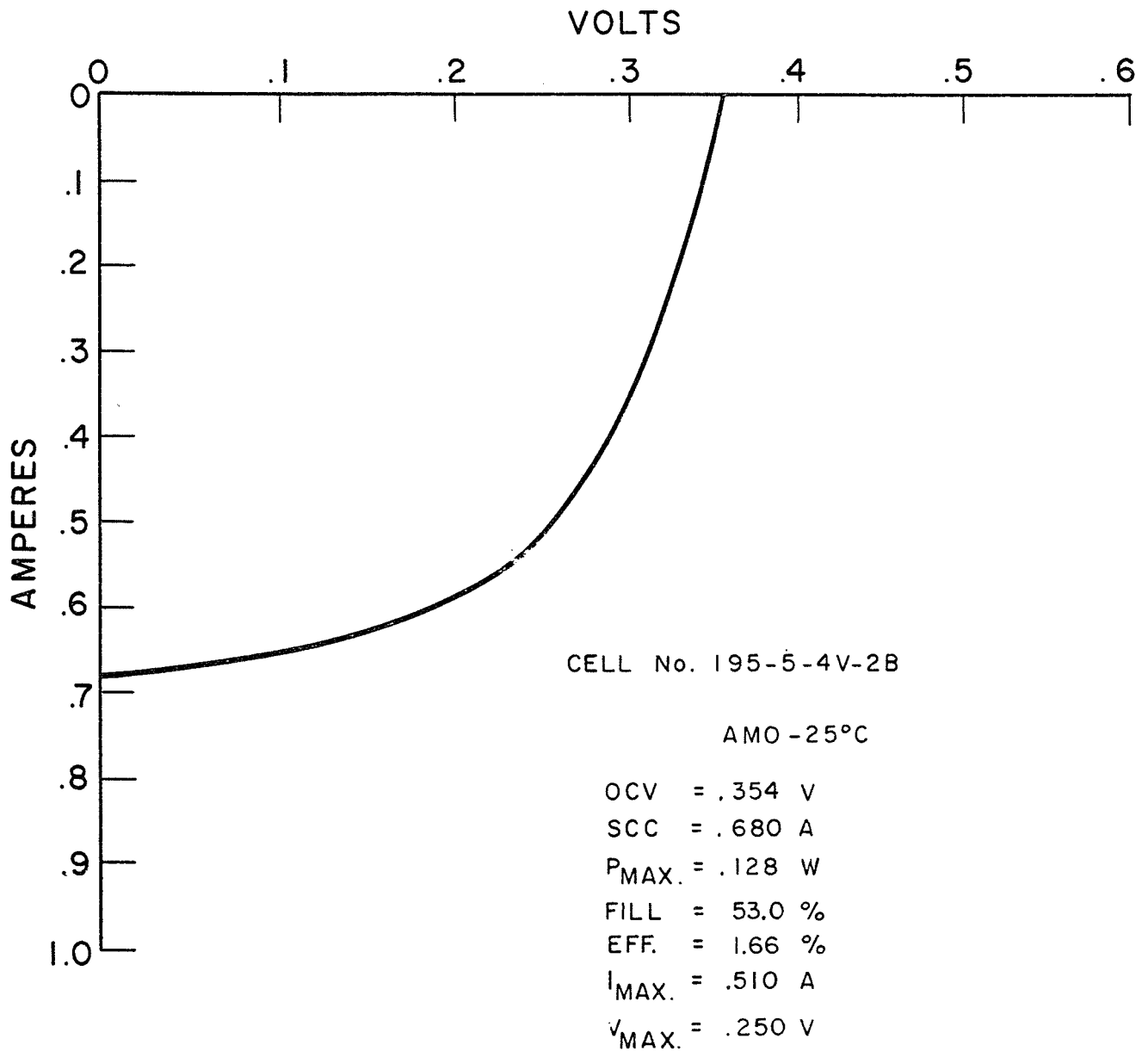


FIG. 18: I-V CHARACTERISTIC OF CELL WITH NO INTERLAYER.

FEP Teflon Cover Plastic

One of the most obvious changes that can be made to improve the efficiency of thin film CdS solar cells appears to be the simple substitution of a more transparent plastic for the Kapton cover plastic. Kapton's optical properties are obviously ill-suited for cover plastic use on solar cells since it absorbs about 25% of the AM0 sunlight. However, it admirably satisfies the other requirements for cover plastic material, that is, resistance to degradation by ultraviolet and particle radiation. No optically clear plastic material has yet been found that matches Kapton's resistance to radiation degradation. Recent work indicates that FEP Teflon approaches Kapton's radiation resistance,⁽⁶⁾ and it was decided to investigate it as a substitute cover plastic.

The first attempts at using Type C FEP Teflon as a cover plastic were by direct substitution for the Kapton. The same epoxy that is used to attach Kapton was used to attach the FEP with the same curing conditions. The resulting cells were visually acceptable; that is, the epoxy apparently successfully bonded the FEP to the cell. The initial electrical characteristics were also encouraging, see Table XXVIII which lists the ranges and averages of the AM0-25°C performance of 33 of these cells.

Table XXVIII. AM0-25°C Performance of 33 FEP Teflon Covered Cells.

	Max.	Min	Average
OCV	.482	.455	.470 V
SCC	1.120	.870	.975 A
P _{max}	.345	.281	.310 W
Eff.	4.5	3.7	4.2%
Fill	71.0	62.0	67.7%

These values should be compared with the similar values from this year's standard process cells, see Table I. The OCV's as expected, are practically identical, but the SCC's of the FEP cells are about 30% greater, which is somewhat more than the 25% normally seen between uncovered and Kapton covered cells. The average maximum power and efficiency of the FEP cells is about 24% greater than the Kapton covered cells which is approximately what was expected. The average fill of the FEP cells, however, is 3.4% lower than the standard cells. A closer look at the I-V traces reveals that these lower fills mainly appeared on the high SCC and high efficiency cells. This behavior has been noted before on Mylar covered cells and has been assumed to be caused by a limiting

(6) E. Anagnostou, private communication.

series resistance in the cell. Figure 19 is a good example of such a cell. In spite of what previously had been an acceptable series resistance of about 0.07 ohms, the fill is still obviously too low. The IR drop due to the series resistance is about 1.1 amps x 0.07 ohms ~ .077 volts, which means that the maximum power point would be 77 mV higher if the series resistance were zero. This would result in an efficiency of about 6% in the example shown with an extremely high fill.

An attempt to reduce this series resistance in FEP covered cells was made by substituting roll-coated substrates for the standard sprayed substrates. It was thought that the lower sheet resistance of the roll-coated substrates would lower the cells' series resistance, and thus improve its fill. The results of this experiment are tabulated in Table XXIX.

Table XXIX. AM0-25°C Performance of 26 FEP Covered Class I Roll-Coated Substrate Cells.

	Max.	Min.	Average
OCV	.480	.460	.468 V
SCC	1.095	.840	.965 A
P _{max}	.360	.274	.303 W
Eff.	4.7	3.6	4.0%
Fill	70.8	64.5	68.3%

The slight difference in fills is not significant enough to conclude that roll-coated substrates are better than sprayed substrates. As a result of short term outdoor testing it soon became apparent that the epoxy used to attach the FEP to the cell was quite sensitive to ultraviolet radiation. When used to attach Kapton to the cell the Kapton prevented any ultraviolet radiation from reaching the epoxy since it effectively cuts off at about 5100 Å. However, when used to attach the transparent FEP, which allowed the ultraviolet to reach the epoxy, its ultraviolet limitations soon became apparent. Hence an adhesive had to be found that had properties similar to the cover plastic, i. e., it had to be optically transparent and resistant to ultraviolet and particle radiation. Finding an adhesive with these properties turned out to be as difficult as finding a cover plastic with them.

A large number of transparent adhesives were then evaluated, including silicones, urethanes, epoxies and a number of unspecified proprietary ones. Surprisingly, practically all resulted in visually acceptable cells, i. e., they appeared to have successfully bonded the FEP to the cells. But the strengths of these bonds varied considerably, ranging from practically zero to strong enough to pull the CdS film from the substrate. The adhesives that were evaluated and a rough indication of their bond strengths are listed in Table XXX.

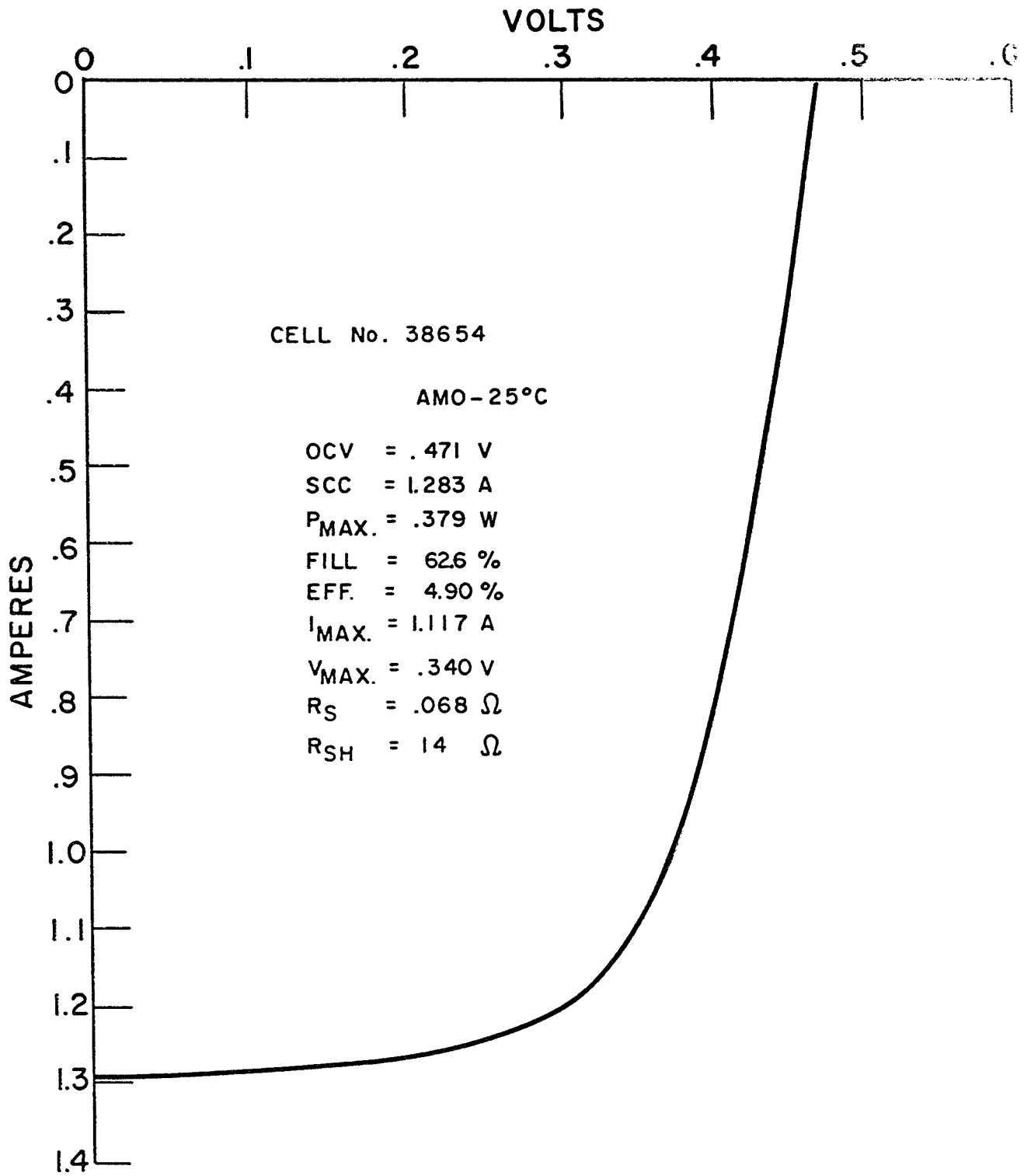


FIG. 19: I-V CHARACTERISTIC OF FEP COVERED CELL.

Table XXX. Adhesives Evaluated for Attaching Type C
FEP Teflon to Gridded Cells.

<u>Adhesive</u>	<u>Company</u>	<u>Comments</u>
RTV 602	G. E.	D
RTV 615	G. E.	D
182	Dow Corning	D
184	Dow Corning	D
281	Dow Corning	C
SR585	G. E.	B
X-30483	Dow Corning	C
RVCT-91	Arvey	A
Epoxy 20	Transene	D
Epoxy 30	Transene	A
Uralane XA-8666	Furane Plastics	A
4475	3M Company	D
77-N	3M Company	D
903-1	Tech. Fluorocarbon Eng.	B
903-2	Tech. Fluorocarbon Eng.	B
Quick Stick Spray	Maker Products	D
Eccobond 45 Clear	Emerson Cuming	D
Epotek 301	Epoxy Technology Inc.	A

Where:

- A - FEP wouldn't separate by itself, pulled off grid and CdS also.
- B - FEP difficult to remove, pulled portions of grid loose
- C - FEP was removable with difficulty.
- D - FEP was easily removable.

The RVCT-91, 903-1 and 903-2 are 2 mil FEP Teflon tapes with proprietary adhesives already applied. At least two samples of each adhesive were evaluated. One sample was cured according to the manufacturer's instructions and a second sample was given the same cure that the present cover plastic epoxy receives. In many cases the second method gave better results than the first.

Many cells have been fabricated with FEP cover plastics using the "A" rated adhesives. These cells are in the process of being tested to determine if their ultraviolet properties are acceptable. However, it is too early to say which, if any, of the adhesives is space acceptable.

A second method of attaching FEP Teflon to gridded cells was also evaluated. In this method the FEP film is heated to above its melting temperature and under pressure forms a strong bond to the gridded cell surface. Bonds strong enough to pull the CdS and grid away from the substrate are easily formed this way. Heating the FEP film in 10° C increments at 100 psi pressure in vacuum showed no reliable bonding until a temperature of 270° C was reached. It was also found that pressure is not a critical parameter. Laminating at 290° C at 50 psi was selected as the tentative laminating conditions for the initial evaluation. It was also observed that stronger bonds are achieved when the modified surface of Type C FEP is in contact with the cell surface. Further, it was found that a modified surface is no longer able to accept adhesives after a heating cycle. Apparently heating above its melt temperature causes a modified surface to revert back to its original form. This fact may become of significance during array fabrication if FEP is found to be acceptable as a cover plastic.

As stated a laminating condition of 290° C at a pressure of 50 psi was selected for the initial evaluation of FEP as a cover plastic. Although not rigorously optimized these conditions do result in bonds of apparently acceptable strength since they always pull away the CdS film and grid from the substrate. Unfortunately the time could not easily be varied for these laminations, the lamination press could only be heated relatively slowly. It normally took 40-50 minutes for the platens in the press to reach the required temperature. The usual practice was to let the plates remain at the desired laminating temperature for 5 minutes, then start the cooling procedure. Cooling was relatively fast, returning to room temperature within several minutes.

The effect of this high temperature lamination cycle on the electrical performance of cells is not consistent. Variations that range from catastrophic failures to slight perturbances have been seen, but the effect most commonly seen is a large decrease in OCV, fill and efficiency and a slight increase in SCC. This large loss is usually followed by a degree of recovery, again, that is not consistent. Figure 20 shows the three curves from a cell which showed this behavior. The degree of recovery depends on the treatment that the cell is subjected to after removal from the lamination press. Oddly enough a 15 hour vacuum bake at 135° C resulted in a greater recovery than room temperature exposure. It may be that the cause of the degradation that occurs in the high temperature lamination is somewhat annealed out during this lower temperature bake. At any rate, there does appear to be a natural tendency for the cell to recover after the high temperature FEP lamination but the conditions for promoting the maximum recovery have yet to be determined.

The large fall-off in cell performance after FEP lamination was duplicated by subjecting a number of standard process Kapton covered cells to the same laminating cycle. In all cases the same type of degradation and recovery resulted, see Fig. 21. In addition, cells with no cover plastics run through the same sequence, see Fig. 22, show the same type of

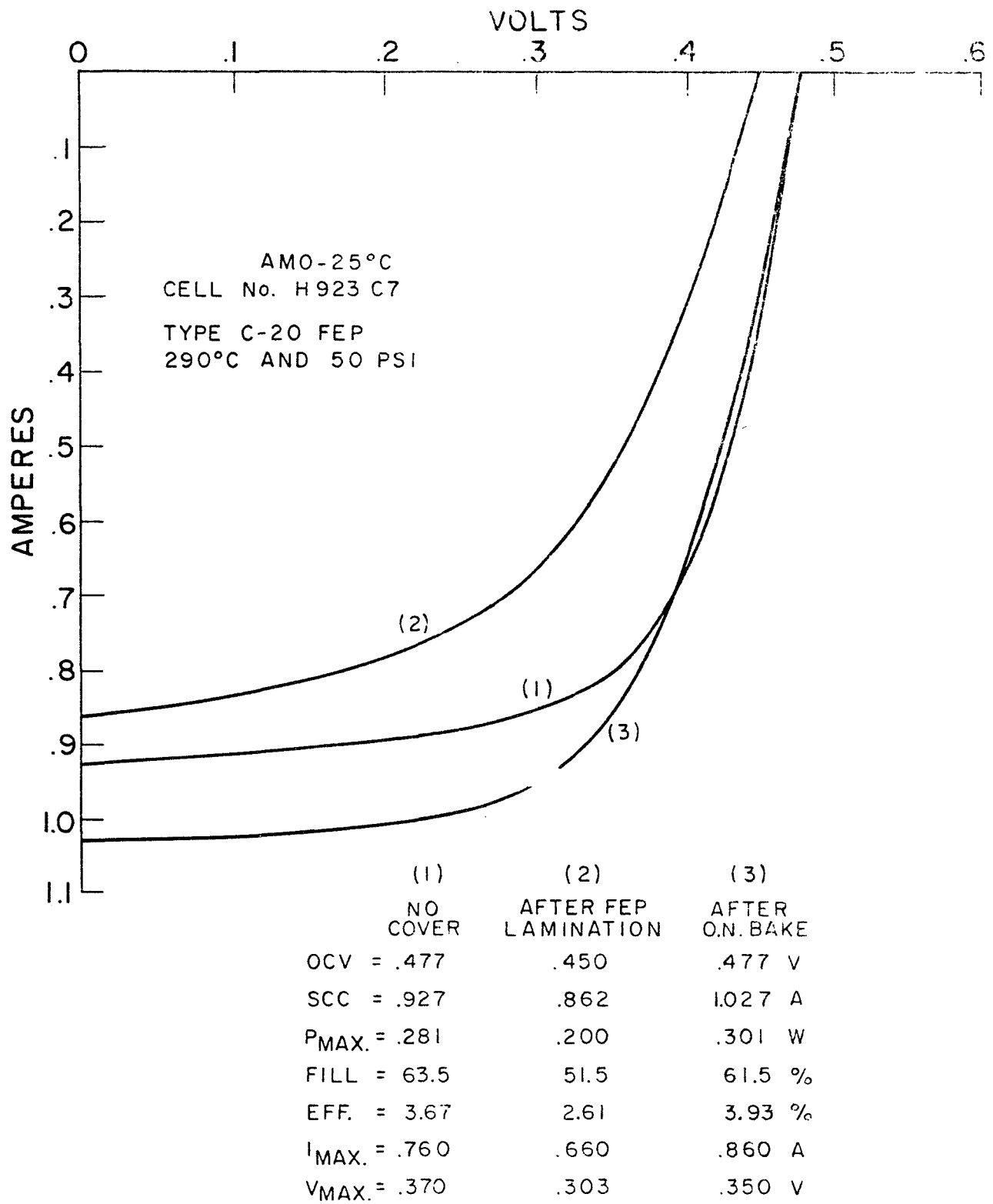
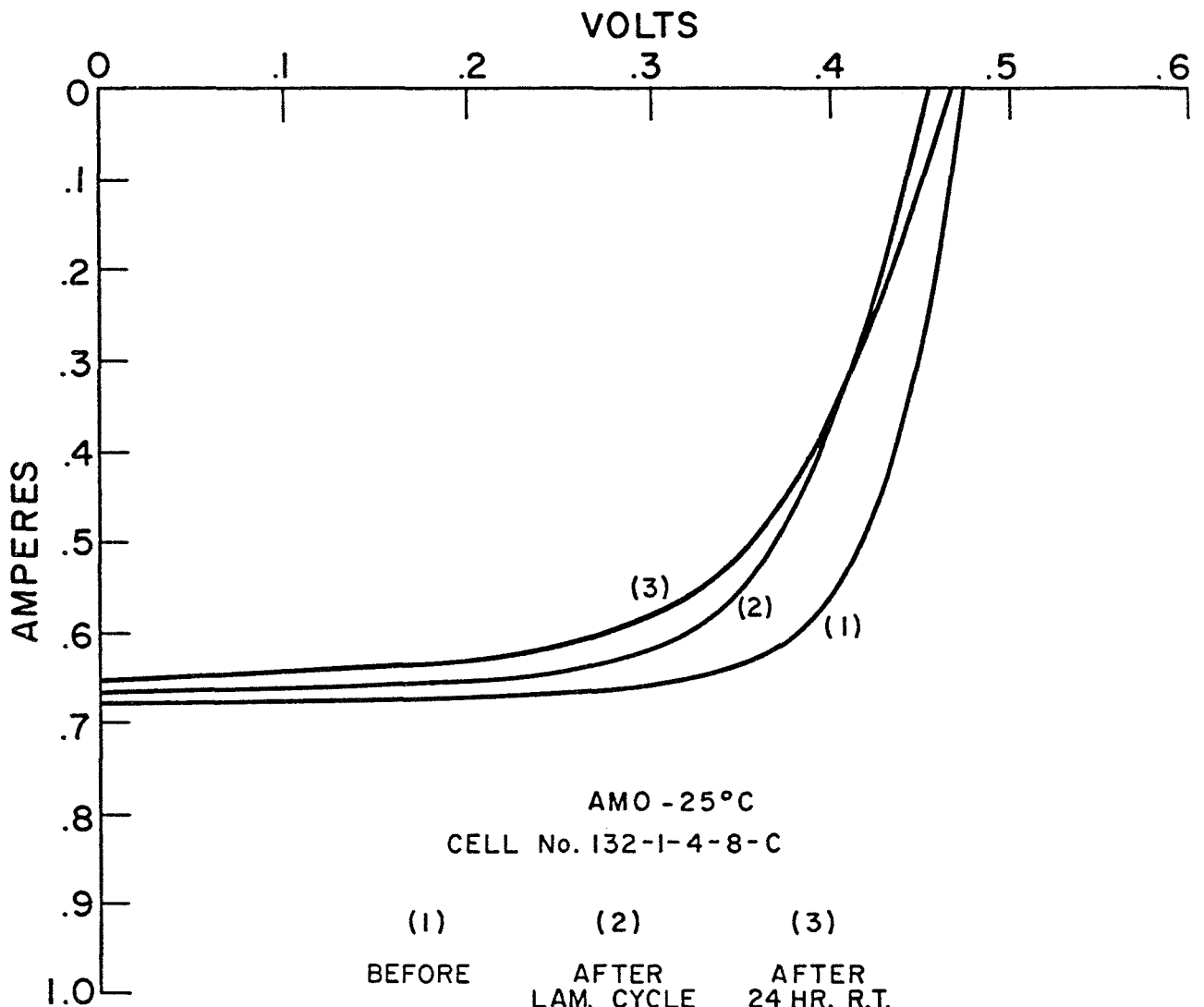


FIG. 20: I-V CHARACTERISTIC OF HEAT SEALED FEP CELL.



	(1) BEFORE	(2) AFTER LAM. CYCLE	(3) AFTER 24 HR. R.T.
OCV =	.472	.455	.466 V
SCC =	.680	.668	.652 A
P _{MAX} =	.229	.194	.179 W
FILL =	71.4	64.0	58.8 %
EFF =	3.00	2.53	2.33 %
I _{MAX.} =	.603	.580	.533 A
V _{MAX.} =	.380	.335	.335 V
R _S =	.064	.130	.147 Ω
R _{SH} =	30.0	18.0	13.6 Ω

FIG. 21: I-V CHARACTERISTICS OF CLASS I STANDARD PROCESS CELL SUBJECTED TO SAME HEATING CYCLE USED TO LAMINATE FEP.

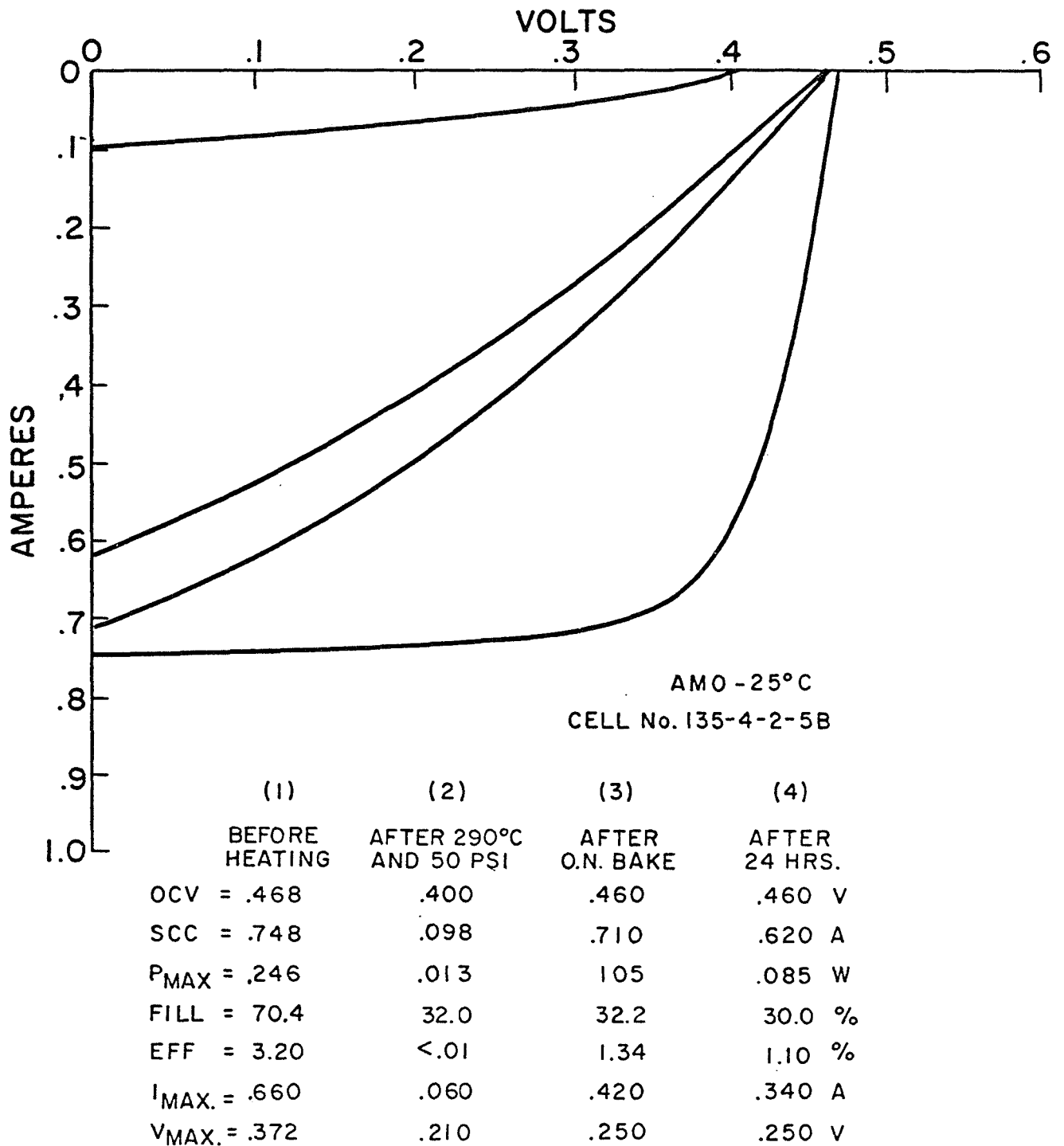


FIG. 22: I-V CHARACTERISTICS OF CELL WITH NO COVER SUBJECTED TO SAME HEATING CYCLE USED TO LAMINATE FEP.

behavior, indicating that the high temperature lamination cycle, rather than the Teflon, was responsible for the decrease and recovery. The reason for this behavior is not known but, as mentioned earlier, might be due to physical damage to the junction region. This is indicated by the lowered shunt resistance and lowered OCV. Fortunately there seems to be a natural tendency for the cell to recover, but again the mechanism is not understood. However, complete recovery has seldom been seen. Final performance is almost always poorer than performance prior to FEP lamination.

It is too early for a complete characterization of the performance and stability of heat bonded FEP covered cells. However some short-term testing data has been collected. Table XXXI shows the performance of a group of six cells over a period of 51 days at room atmosphere. The three pairs of cells were laminated at slightly different temperatures, as indicated in the Table.

Table XXXI. AM0-25° C Performance of Heat Bonded FEP Covered Cells.

	OCV	SCC	P _{max}	Fill	Eff.
	mV	mA	mW	%	%
234435 (280° C)					
Initial	489	950	319	69.0	4.16
19 days	482	910	289	65.9	3.76
35 days	484	890	281	65.5	3.66
51 days	475	890	273	64.6	3.56
234436 (280° C)					
Initial	491	961	330	70.0	4.31
19 days	491	940	314	68.7	4.10
35 days	485	920	298	66.8	3.88
51 days	485	925	297	66.3	3.88
178-718 (290° C)					
Initial	473	1092	336	65.0	4.38
20 days	468	1058	307	62.2	4.00
36 days	466	1038	292	60.4	3.81
52 days	465	1040	294	56.5	3.56
178-715 (290° C)					
Initial	462	1108	339	66.5	4.42
20 days	458	1052	302	62.8	3.94
36 days	452	1024	287	62.0	3.74
52 days	454	1015	283	61.5	3.70
178-712 (300° C)					
Initial	478	1095	352	68.5	4.59
21 days	466	1059	313	63.5	4.08
37 days	465	1035	295	61.2	3.84
53 days	462	1040	290	60.4	3.78
178-716 (300° C)					
Initial	464	1062	328	68.0	4.27
21 days	454	1007	284	62.2	3.70
37 days	450	988	270	60.8	3.52
53 days	452	985	270	60.7	3.52

There is obviously a period of readjustment for these cells which is similar to what occurs in standard process cells. However the time involved here is much greater than that in standard cells. One common characteristic in this readjustment period appears to be an increasing series resistance, which seems to be the main cause of the decreasing fill in all of the cells. This can be caused by a number of reasons in the cell but the grid contact, barrier layer and/or insulating layer resistance are immediately suspect.

The heat bonded cells do not appear to hold up as well as the adhesive bonded FEP cells on outdoor exposure. After about a month outdoors two heat bonded cells showed many areas of cover plastic delamination. Adhesive bonded cells on the same test show no adverse signs. However, more test data are necessary before a conclusion can be drawn regarding the acceptability of heat bonded FEP Teflon as a cover plastic.

Characterization of CdS Evaporation Process

The purpose of this task was to characterize the most critical parameters in the CdS evaporation cycle with respect to uniformity and repeatability from one evaporation cycle to the next. Standard cell production has always been plagued by a wide variation in cell performance, the cause of which has remained unknown. The intent was to determine if large variations were occurring in the CdS evaporation process which might be responsible for the variation in the production cells. The evaporation rate profile of the CdS evaporation sources was studied as a function of time and the temperature distribution that occurred across the Ag-Pyre ML coated Kapton substrate during CdS evaporation was also studied.

(1) Evaporation Rate Profile

It has always been suspected that as the CdS evaporation sources are continuously cycled they must be changing their evaporation characteristics as a result of aging effects. Specifically, it was thought that there must be increase in resistance with age and since a constant power application is specified it would appear that a decrease in evaporation rate must be occurring. This was evidenced by the appearance of unevaporated CdS in the sources as they aged. In order to completely evaporate all of the CdS it was necessary to increase the input power, contrary to the constant power requirement.

To determine more thoroughly what was occurring the evaporation rate profile of two types of sources was followed as a function of time. The two sources were quite similar, differing only by the inclusion of a thermal stress relief in the connecting straps. An Allen-Jones Model 600 Evaporation Rate Monitor was used to determine evaporation rates under actual CdS evaporation conditions. Figure 23 shows a sketch of the most frequently observed evaporation rate versus time curve and was considered to be the normal evaporation rate profile. Only the height of the curve showed any variation from one cycle to another.

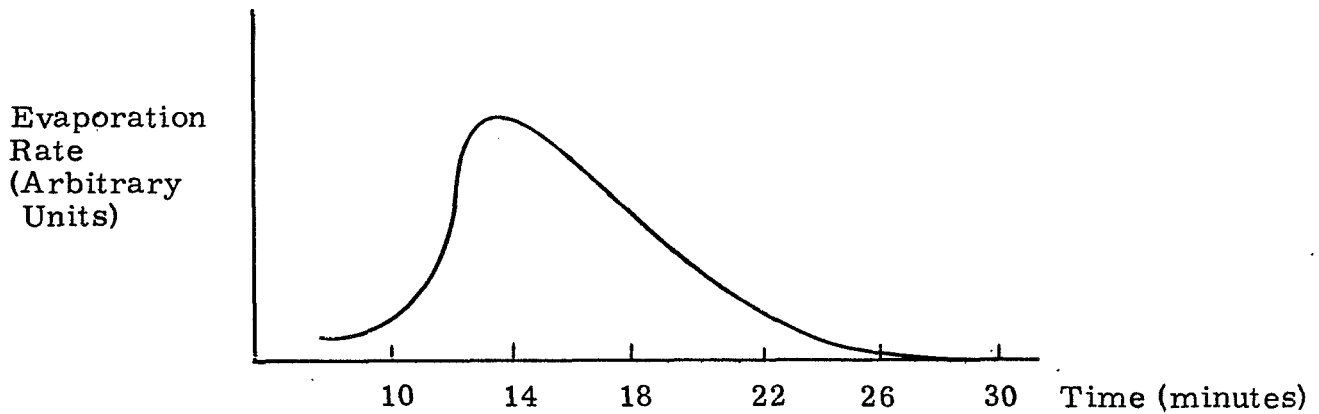


Fig. 23 Typical Evaporation Rate Profile of CdS Evaporation Source

The evaporation sources which did not have the thermal stress reliefs showed normal profiles through 40 evaporation cycles and rather erratic behavior after that. Physical changes were apparent much sooner, at about 20 cycles. Complete failure occurred after 51 cycles. The lack of stress reliefs showed up initially as a warpage in the geometry of the source followed by breaking of the Mo-Ta welds.

The evaporation sources which had the stress reliefs held up remarkably longer. The test was terminated after 85 cycles at which time the profile had shown no significant change nor was there any physical change apparent in the source. Since the normal cycle life between source replacements is about 60 cycles, there was no immediate need for carrying the test further.

The superiority of the stress relieved sources was also evident after they had been incorporated into the production evaporator. Previously, source failure and replacement between evaporator shutdowns for clean up was a frequent occurrence. However the use of the stress relieved sources has almost eliminated this problem.

(2) Substrate Temperature Uniformity

During CdS evaporation the Ag-Pyre ML covered Kapton substrate is maintained at a nominal temperature of 220°C. The substrate is clamped between two thin aluminum frames which hold it in place. The lower frame, which is in contact with the Ag-Pyre ML surface, also serves as an evaporation mask and defines the areas to be covered with CdS. The entire frame-substrate package is radiation heated by a large area tantalum heater positioned a half inch above the package. An additional strip of tantalum, which runs around the periphery of the main substrate heater, serves to heat the edges of the aluminum frames.

Radiation heating has been suspected of resulting in temperature gradients across the substrate during CdS evaporation because of the large area involved, about 10-1/2 x 11 inches. To study this possible effect a thermocoupled test substrate was substituted for standard substrates during a number of simulated evaporation cycles. Four thermocouples were attached to the silvered surface of a standard substrate with thermally conductive epoxy. The same type and size thermocouples that are normally used to control substrate temperature during standard depositions were used. The experimental arrangement consisted of the two control thermocouples in pressure contact with the back or unsilvered side of the Kapton substrate, the side facing the substrate heater. The four test thermocouples were attached with epoxy to the silvered or front surface of the substrate, the side facing the CdS evaporation sources. In addition, three test thermocouples were attached directly to the bottom aluminum frame. A control thermocouple was attached to the top frame and was used to control the peripheral frame heater. The control thermocouples are present during all standard CdS evaporations.

Fifteen minutes after the substrate and frame heaters had been turned on, at which time power is normally applied to the evaporation sources to start the CdS deposition process, a temperature gradient of 45° C was measured between test thermocouples at the center of the substrate and at the edge. In addition, a test thermocouple mounted opposite one of the substrate control thermocouples, i. e. , separated only by the thickness of the 1 mil Kapton film and the 0.3 mil Ag-Pyre ML layer, read about 40° C lower than the control. Hence, in addition to demonstrating that a temperature gradient exists at the substrate during a simulated CdS evaporation run, it was also shown that there may have been a large uncertainty as to what the actual temperature was.

When normal power was applied to the evaporation sources, but with no CdS present, the gradient was largely reduced; the maximum temperature difference between any two test thermocouples was about 12° C. This indicated that although radiant heat from the evaporation sources does tend to eliminate the temperature gradients on the substrate this method ought not to be relied on since the evaporation process is well in progress before the gradients are significantly reduced.

The thermocoupled substrate was then turned over so that the test thermocouples as well as the control thermocouples faced the substrate heater. All of the test thermocouples read within 10° C of the control thermocouple temperature. Since the test thermocouples read about 40° C lower than the control thermocouple when the test couples were attached to the bottom side of the substrate, it was assumed that radiation heating of the control thermocouple by the substrate heater occurs normally. Obviously, there is some doubt as to what the actual substrate temperature is during CdS evaporation.

In order to determine more fully the effects of the frames on the substrate temperature distribution the center strips of both the front and back frames were removed from a pair. The thermocoupled substrate was held only by the periphery of the frames. The maximum temperature difference with only the substrate and frame heaters was 23° C. This indicated that the frame center strips were possibly acting as heat sinks, particularly the lower one since its only source of heat is radiation from the frame heater along its edges.

In another attempt to determine the cause of the substrate temperature gradient a standard front frame was conduction heated by attaching a chromel heater wire along its center strips with a conductive epoxy. The maximum temperature difference between the same two thermocouples that read the largest differences before was about 23° C. Initially, a temperature difference of 47° C was read between these two couples.

The effect of other frame materials on the substrate temperature distribution was then determined. First, the use of a stainless steel mask was attempted. Again the center temperature was lowest, and in fact lower than previously, and continued decreasing with time. The mass of this particular mask was greater than the aluminum mask but its specific heat was less by an equivalent amount. However, the thermal conductivity of the stainless was a factor of ten less than the aluminum frame, and this very easily could have accounted for the observed gradient.

An H-film mask was also evaluated in which no metal was in contact with the substrate other than very small clamps which held the substrate suspended from a wire frame but not in contact with it. All thermocouple readings came within 20° C of the control temperature of 220° C within the same 15 minute warm up cycle. This indicated that the small thermal mass of the H-film mask tended not to act as much of a heat sink as the metal frames. CdS evaporations using these masks resulted in poor edge definition due to motion of the H-film during the evaporation process.

These experiments were done in the large three position evaporator that is also used in normal production of CdS cells. The three positions are identical in design and construction and as such should have roughly the same operating characteristics. As a matter of fact, one indication of evaporation uniformity should be the degree of uniformity of the operating characteristics of the three stations. Elapsed time indicators were connected across each of the three substrate heaters in order to help determine if the three substrates were seeing approximately the same conditions. The indicators showed however, that a wide variation in power consumption among the three stations, not only from station to station but from run to run as well was occurring. Substrates are normally heated for about an hour during a typical evaporation cycle but the actual elapsed time that the heaters are on varied from 4.5 minutes to 17 minutes. The only pattern apparent in the results was that one station, No. 3, consistently was on the longest of the three stations. These wide variations

ought not have occurred if the three positions were operating identically. It is not too unreasonable to assume that substrate temperatures were also varying in a similar manner.

However, the effect of this assumed temperature variation, as well as the temperature gradients discussed earlier, on the CdS film structure and ultimately on cell performance is unknown. In fact, there may be no effect at all since many excellent cells have been fabricated in spite of their occurrence; or, it may be that they do partially account for the rather wide variation in cell performance normally present in cell production.

FINAL REPORT DISTRIBUTION LIST

CONTRACT NAS3-11845

National Aeronautics & Space Administration
Washington, D.C. 20546
Attn: RNW/Ernst Cohn, (2 copies)
RN/William H. Woodward

National Aeronautics & Space Administration
Lewis Research Center
21000 Brookpark Road
Cleveland, Ohio 44135
Attn: John E. Dilley, MS 500-309
A. F. Forestieri, MS 302-1
B. Lubarsky, MS 3-3
D. T. Bernatowicz, MS 302-1
L. R. Scudder, MS 302-1 (5 copies)
L. Rosenblum, MS 302-1
A. E. Spokowski, MS 302-1
H. W. Brandhorst, MS 302-1
Report Control Office, MS 5-1
Technology Utilization Office, MS 3-19
V. F. Hlavin, MS 3-14
Library, MS 60-3

Naval Research Laboratory
Department of the Navy
Washington, D.C. 20390
Attn: E. Broncato, Code 6464
M. Wotaw, Code 5170
Dr. V. Limmenhom, Code 7450
Dr. C. Klick, Code 6440

Air Force Ballistic Missile Division
Air Force Unit Post Office
Los Angeles, California 91745
Attn: Col. L. Norman, SSEM
Lt. Col. G. Austin, SSZAS
Lt. Col. A. Bush, SSZME
Capt. A. Johnson, SSZDT
Capt. W. Hoover, SSTRE

Aerospace Corporation
P.O. Box 95085
Los Angeles, California 91745
Attn: Technical Library Documents Group

Bell Telephone Laboratories, Inc.
Murray Hill, New Jersey 07971
Attn: W. L. Brown
U. B. Thomas

The Eagle-Picher Company
Chemical & Material Division
Miami Research Laboratories
200 Ninth Avenue, N.E.
Miami, Oklahoma 74354
Attn: John R. Musgrave

Material Research Corporation
Orangeburg, New York 10962
Attn: Vernon F. Adler

National Cash Register Company
Physical Research Department
Dayton, Ohio 45409
Attn: J. S. Skarman

Radio Corporation of America
Semiconductor & Materials Division
Somerville, New Jersey 08876
Attn: Dr. F. L. Vogel
M. L. Topter

Sylvania Electronics Products, Inc.
Electron Tube Division
Emporium, Pennsylvania 15834
Attn: Georgian Larrabee, Librarian

Westinghouse Electric Corporation
Research & Development Laboratories
Churchill Borough, Pennsylvania 15235
Attn: B. Chang

Hughes Aircraft Corporation
Space System Division
P.O. Box 90919, Airport Station
Los Angeles, California 90009
Attn: Preston DuPont

Ion Physics Corp.
P.O. Box 98
Burlington, Massachusetts 01803
Attn: A. M. Huang

Navy Space Systems Activity
Air Force Unit Post Office
Los Angeles, California 90045
Attn: Richard Silverman

Lockheed Missiles & Space Company
P.O. Box 504
Dept. 70-01, Bldg. 151
Sunnyvale, California 94088
Attn: Kenneth A. Ray

Semi-Elements, Inc.
Saxonburg Blvd.
Saxonburg, Pennsylvania 16056
Attn: R. W. Christensen

Martin-Marietta Corporation
Electronics Research & Development
P.O. Box 179
Denver, Colorado 80201
Attn: John H. Martin

National Aeronautics & Space Administration
Scientific & Technical Information Facility
P.O. Box 33
College Park, Maryland 20740
Attn: Acquisition Branch (SQR-34-54)
2+1 reproducible

National Aeronautics & Space Administration
Langley Research Center
Langley Station
Hampton, Virginia 23365
Attn: W. C. Hulton
K. Rind
John L. Patterson, MS 234

Jet Propulsion Laboratory
4800 Oak Grove Drive
Pasadena, California 91103
Attn: John V. Goldsmith
Don W. Ritchie
R. J. Sturn

U.S. Army Signal Res. & Dev. Laboratory
Fort Monmouth, New Jersey 07703
Attn: Power Sources Branch

Office of the Chief of Engineers
Technical Development Branch
Washington, D.C. 20390
Attn: James E. Malcon/ENGMCRD

Wright-Air Development Division
Wright-Patterson AF Base, Ohio 45433
Attn: P. R. Betheand
Mrs. E. Tarrant/WWRNEM-1

Battelle Memorial Institute
505 King Avenue
Columbus, Ohio 43201
Attn: L. W. Aukerman
R. E. Bowman
T. Shielladay

COMSAT Laboratories
P.O. Box 115
Clarksburg, Maryland 20734
Attn: W. Billerbeck
Denis J. Curtin

Harshaw Chemical Company
Crystal Electronics Division
6801 Cochran Road
Solon, Ohio 44139

Heliotek Corporation
12500 Gadstone Avenue
Sylmar, California 74820
Attn: Eugene Ralph

North American Aviation, Inc.
Autonetics Division
Anaheim, California 92805
Attn: P. R. August

Sandia Corporation
P.O. Box 5800
Albuquerque, New Mexico 87115
Attn: K. D. Hardin, 1433

Union Carbide Corporation
Parma Research Center
Technical Information Services
P.O. Box 6116
Cleveland, Ohio 44101

Westinghouse Electric Corporation
Semiconductor Division
Youngwood, Pennsylvania 15697
Attn: Don Gunther
Peter Brody

University of Maryland
Department of Mechanical Engineering
College Park, Maryland 20740
Attn: M. E. Talaat

G. T. Schjeldahl Company
Box 170
Northfield, Minnesota 55057
Attn: Don Roiseland

Lockheed Missiles & Space Company
P.O. Box 504, Dept. 58-30
Sunnyvale, California 94088
Attn: S. H. Lee, Bldg. 538

General Electric Company
Research & Development Center
One River Road
Schenectady, New York 12305
Attn: D. A. Cusano

McDonnell Douglas Corporation
Missile & Space Systems Division
3000 Ocean Park Boulevard
Santa Monica, California 90406
Attn: Howard Weiner

National Aeronautics & Space Administration
Goddard Space Flight Center
Greenbelt, Maryland 20771
Attn: W. R. Cherry
H. Schach
B. Mermalstain, Code 672
J. W. Callaghan, Code 621
Librarian

National Aeronautics & Space Administration
Manned Spacecraft Center
Houston, Texas 77058
Attn: S. Caudiano
A. E. Potter

Institute for Defense Analyses
Science and Technology Division
400 Army Navy Drive
Arlington, Virginia 22202
Attn: R. C. Hamilton

Air Force Cambridge Research Center
Air Research & Development Command
USAF, Hanscom Field
Bedford, Massachusetts 01731
Attn: Col. G. deGiacomo

Aeronautical Research Laboratories
Office of Aerospace Research, USAF
Wright-Patterson AF Base, Ohio 45433
Attn: Mr. D. C. Reynolds, ARX
Chief, Solid State Physics Research Lab.

Flight Accessories Aeronautics Systems Division
Wright-Patterson AF Base, Ohio 45433
Attn: Joe Wise/Code APIP-2
James L. Mattice, ASRCN-22

Bell & Howell Research Center
360 Sierre Madre Villa
Pasadena, California 91102
Attn: Alan G. Richards

University of Delaware
Physics Department
Newark, Delaware 19711
Attn: K. W. Boer

Hughes Aircraft Company
Aerospace Group, R&D Division
Culver City, California 90230
Attn: C. A. Escoffery

Martin Company
Orlando, Florida 32805
Attn: Library

Philco Corporation
Blue Bell, Pennsylvania 19422
Attn: Mr. A. E. Mace

RCA Laboratories
Princeton, New Jersey 08540
Attn: Paul Rappaport

Sigmatron, Inc.
849 Ward Drive
Santa Barbara, California 93105
Attn: Sharon Marsellos

Solid-State Electronics Laboratory
Stanford Electronics Laboratories
Stanford University
Stanford, California 94305
Attn: Prof. G. L. Pearson
Prof. R. Bube

Massachusetts Institute of Technology
Lincoln Laboratory
Lexington, Massachusetts 02139
Attn: Dr. William L. Black, Rm L-255
Dr. A. G. Stanley, Rm D-025

The Boeing Company
P.O. Box 3999
Seattle, Washington 98124
Attn: H. Oman, MS 88-06
R. A. Mickelson, MS 88-43

Physics Technology Labs, Inc.
7841 El Cajon Boulevard
La Mesa, California 92041
Attn: W. E. Richards

Goodyear Aerospace Corporation
1210 Massillon Road
Akron, Ohio 44315
Attn: Richard Hose

General Telephone & Electronics Labs, Inc.
Advanced Materials & Devices
208-20 Willets Pt. Blvd.
Bayside, New York 11360
Attn: M. Wasserman
A. L. Swygard

INITIAL DISTRIBUTION LIST

Copy No.

1. D. B. Parkinson
2. Hans Jaffe
3. Project Administrator
4. Patent
- 5-7. Library
8. H. E. Nastelin
- 9-11. F. A. Shirland
12. L. R. Shiozawa
13. W. F. Dunn
14. J. Smith
15. J. Beller
16. T. Deucher
- 17-114. NASA Distribution List (98 copies)